Doctoral Thesis

Synthesis, Conformation, and Chiral Properties of Optically Active Polyfluorenevinylene Derivatives

(光学活性ポリフルオレンビニレン誘導体の

合成、コンホメーションおよびキラル特性)

Pengfei WU (呉 鵬飛)

Hokkaido University

Contents

Chapter 1. General Introduction

1.1 Polymer chirality

Chirality of Polymer chirality plays various roles in life as well as in synthetic material applications, and helix is the focus in studies on synthetic polymer chirality. Helix is the molecular conformation of a spiral nature, generated by regularly repeating rotations around the backbone bonds of a macromolecule, and a polymer consisting of single-handed helical or preferred-handed helical macromolecules may be optically active exhibiting chiroptical properties. Natural polymers including proteins (peptides), DNAs, and polysaccharides are in many cases single-handed helical where the handedness is based upon handedness of centers of chirality in the monomeric unit. Helical folding of proteins and DNAs is closely related to their biological activities.

On the other hand, for synthetic polymers, helicity can be introduced by designing monomer and polymerization reaction and by controlling interactions of random chain with external molecule. Single-handed or preferred-handed helix can be created on the basis of chirality of ligand or monomeric units or external molecules. Optically active, helical synthetic polymers find various functions including resolution of racemic small molecules,[1] asymmetric catalysis,[2] optical non-linearity,[3] chiroptical switch,[4] and circularly polarized light (CPL) emission.[5]

1.2 Optically active, synthetic polymers having helical conformation

Following the early and important studies on helical structures of natural macromolecules including polysaccharide (α-amylose) (1936),[6] polypeptides (1951),[7] and DNAs (1953),[8] research aiming at synthetic helical polymers came into bloom. The first synthetic helix was made for isotactic polypropylene by Natta in 1955 where the helix was racemic and was stable only in the solid state.[9] Later, preferred-handed helix of isotactic polyolefins which can be maintained in solution was realized based on the effect of side-chain chirality.[10] A major break-through in this field was the synthesis of

single-handed helical, isotactic poly(triphenylmethacrylate methacrylate) (poly(TrMA)) by asymmetric anionic polymerization (helix-sense-selective polymerization, asymmetric helix-chirogenic polymerization) using chiral ligand as chirality source reported in 1979.[11] Poly(TrMA) is the first example of single-handed helical polymer having no configurational chirality. This polymer can hold its single-handed helical conformation through steric repulsion between the bulky side-chain groups. Examples of other synthetic helical polymers include polyolefins,[10] polyisocyanates,[12] polyisocyanides,[13] polychloral,[14] poly(meth)acryaltes,[15] polysilanes,[16] polyacetylenes,[17] and main-chain conjugated polymers (**Chart. 1-1**).[18]

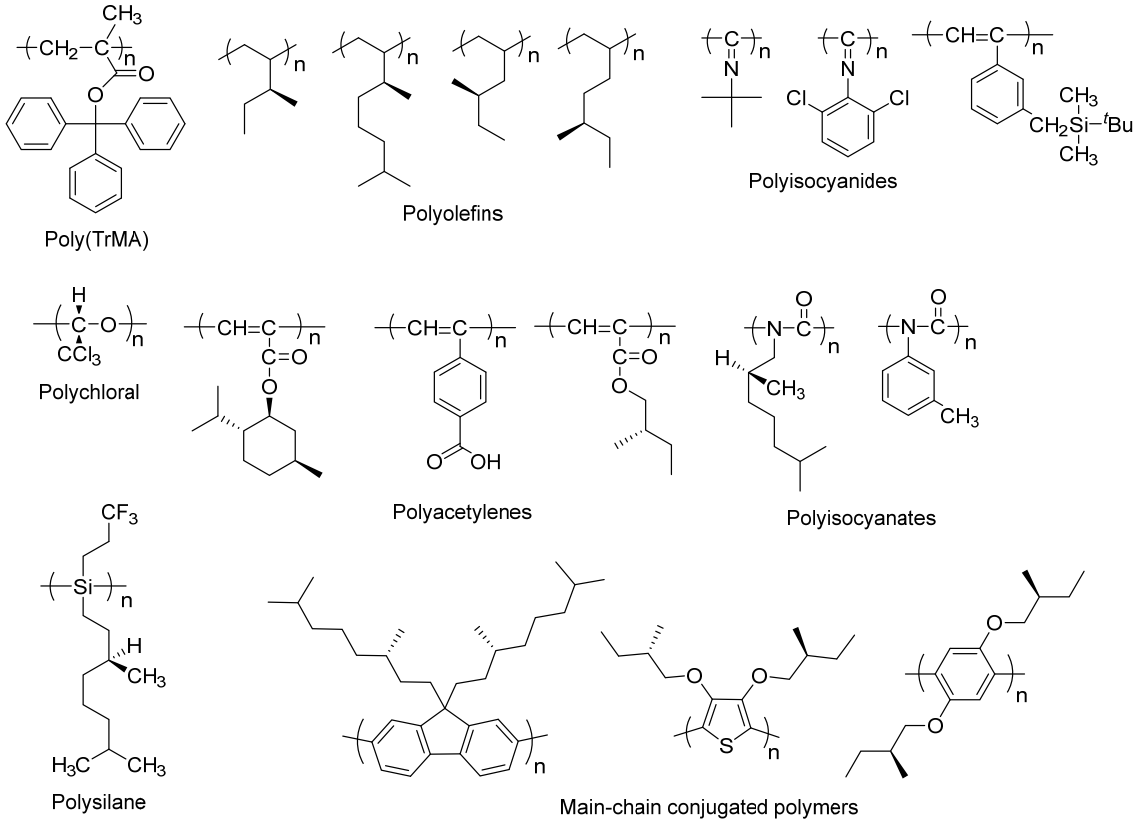

Chart. 1-1. Representative examples of synthetic helical polymers.

Generation of helical structure regardless of handedness can be based on one or more

among the following factors: (1) steric repulsion between side-chain groups, (2) attraction between side-chain or main-chain moieties, (3) inherent rigidity of the main chain, and (4) non-covalent interactions with external molecules which temporarily modify the chain structure. Single-handedness or preferred-handedness is introduced (1) by polymerization through kinetic control, or (2) on the basis of configurational chirality present in the monomeric unit or in the main chain through static stability, or (3) by the effect of external chiral molecule interacting with polymer chain. Helical structures and preferred handedness of the polymers noted above are controlled by these methods through ground-state chemistry.

Chirality of polymers is analyzed mainly using circular dichroism (CD) spectra which quantifies the difference in molar absorptivity toward right- and left-handed CPL's of a chiral polymer at different wavelengths. The extent of this difference is generally evaluated by Kuhn's anisotropy factor (g_{CD}):[19]

$$g_{CD} = 2(\varepsilon_L - \varepsilon_R)/(\varepsilon_L + \varepsilon_R)$$

where ε_L and ε_R denote molar absorptivities for left- and right-handed CPL's.

The magnitude of g_{CD} value is generally very small; g_{CD} for aromatic chromophores is in the order of 10^{-3}~10^{-4}. Ketones have rather large g_{CD} values in the order of 10^{-2}.

1.3 Linear and hyperbranched polyfluorenevinylenes

Polyfluorenevinylenes [poly(9,9-disubstitutedfluorene-2,7-diylethene- 1,2-diyl)] as well as polyphenylenevinylenes [poly(2,5-disubstitutedbenzene-1,4-diylethene-1,2-diyl)] have been widely studied as light- emitting and photovoltaic polymers whose long π-conjugation is responsible for visible light emission.[20] Such polymers can be prepared by the Gilch reaction of 2,7-bis(bromomethyl)fluorene derivatives in the presence of a base such as *t*-BuOK and also by metathesis polymerization of 2,7-divinylfluorne derivatives.[21] The two reactions can create double bond (ethane-1,2-diyl unit) between fluorene core units at high efficiency. While a variety of

linear polyfluorenevinylenes have been studied as organic light-emitting diode (OLED) material candidates, work on chirality of such polymers has been limited while chiral, linear polyfluorenevinylenes are considered to be potentially interesting as CPL emitters. The existing examples of linear, chiral polyfluorenevinylenes include polymers with two linear, chiral side-chain groups with the same structure attached to the 9(9')-position of fluorene core where the effects of the distance between fluorene core and the center of chirality of the side-chain group on CD and CPL spectra.[22] In this work, CD and CPL efficiency was amplified in suspension as compared with solution, and the amplification was ascribed to inter-chain aggregates formation, which is quite different from what this work discussed in Chapter 2 where self-folding of polymer chain leads to extreme amplification of chirality in the ground and excited states.

As well as linear polymers, hyperbranched polyfluorenevinylenes have also been studied.[23] As for the synthesis, the Gilch reaction of 2,4,7-tris(bromomethyl) fluorene derivatives has been used. Hyperbranched polyfluorenevinylenes were originally devised to avoid the formation of excimer between fluorene core units which can occur for linear polymers and decreases emission efficiency as well as changes emission wavelengths (colors). Complex structures of hyperbranched polymers would not allow chain alignment which tends to facilitate excimer formation in excited states. Hyperbranched polyfluorenevinylenes indeed do not show decreased emission intensity or changes in emission color.

However, hyperbranched polyfluorenevinylene with chirality was reported in only short communication[23f], and details of the synthesis and properties have not been disclosed while such polymer may be an interesting material of CPL emission. In addition, complex molecular architecture may allow interactions with external molecules that may enter or penetrate into the interior space of complex hyperbranched structures, which is the subject discussed in Chapter 3 of this thesis.

1.4 Thesis contents

In this work, linear and hyperbranched polyfluourenevinylenes whose chirality arises from neomenthyl group attached to the 9-position of fluorene core were synthesized, and their structure and functions were studied. The polymers are copolymers composed of chiral and achiral monomeric units at different ratios which allowed investigations on how chain (segment) chirality affects chiroptical properties of entire polymers. As briefly discussed above, chiroptical properties have been demonstrated to be enhanced by inter-chain aggregation which may form helical bundles that amplify chirality. Such examples are based on the widely accepted concept of controlling "uniform" structure which is believed to result in enhanced properties in chirality sciences. In a sharp contrast, this thesis discusses "non-uniform" chain folding of linear polymers and "complex structure" of hyperbranched polymers in connection with chiroptical properties of the polymers, which led to largely enhanced chiroptical properties not only in the ground state but also in excited states. The findings presented in this thesis may shed light on seemingly "unordered" structures of polymers which have been overlooked or unnoticed so far but actually can strongly contribute to the realization of desired properties.

The following summarizes the contents of each chapter of this thesis:

Chapter 1 introduced the background of this thesis work encompassing the background including from the classic methods of chiral polymer synthesis and also briefly introduces the examples of polyfluorenevinylenes with chiraltiy.

Chapter 2 describes the synthesis and "non-uniform" self-folding of linear polyfluorenevinylenes. An unprecedented non-uniform self-folding of artificial polymer chains composed of turn moieties and stretched segments is presented through the design of a set of optically active poly(fluorene-2,7-diylethene-1,2-diyl) (poly(fluorenevinylene)) derivatives bearing a neomenthyl group and a pentyl group

attached at the 9-position of fluorene backbone at various ratios. The folded structure is formed and stabilized through inter-chain interactions in the solid state, leading to remarkably enhanced chiroptical properties (chirality amplification) in terms of circular dichroism (CD) and circularly polarized light (CPL) emission. This phenomenon is rationalized by experimental and theoretical CD and CPL spectral analyses. The polymer arrangements in the solid state were further assessed through transmission electron microscopic observations combined with enhanced sampling molecular dynamics simulations in the solid state revealing the thin film organizations.

Chapter 3 presents the synthesis of hyperbranched polyfluorenvinylenes and their interactions with external molecules that are given intermolecular structural order when they enter or penetrate into the complex structure of hyperbranching. Hyperbranched, optically active poly(fluorene-2,4,7- triylethene-1,2-diyl) [poly(fluourenevinylene)] derivatives bearing a neomenthyl group and a pentyl group at the 9-position of fluorene backbone at various ratios as chirality donor, host polymers efficiently included naphthalene, anthracene, pyrene, 9-phenylanthracene, and 9,10-diphenyanthracene as chirality acceptor, guest molecules in their interior space in film as well as in solution, and the guest molecules exhibited intense circular dichroism through chirality transfer with chirality amplification. The chirality transfer efficiency was much higher with a higher-molar-mass polymers and also compared with linear poly(fluorene-2,7-diylethene-1,2-diyl) derivatives bearing the same side-chain groups. The polymers may include the small molecules in their complex structure without any specific interactions. The included molecules may be in intermolecular order which may be similar to those known for liquid crystals. Naphthalene, anthracene, pyrene, and 9-phenylanthracene included in the polymer exhibited efficient circularly polarized light emission where chirality is remarkably amplified.

Chapter 4 summarizes this thesis and presents general conclusions.

References

1. (a) H. Yuki, Y. Okamoto, I. Okamoto, Resolution of racemic compounds by optically active poly (triphenylmethyl methacrylate), *J. Am. Chem. Soc.* **1980,** *102* (20), 6356-6358; (b) Y. Okamoto, S. Honda, I. Okamoto, H. Yuki, S. Murata, R. Noyori, H. Takaya, Novel packing material for optical resolution:(+)-poly (triphenylmethyl methacrylate) coated on macroporous silica gel, *J. Am. Chem. Soc.* **1981,** *103* (23), 6971-6973; (c) Y. Okamoto, K. Hatada, Resolution of Enantiomers by HPLC on Optically Active Poly(triphenylmethyl Methacrylate), *J. Liq. Chromatogr.* **1986,** *9* (2-3), 369-384; (d) T. Nakano, Optically active synthetic polymers as chiral stationary phases in HPLC, *J. Chromatogr. A* **2001,** *906* (1–2), 205-225; (e) K. Shimomura, T. Ikai, S. Kanoh, E. Yashima, K. Maeda, Switchable enantioseparation based on macromolecular memory of a helical polyacetylene in the solid state., *Nature chemistry* **2014,** *6* (5), 429-434.

2. (a) M. Reggelin, M. Schultz, M. Holbach, Helical chiral polymers without additional stereogenic units: A new class of ligands in asymmetric catalysis, *Angew. Chem. Int. Ed.* **2002,** *114* (9), 1684-1687; (b) A. F. Trindade, P. M. P. Gois, C. A. M. Afonso, Recyclable Stereoselective Catalysts, *Chem. Rev.* **2009,** *109* (2), 418-514; (c) T. Yamamoto, M. Suginome, Helical Poly (quinoxaline-2, 3-diyl) s Bearing Metal-Binding Sites as Polymer-Based Chiral Ligands for Asymmetric Catalysis, *Angew. Chem. Int. Ed.* **2009,** *48* (3), 539-542; (d) A. J. Boersma, D. Coquière, D. Geerdink, F. Rosati, B. L. Feringa, G. Roelfes, Catalytic enantioselective syn hydration of enones in water using a DNA-based catalyst, *Nature chemistry* **2010,** *2* (11), 991-995; (e) T. Yamamoto, T. Yamada, Y. Nagata, M. Suginome, High-molecular-weight polyquinoxaline-based helically chiral phosphine (PQXphos) as chirality-switchable, reusable, and highly enantioselective monodentate ligand in catalytic asymmetric hydrosilylation of styrenes. *J. Am. Chem. Soc.* **2010,** *132* (23), 7899-7901; (f) Z. Tang, H. Iida, H.-Y. Hu, E. Yashima, Remarkable enhancement of the enantioselectivity of an organocatalyzed asymmetric Henry reaction assisted by helical poly (phenylacetylene) s bearing cinchona alkaloid pendants via an amide linkage, *ACS Macro Lett.* **2012,** *1* (2), 261-265.

3. P. N. Prasad, Polymeric materials for non-linear optics and photonics, *Polymer* **1991,** *32* (10), 1746-1751.

4. (a) N. Hida, F. Takei, K. Onitsuka, K. Shiga, S. Asaoka, T. Iyoda, S. Takahashi, Helical, chiral polyisocyanides bearing ferrocenyl groups as pendants: synthesis and properties, *Angew. Chem. Int. Ed.* **2003,** *115* (36), 4485-4488; (b) E. Gomar-Nadal, J. Veciana, C. Rovira, D. B. Amabilino, Chiral teleinduction in the formation of a macromolecular multistate chiroptical redox switch, *Adv. Matter.* **2005,** *17* (17), 2095-2098; (c) E. Gomar-Nadal, L. Mugica, J. Vidal-Gancedo, J. Casado, J. T. L. Navarrete, J. Veciana, C. Rovira, D. B. Amabilino, Synthesis and doping of a multifunctional tetrathiafulvalene-substituted poly (isocyanide),

Macromolecules **2007,** *40* (21), 7521-7531; (d) H. Iida, T. Mizoguchi, S.-D. Oh, E. Yashima, Redox-triggered switching of helical chirality of poly (phenylacetylene) s bearing riboflavin pendants, *Polym. Chem.* **2010,** *1* (6), 841-848.

5. (a) E. Peeters, M. P. Christiaans, R. A. Janssen, H. F. Schoo, H. P. Dekkers, E. Meijer, Circularly polarized electroluminescence from a polymer light-emitting diode, *J. Am. Chem. Soc.* **1997,** *119* (41), 9909-9910; (b) S. Meskers, E. Peeters, B. Langeveld-Voss, R. Janssen, Circular Polarization of the Fluorescence from Films of Poly (p-phenylene vinylene) and Polythiophene with Chiral Side Chains, *Adv. Matter.* **2000,** *12* (8), 589-594; (c) M. Oda, H. G. Nothofer, G. Lieser, U. Scherf, S. Meskers, D. Neher, Circularly Polarized Electroluminescence from Liquid-Crystalline Chiral Polyfluorenes, *Adv. Matter.* **2000,** *12* (5), 362-365; (d) Y. Nakano, M. Fujiki, Circularly Polarized Light Enhancement by Helical Polysilane Aggregates Suspension in Organic Optofluids, *Macromolecules* **2011,** *44* (19), 7511-7519; (e) K. Watanabe, T. Sakamoto, M. Taguchi, M. Fujiki, T. Nakano, A chiral π-stacked vinyl polymer emitting white circularly polarized light, *Chem. Commun.* **2011,** *47* (39), 10996-10998; (f) B. A. San Jose, J. Yan, K. Akagi, Dynamic switching of the circularly polarized luminescence of disubstituted polyacetylene by selective transmission through a thermotropic chiral nematic liquid crystal, *Angew. Chem. Int. Ed.* **2014,** *126* (40), 10817-10820.

6. (a) C. S. Hanes, THE ACTION OF AMYLASES IN RELATION TO THE STRUCTURE OF STARCH AND ITS METABOLISM IN THE PLANT. PARTS IV-VII, *New Phytologist* **1937,** *36* (3), 189-239; (b) K. Freudenberg, E. Schaaf, G. Dumpert, T. Ploetz, Neue Ansichten über die Stärke, *Naturwissenschaften* **1939,** *27* (51), 850-853.

7. L. Pauling, R. B. Corey, Configurations of Polypeptide Chains With Favored Orientations Around Single Bonds: Two New Pleated Sheets, *Proc. Natl Acad. Sci. USA* **1951,** *37* (11), 729-740.

8. J. D. Watson, F. H. C. Crick, Molecular Structure of Nucleic Acids: A Structure for Deoxyribose Nucleic Acid, *Nature* **1953,** *171* (4356), 737-738.

9. G. Natta, P. Pino, P. Corradini, F. Danusso, E. Mantica, G. Mazzanti, G. Moraglio, CRYSTALLINE HIGH POLYMERS OF α-OLEFINS, *J. Am. Chem. Soc.* **1955,** *77* (6), 1708-1710.

10. P. Pino, G. P. Lorenzi, OPTICALLY ACTIVE VINYL POLYMERS. II. THE OPTICAL ACTIVITY OF ISOTACTIC AND BLOCK POLYMERS OF OPTICALLY ACTIVE α-OLEFINS IN DILUTE HYDROCARBON SOLUTION, *J. Am. Chem. Soc.* **1960,** *82* (17), 4745-4747.

11. Y. Okamoto, K. Suzuki, K. Ohta, K. Hatada, H. Yuki, Optically active poly (triphenylmethyl methacrylate) with one-handed helical conformation, *J. Am. Chem. Soc.* **1979,** *101* (16), 4763-4765.

12. (a) M. M. Green, C. Andreola, B. Munoz, M. P. Reidy, K. Zero, Macromolecular stereochemistry: a cooperative deuterium isotope effect leading to a large optical rotation, *J. Am. Chem. Soc.* **1988,** *110* (12), 4063-4065; (b) Y. Okamoto, M. Matsuda, T. Nakano, E. Yashima, Asymmetric polymerization of aromatic isocyanates with optically active anionic initiators, *J. Polym. Sci., Part A: Polym. Chem.* **1994,** *32* (2), 309-315.

13. P. C. J. Kamer, R. J. M. Nolte, W. Drenth, Screw sense selective polymerization of achiral isocyanides catalyzed by optically active nickel(II) complexes, *J. Am. Chem. Soc.* **1988,** *110* (20), 6818-6825.

14. K. Ute, K. Hirose, H. Kashimoto, K. Hatada, O. Vogl, Haloaldehyde polymers. 51. Helix-sense reversal of isotactic chloral oligomers in solution, *J. Am. Chem. Soc.* **1991,** *113* (16), 6305-6306.

15. Y. Okamoto, K. Suzuki, K. Ohta, K. Hatada, H. Yuki, Optically active poly(triphenylmethyl methacrylate) with one-handed helical conformation, *J. Am. Chem. Soc.* **1979,** *101* (16), 4763-4765.

16. M. Fujiki, Optically Active Polysilane Homopolymer: Spectroscopic Evidence of Double-Screw-Sense Helical Segmentation and Reconstruction of a Single-Screw-Sense Helix by the "Cut-and-Paste" Technique, *J. Am. Chem. Soc.* **1994,** *116* (26), 11976-11981.

17. (a) E. Yashima, S. Huang, T. Matsushima, Y. Okamoto, Synthesis and Conformational Study of Optically Active Poly(phenylacetylene) Derivatives Bearing a Bulky Substituent, *Macromolecules* **1995,** *28* (12), 4184-4193; (b) E. Yashima, T. Matsushima, Y. Okamoto, Chirality Assignment of Amines and Amino Alcohols Based on Circular Dichroism Induced by Helix Formation of a Stereoregular Poly((4-carboxyphenyl)acetylene) through Acid−Base Complexation, *J. Am. Chem. Soc.* **1997,** *119* (27), 6345-6359; (c) H. Nakako, R. Nomura, M. Tabata, T. Masuda, Synthesis and Structure in Solution of Poly[(−)-menthyl propiolate] as a New Class of Helical Polyacetylene, *Macromolecules* **1999,** *32* (9), 2861-2864; (d) H. Nakako, Y. Mayahara, R. Nomura, M. Tabata, T. Masuda, Effect of Chiral Substituents on the Helical Conformation of Poly(propiolic esters), *Macromolecules* **2000,** *33* (11), 3978-3982.

18. (a) T. Nakano, Y. Okamoto, Synthetic Helical Polymers: Conformation and Function, *Chem. Rev.* **2001,** *101* (12), 4013-4038; (b) M. Oda, H.-G. Nothofer, U. Scherf, V. Šunjic, D. Richter, W. Regenstein, D. Neher, Chiroptical properties of chiral substituted polyfluorenes, *Macromolecules* **2002,** *35* (18), 6792-6798; (c) G. Tian, Y. Lu, Novak, B. M. Helix-Sense Selective Polymerization of Carbodiimides: Building Permanently Optically Active Polymers from Achiral Monomers, *J. Am. Chem. Soc.* **2004,** *126* (13), 4082-4083.

19. (a) W. Kuhn, The physical significance of optical rotatory power,. *Transactions of the Faraday Society* **1930**, *26*, 293-308; (b) W. Kuhn, E. Knopf, The preparation of optically active compounds by the aid of light, *Z Phys Chem* **1930**, *7*, 292-310; (c) W. Kuhn, E. Knopf,

Photochemische erzeugung optisch aktiver stoffe, *Naturwissenschaften* **1930**, *18* (8), 183-183.

20. (a) A. C. Grimsdale, K. Leok Chan, R. E. Martin, P. G. Jokisz, A. B. Holmes, Synthesis of light-emitting conjugated polymers for applications in electroluminescent devices, *Chem. Rev.* 2**009**, *109*, 897-1091; (b) O. Inganas, F. Zhang, M. R. Andersson, Alternating polyfluorenes collect solar light in polymer photovoltaics, *Acc. Chem. Res.* **2009**, *42*, 1731-1739; (c) C. Li, M. Liu, N. G. Pschirer, M. Baumgarten, K. Muellen, Polyphenylene-based materials for organic photovoltaics, *Chem. Rev.* **2010**, *110*, 6817-6855; (d) H. Tsuji, E. Nakamura, Carbon-bridged oligo (phenylene vinylene) s: a de novo designed, flat, rigid, and stable π-conjugated system, *Acc. Chem. Res.* **2019**, *52*, 2939-2949.

21. (a) H. Gilch, W. Wheelwright, Polymerization of α-halogenated π-xylenes with base, *Journal of Polymer Science Part A-1: Polymer Chemistry* **1966**, *4*, 1337-1349; (b) N. Yamamoto, R. Ito, Y. Geerts, K. Nomura, Synthesis of All-Trans High Molecular Weight Poly(N- alkylcarbazole-2,7-vinylene)s and Poly(9,9-dialkylfluorene-2,7-vinylene)s by Acyclic Diene Metathesis (ADMET) Polymerization Using Ruthenium −Carbene Complex Catalysts, *Macromolecules* **2009**, *42*, 5104-5111; (c) T. Miyashita, M. Kunisawa, S. Sueki, K. Nomura, Synthesis of Poly (arylene vinylene)s with Different End Groups by Combining Acyclic Diene Metathesis Polymerization with Wittig-type Couplings, *Angew. Chem. Int. Ed.* **2017**, *56*, 5288-5293.

22. (a) T. Yamada, K. Nomura, M. Fujiki, Noticeable Chiral Center Dependence of Signs and Magnitudes in Circular Dichroism (CD) and Circularly Polarized Luminescence (CPL) Spectra of all-trans-Poly(9,9-dialkylfluorene-2,7-vinylene)s Bearing Chiral Alkyl Side Chains in Solution, Aggregates, and Thin Films, *Macromolecules* **2018**, *51*, 2377-2387; (b) S. Yorsaeng, Y. Kato, K. Tsutsumi, A. Inagaki, B. Kitiyanan, M. Fujiki, K. Nomura, Synthesis of Well-Defined Oligo (2, 5-dialkoxy-1, 4-phenylene vinylene) s with Chiral End Groups: Unique Helical Aggregations Induced by the Chiral Chain Ends, *Eur. J. Chem.* **2015**, *21*, 16764-16768; (c) A. Satrijo, T. M. Swager, Facile control of chiral packing in poly (p-phenylenevinylene) spin-cast films, *Macromolecules* **2005**, *38*, 4054-4057; (d) E. Peeters, M. P. T. Christiaans, R. A. J. Janssen, H. F. M. Schoo, H. P. J. M. Dekkers, E. W. Meijer, Circularly polarized electroluminescence from a polymer light-emitting diode, *J. Am. Chem. Soc.* **1997**, *119*, 9909-9910; (e) A. Satrijo, S. C. Meskers, T. M. Swager, Probing a conjugated polymer's transfer of organization-dependent properties from solutions to films, *J. Am. Chem. Soc.* **2006**, *128*, 9030-9031.

23. (a) L. Jing, B. Zhishan, “AB2 + AB” Approach to Hyperbranched Polymers Used as Polymer Blue Light Emitting Materials, *Macromolecules* **2004**, *37*, 2013-2015; (b) L.-R. Tsai, Y. Chen, Hyperbranched and thermally cross-linkable oligomer from a new 2, 5, 7-tri-functional fluorene monomer, *J. Polym. Sci., Part A: Polym. Chem.* **2007**, *46*, 70-84; (c) L.-R. Tsai, Y.

Chen, Hyperbranched poly (fluorenevinylene) s obtained from self-polymerization of 2, 4, 7-tris (bromomethyl)-9, 9-dihexylfluorene, *Macromolecules* **2008**, *41*, 5098-5106; (d) J.-M. Yu, Y. Chen, Multifunctional hyperbranched oligo (fluorene vinylene) containing pendant crown ether: synthesis, chemosensory, and electroluminescent properties, *Macromolecules* **2009**, *42*, 8052-8061; (e) J.-M. Yu, Y. Chen, Thermally cross-linkable hyperbranched polymers containing triphenylamine moieties: Synthesis, curing and application in light-emitting diodes, *Polymer* **2010**, *51*, 4484-4492; (f) J.-M. Yu, T. Sakamoto, K. Watanabe, S. Furumi, N. Tamaoki, Y. Chen, T. Nakano, Synthesis and efficient circularly polarized light emission of an optically active hyperbranched poly (fluorenevinylene) derivative, *Chem. Commun.* **2011**, *47*, 3799-3801.

Chapter 2. Non-uniform self-folding of linear polyfluorenevinylenes

2.1 Introduction

Macromolecules having a controlled conformation such as single-handed helix are known to be useful sources of optically active polymeric materials.[1-4] Macromolecular helix can be divided into the two major classes, i.e., stable helix and dynamic helix.[1-2] Stable helices can be made mainly by helix-sense selective polymerization (asymmetric helix-chirogenic polymerization) where single-handedness arises from chiral ligands or chiral monomeric units.[3-4] As for dynamic helices, single-handedness may arise through interactions with external molecules or by chiral moieties embedded in the chain.[1,2] Also, chirality of dynamic helices can be amplified by cooperation between helical units in a chain[5] or inter-chain interactions forming aggregates.[6-10] With such a background, we herein report the synthesis and properties of poly(fluorene-2,7-diylethene-1,2-diyl) (poly(fluorenevinylene)) derivatives composed of chiral monomeric units with neomenthyl group derived from *L*-menthol ((1R,2S,5R)-2-isopropyl-5-methylcyclohexanol) as the chirality source and achiral units. The polymer composed only of the chiral units exhibited remarkable chirality amplification through self-folding. Self-folding is most well recognized for peptide chains which leads to specific conformations such as α-helix and β-sheet which are fundamental stereo structures in higher order structures of proteins.[7-9] In contrast, only limited examples of self-folding are known for artificial polymers.[10]

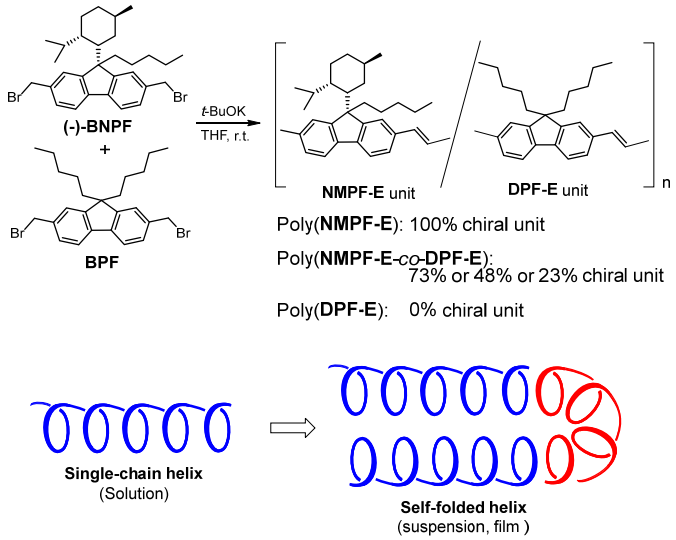

Scheme 2-1. Synthesis and self-folding of chiral poly(fluorene-2,7- diylethene-1,2-diyl) derivatives.

Homopolymerization and copolymerization of 2,7-bis(dibromomethyl)-9-neomenthyl-9-pentylflourene ((-)-BNPF) and 2,7-bis(dibromomethyl)-9,9-dipentylflourene (BPF) through the Gilch reaction[11,12] using *t*-BuOK in tetrahydrofuran (THF) at 24 °C led to homopolymers and copolymers composed of chiral 9-neomenthyl-9-pentylfluorene-2,7-diylethene-1,2-diyl (NMPF-E) units and/or achiral 9,9-dipenthylfluorene-2,7-diylethene- 1,2-diyl (DPF-E) units at different ratios: poly(9-neomenthyl-9- pentylfluorene-2,7-diylethene-1,2-diyl) [poly(NMPF-E)] (100% chiral units), poly[(9-neomenthyl-9-pentyl-2,7-diyl-ethene-1,2-diyl-co-9-dipentyl fluorene-2,7-diyl-ethene-1,2-diyl] [poly(NMPF-E-co-DPF-E)] (73% or 48% or 23% chiral units) and poly(9,9-dipentylfluorene-2,7-diylethene- 1,2-diyl) [poly(DPF-E)] (0% chiral units) (Scheme 2-1). The conditions and results of polymerization as well as synthetic details are reported in Table 2-1. The crude polymerization products had broad dispersity and were separated into higher-molar-mass (Mn 21.9-25.7 x 10^3) and lower-molar-mass (Mn 1.3-1.4 x 10^3) parts by preparative size exclusion chromatography. The ^{1}H NMR and SEC results are shown in Figure 2-1, 2-2 and 2-3.

The two parts had similar ratios of chiral units. Although the polymers with NMPF-E units may have regularity in relative configuration of chirality centers at the 9-position of fluorene backbone, tacticity is so far not known. Since steric repulsion between side-chain groups may not be significant, the polymers may be considered atactic.

Table 2-1. Synthesis of poly(fluorene-2,7-diylethene-1,2-diyl) derivatives composed of chiral NMPF-E unit and achiral DPF-E unit from chiral (-)-BNPF and achiral BPF by the Gilch reaction inTHF at 24°C for 12 h[a]

Run	(-)-**BNPF** (M)	**BPF** (M)	Conv.[b] (%)	Higher-molar-mass part[c]				Lower-molar-mass part[c]			
				Yield (%)	M_n[d]	M_w/M_n[d]	Unit ratio in polymer[e] [NMPF-E]/[DPF-E]	Yield (%)	M_n[d]	M_w/M_n[d]	Unit ratio in polymer; [NMPF-E]/[DPF-E]
1	0	0.08	99	14	25100	1.75	0/100	58	1300	1.08	0/100
2	0.02	0.06	99	13	24900	2.19	23/77	54	1300	1.09	27/73
3	0.04	0.04	99	14	25700	2.19	48/52	67	1400	1.11	46/54
4	0.06	0.02	99	17	23400	1.56	73/27	77	1400	1.26	72/28
5	0.08	0	99	13	21900	1.55	100/0	60	1400	1.37	100/0

[a][*t*-BuOK] = 0.33 M; (-)-BNPF 21.3 mg (0.038 mmol) (run 2), 24.9 mg (0.084 mmol) (run 3), 89.2 mg (0.160 mmol) (run 4), 84.3 mg (0.151 mmol) (run 5); BPF 85.3 mg (0.174 mmol) (run 1), BPF 57.3 mg (0.112 mmol) (run 2), BPF 43.7 mg (0.089 mmol) (run 3), BPF 26.2 mg (0.053 mmol) (run 4). [b]Determined by ^{1}H NMR analysis of crude products. [c]Purified by reprecipitation in MeOH and further separted by preparative SEC into higher- and lower-molar-mass parts. [d]Determined by SEC (eluent THF) using standard polystyrene samples. [e]Determined by ^{1}H NMR analysis.

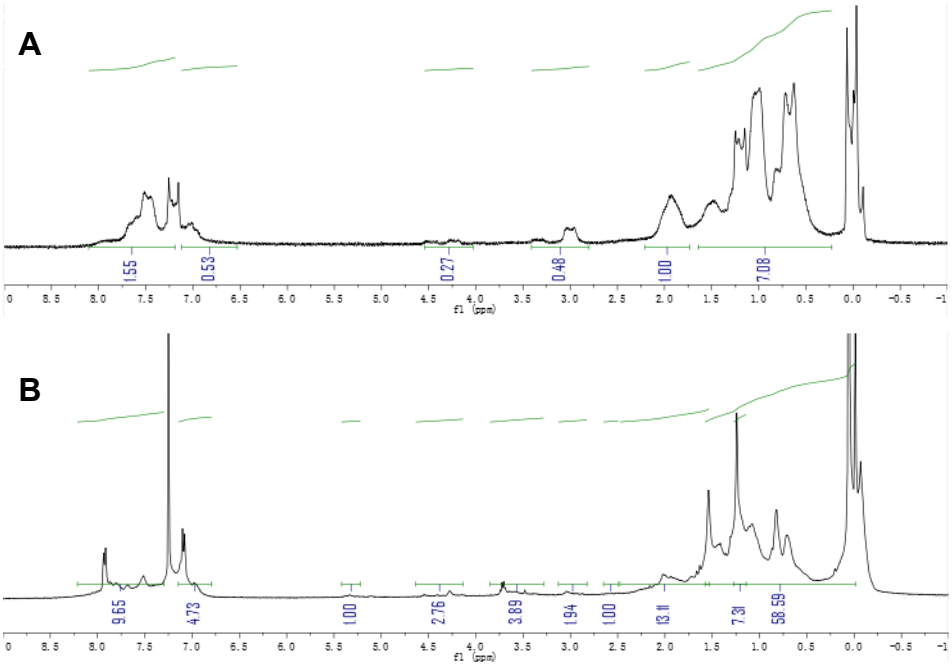

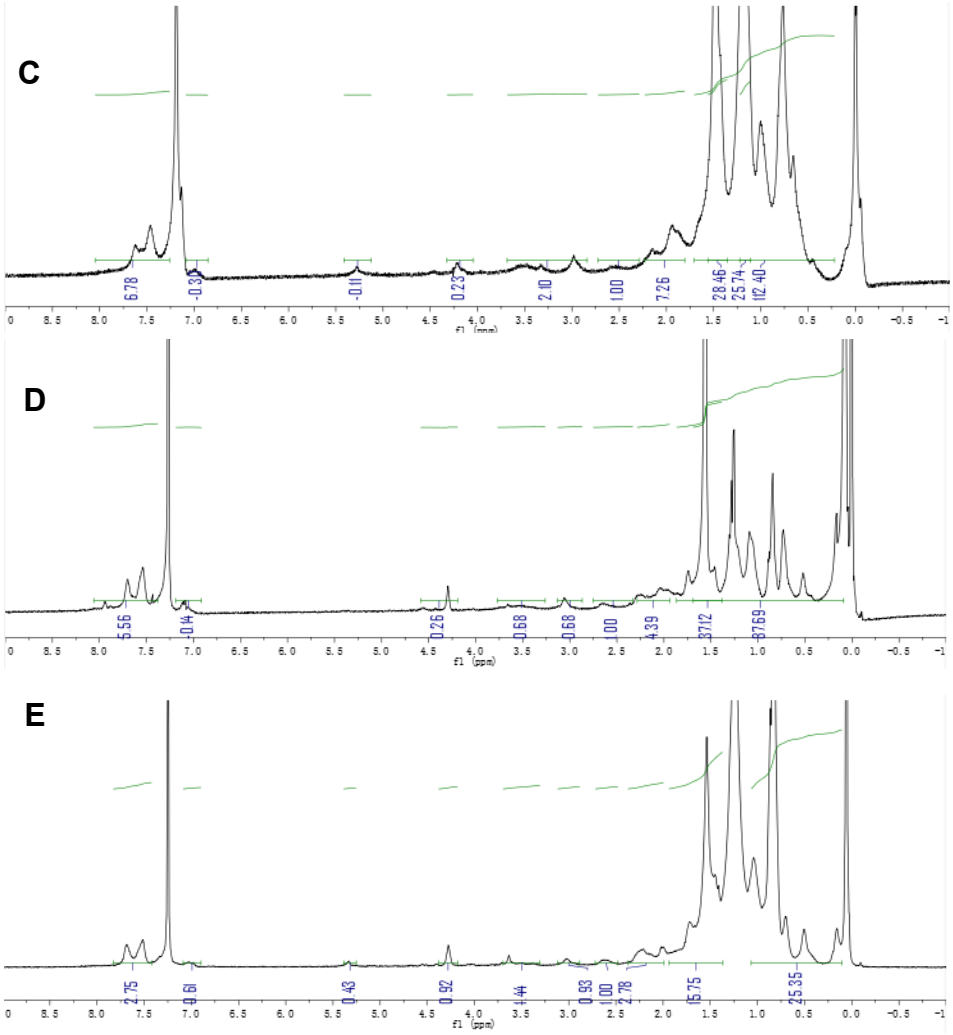

Figure 2-1. ^{1}H NMR spectra of higher-molar-mass products from run 1 (A), run 2 (B), run 3 (C), run 4 (D), run 5 (E) in Table 2-1 [400/600 MHz, $CDCl_3$, r.t.].

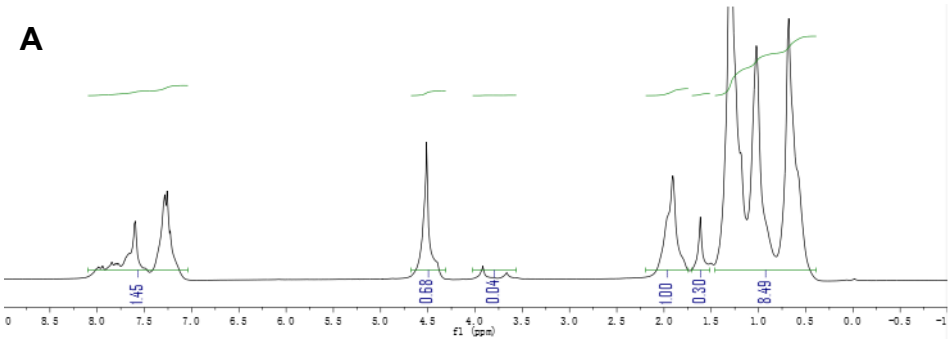

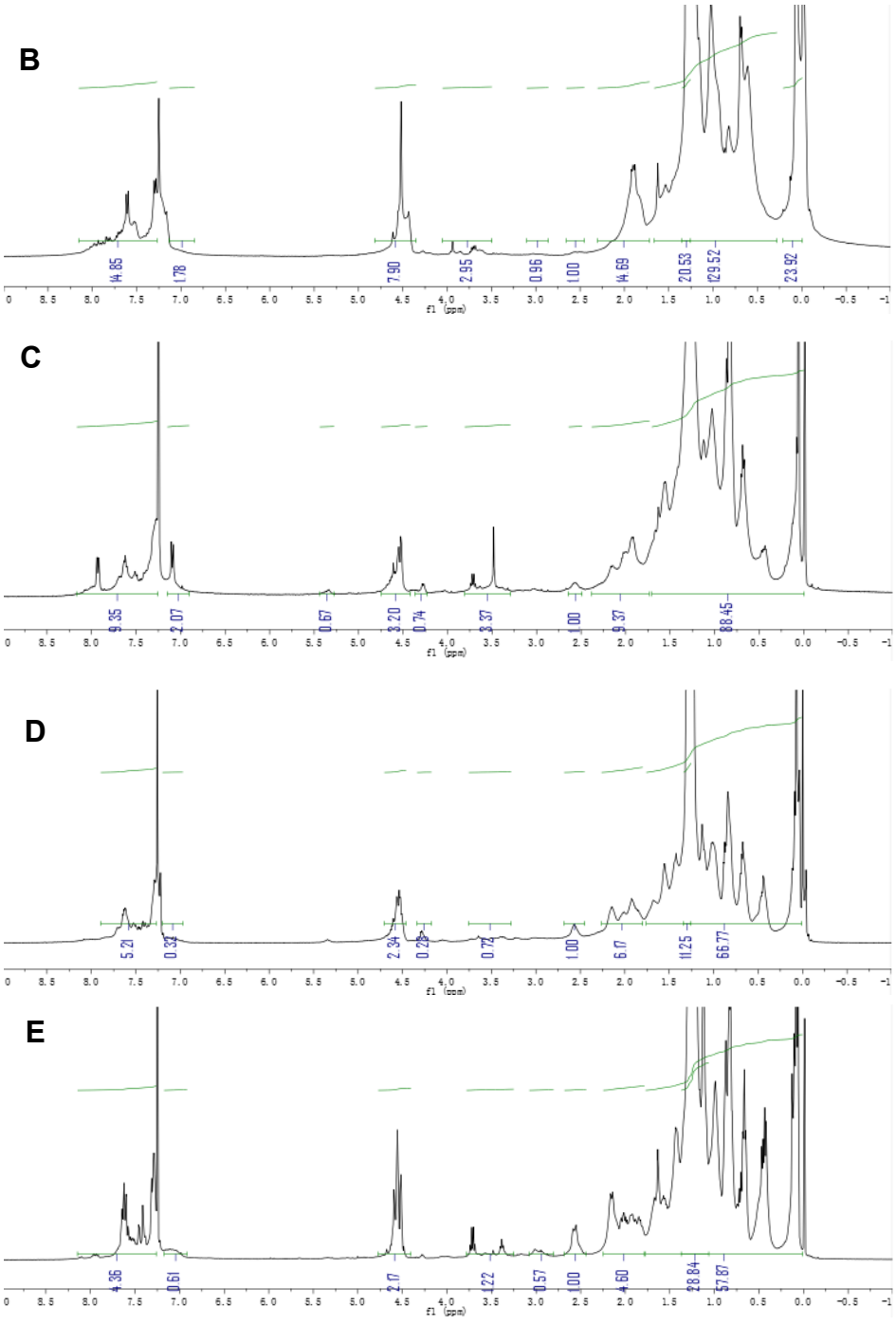

Figure 2-2. ^{1}H NMR spectra of lower-molar-mass products from run 1 (A), run 2 (B), run 3 (C), run 4 (D),and run 5 (E) in Table 2-1 [400/600 MHz, $CDCl_3$, r.t.].

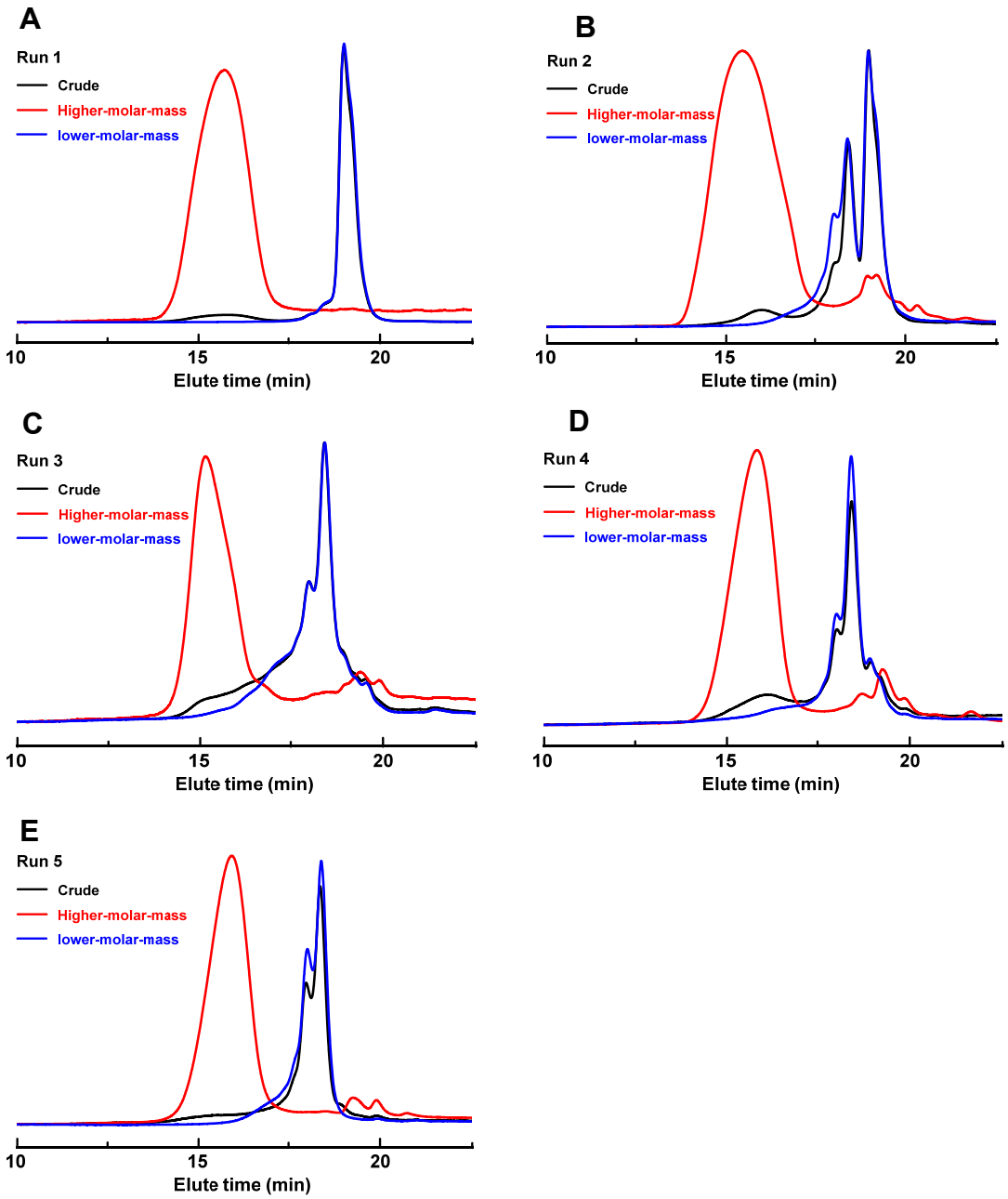

Figure 2-3. SEC profiles of crude mixtures, higher-molar-mass products, and lower-molar-mass products from run 1 (A), run 2 (B), run 3 (C), run 4 (D), and run 5 (E) in Table 2-1.

2.2 Results and Discussions

2.2.1 Chiroptical properties of polymers

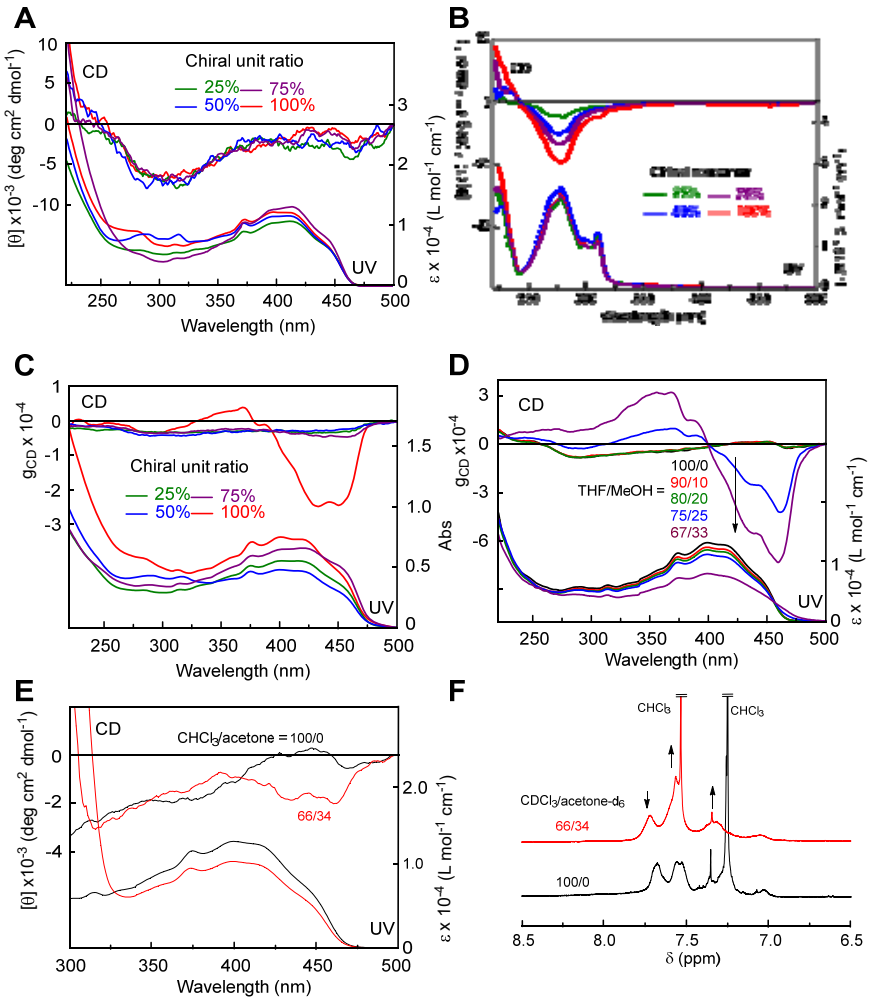

Figure 2-4. CD-UV spectra of higher-molar-mass (A) and lower-molar-mass (B) polymers at different ratios of chiral units in THF solution, g_{CD}-UV spectra of higher-molar-mass polymers in film (C) and of higher-molar-mass poly(NMPFE) in suspension in THF-MeOH mixtures (D), CD-UV spectra of higher-molarmass poly(NMPF-E) in $CHCl_3$ and in $CHCl_3$-acetone (66/34) solutions (E), and 1H NMR spectra higher-molar-mass poly(NMPF-E) in $CDCl_3$ and in $CDCl_3$-acetone-d_6 (66/34) solution (F). [conc. 3 x 10^{-3} M (per residue), cell path 1-mm in A, B, C, and E].

Chirality of the polymers was examined first by circular dichroism (CD) spectra in a THF solution (Figure 2-4 A,B). The higher molar-mass polymers showed very similar

CD spectral shapes in the range of up to 475 nm due to long π-conjugation of fluorene-2,7-diylethene-1,2-diyl units connected in a chain, and very similar intensities regardless of ratios of chiral units (23-100%) (Figure 2-4A). On the other hand, the spectral shapes of the lower molar-mass polymers were similar to that of (-)-9-neomenthyl-9-pentylfluorene as a model of monomeric unit lacking the bands due to the long π-conjugation (Figure 2-5), and the spectral intensity was almost proportional to the ratio of chiral units (23-73%) (Figure 2-4B). These results suggest that the higher-molar mass polymers have a single-handed helical conformation of the conjugated chain while the chiroptical properties of the lower molar-mass polymers are based mainly of 9-neomenthyl-9-pentylfluorene monomeric units and do not have any specific conformation.

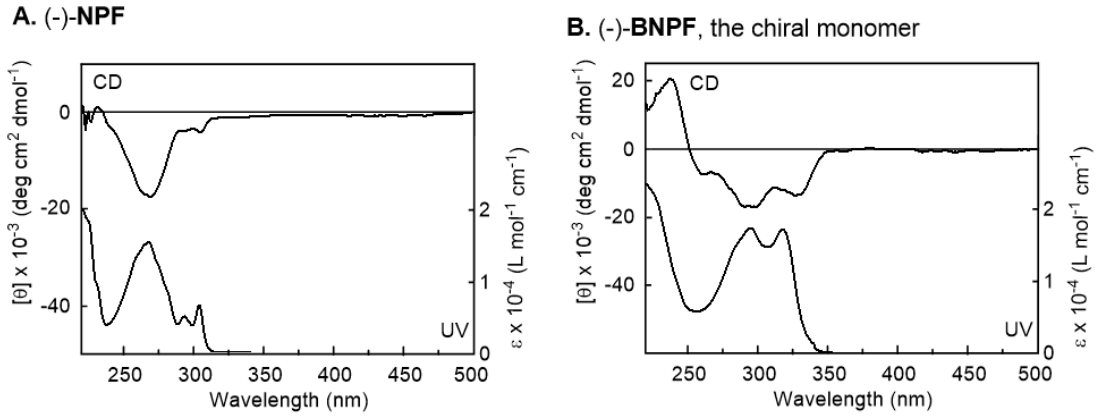

Figure 2-5. CD-UV spectra of (-)-NPF (A) and (-)-BNPF (B) in THF. [concentration 3.86 x 10^{-4} (A), 2.54 x 10^{-4} M (B); cell path 1 mm]

The higher-molar-mass poly(NMPF-E) presented remarkable chirality amplification for CD intensity in film and in suspension (Figure 2-4 C,D). The films were prepared on a quartz glass plate by casting from a THF solution. The poly(NMPF-E) exhibited a CD spectrum having far higher intensities in film than that in solution with monotonous spectra (Figure 2-4C). The film CD has a characteristic splitting pattern composed of intense negative signals in the lowest-energy region (around 450 nm) with a weaker

positive signal. Similar changes from solution to the solid state were observed for the other polymers at lower ratios of chiral units while g_{CD} values in film were smaller than that of poly(NMPF-E) (Figure 2-6). In addition, g_{CD} in film was found to be greater when a solution at higher concentration was used to cast a film (Figure 2-7).

A. Poly(**NMPF-E**-*co*-**DPF-E**) with 73% chiral unit

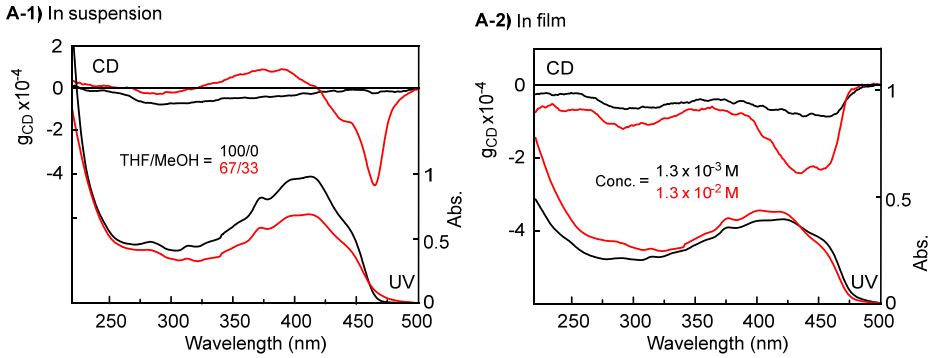

B. Poly(**NMPF-E**-*co*-**DPF-E**) with 48% chiral unit

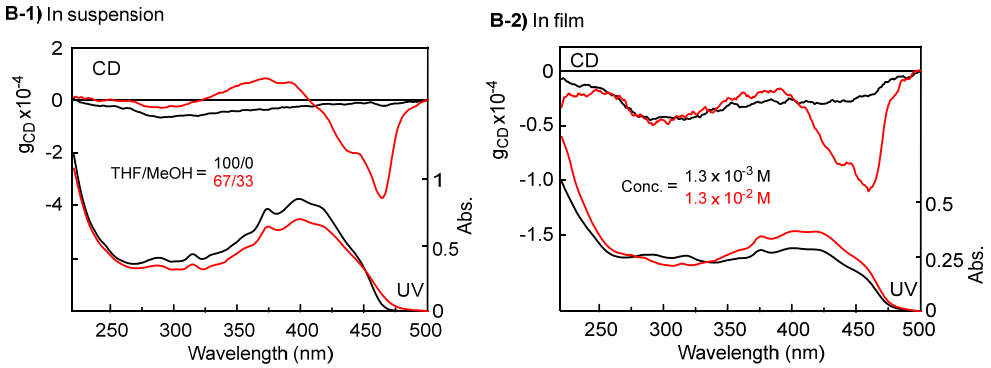

C. Poly(**NMPF-E**-*co*-**DPF-E**) with 23% chiral unit

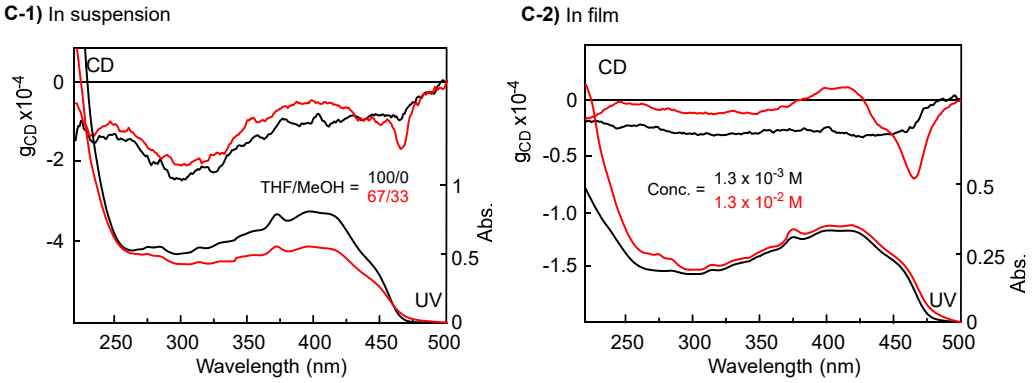

Figure 2-6. CD-UV spectra of higher-molar-mass poly(**NMPF-E**-*co*-**DPF-E**)'s with 73% (A), 48% (B), and 23% (C) chiral units in suspension (left: A-1, B-1, C-1) and in film (right: A-2,

B-2, C-2). The suspension spectra were taken in THF/MeOH (67/33, v/v) and are shown in comparison with those in THF solution (left: A-1, B-1, C-1), and the films were prepared from THF solutions at different concentrations, *i.e.*, 1.3 x 10^{-3} M and 1.3 x 10^{-2} M.

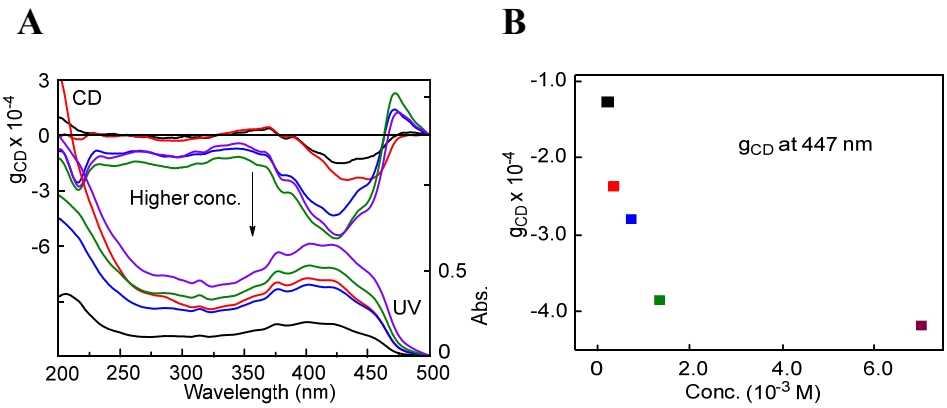

Figure 2-7. CD-UV spectra of films of poly(**NMPF-E**) prepared from solutions at different concentrations (concentration range: 1.3-70 x 10^{-3} M (per residue)) (A) and g_{CD}-vs. -concentration plots (B)

It was confirmed that the orientation (angle) of the film and the surface of the film facing the incident light source, front face or back face, had virtually no significant effects on CD spectral shape of the poly(NMPF-E) film, supporting that the CD spectra are based on macromolecular chirality but NOT on solid-state anisotropies (Figure 2-8).

I. CD spectra of different angles

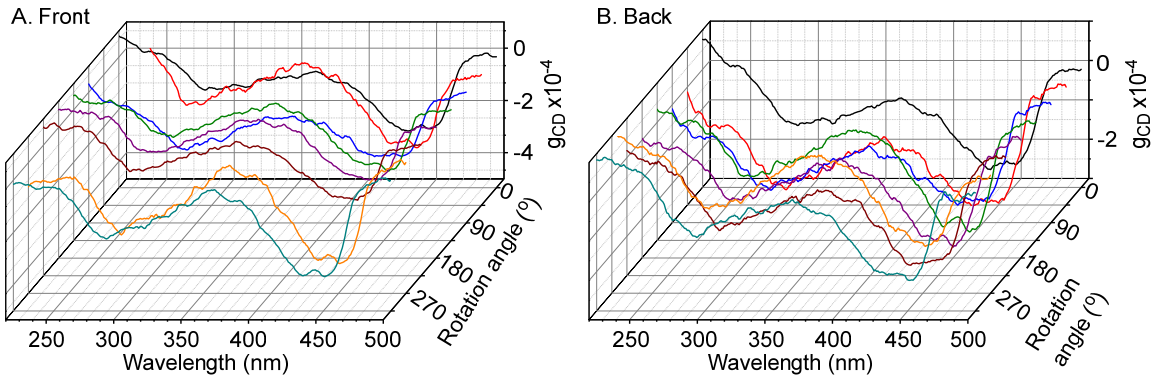

II. LD spectra of different angles

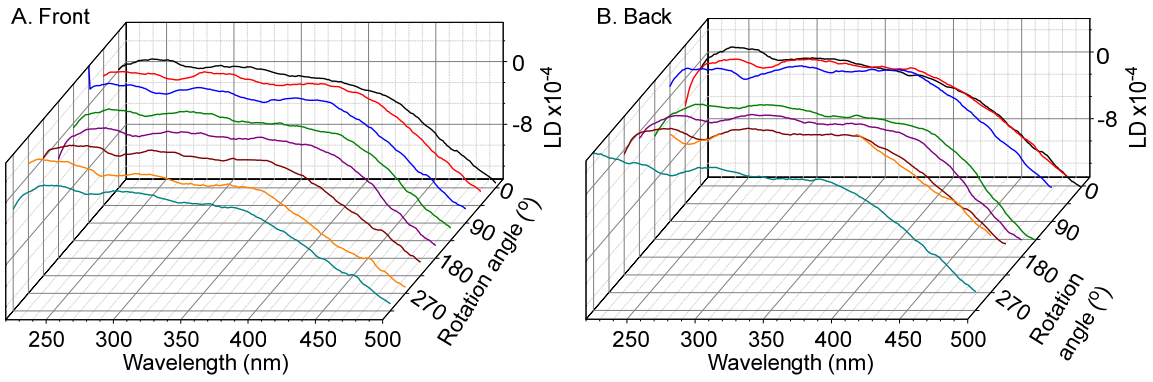

III. UV spectra of different angles

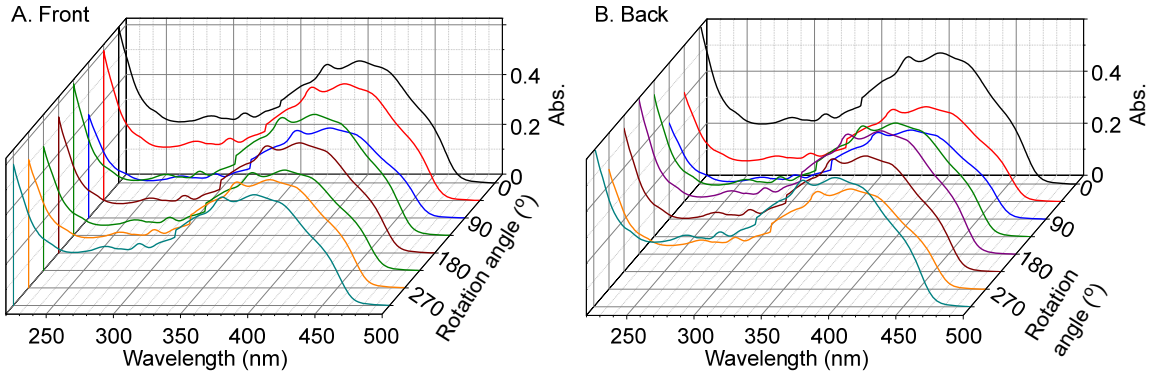

Figure 2-8. CD (I), LD (II) and UV (III) spectra of poly(NMPF-E) film measured at different angles (orientations) of the film with the incident light going through from the front face (A) and from the back face (B). The film face was set orthogonal to the incident light beam.

Chirality amplification of the poly(NMPF-E) was observed also in slightly opaque suspensions in THF-MeOH mixtures where MeOH was gradually added to a THF solution at different ratios (Figure 2-4D). With an increase in the ratio of MeOH, the CD spectrum changed from the monotonous pattern to the splitting pattern with intense negative signals in the lowest-energy region, and the overall intensity largely increased. The maximum absolute g_{CD} value was even greater in suspension than in film (max. g_{CD} -2.5 x 10^{-4} at 425 nm in film, -7.0 x 10^{-3} in THF-MeOH (67/33 (v/v))).

In a suspension, the formation of large aggregates was confirmed by dynamic light scattering (DLS) (Figure 2-9). This suggests that inter-chain interactions in film and in suspension are responsible for the chirality amplification.

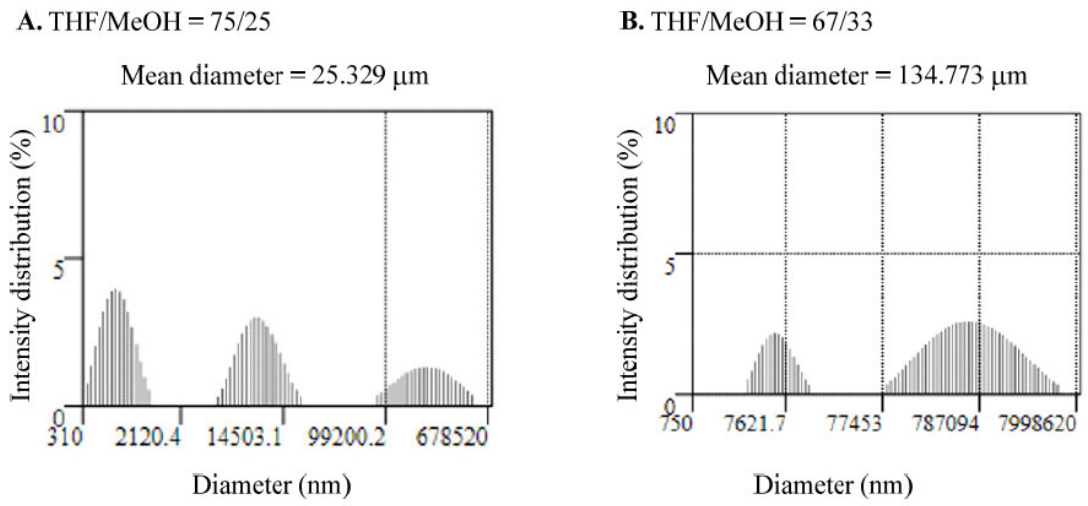

Figure 2-9. DLS profiles of poly(NMPF-E) in THF-MeOH suspensions at THF/MeOH = 75/25 (A) and 67/33 (B) at 3.0 x 10^{-3} M (per residue). [5-mm cell, ambient temperature]

Further, CD spectral changes were observed also in $CHCl_3$ solution on the addition of acetone which alone does not dissolve the polymer (Figure 2-4E). Though the changes in CD intensity were not as remarkable as those in Figure 2-4 C,D, clear negative signals in the lowest-energy region emerged on the addition of acetone. Moreover, 1H NMR spectral shape in the aromatic region in $CDCl_3$ solution changed on the addition of acetone-d_6 (Figure 2-4F), which suggests a role of inter-chain interactions in the chirality amplification in solution.

2.2.2 “Non-uniform” self-folding

The mechanism of the chirality amplification was assessed by molecular dynamics (MD) and steered MD simulations of an ensemble of ten chains on the top of amorphous silicon dioxide slab as a model of a film sample cast on glass plate (Figure 2-9 A). 55-mer models of atactic poly(NMPF-E) corresponding to Mn 22 x 10^3 were used. The MD simulated chain models can be identified from segments of stretched and self-folded chains. In the self-folded segments, stretched segments are connected through “turn” moieties as represented by the 13-monomeric-unit segment shown in Figure 2-9B which corresponds to the part marked by a circle in Figure 2-4A. The “turn”

moieties appear to be formed by two neighboring units.

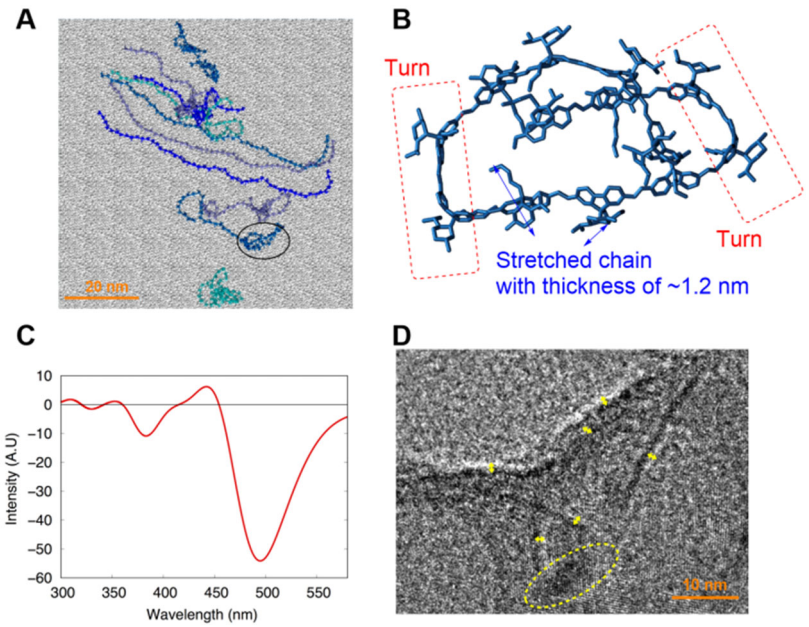

Figure 2-9. Representation of ten chains of 55-mer models of poly(NMPF-E) (100% chiral units) on amorphous silicon dioxide slab obtained through MD simulations (A), a self-folded 13-monomeric-unit segment corresponding to the circled part in A (B), theoretical CD spectrum of the self-folded model in B (C), and TEM image of poly(NMPF-E) of Mn 21.9 x 10^3 in which the yellow arrows show single-strand thickness of 1.2 nm and the yellow circle marks a folded part (D).

Figure 2-9C shows the theoretical CD spectrum calculated for the self-folded 13-monomeric-unit segment. The spectrum is characterized by a split with an intense negative signal in the lowest-energy region accompanied with a smaller, positive signal showing good agreement with the experimental spectra in film, in suspension, and in $CHCl_3$-acetone solution. These results suggest that self-folding of the chains occurred in film, in suspension, and in $CHCl_3$-acetone solution.

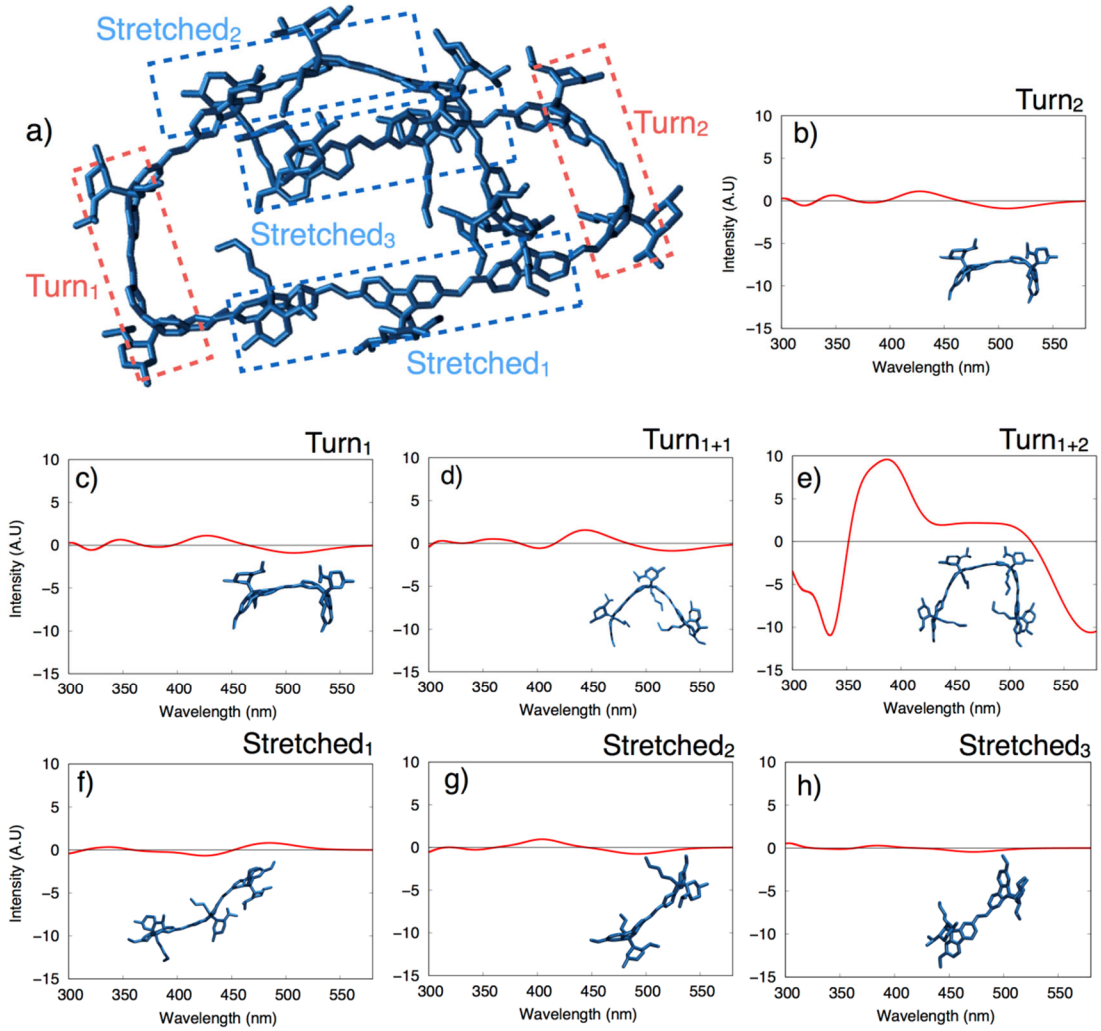

Figure 2-10. The 13-monomeric-unit segment in Figure 2B (main text) further divided in turn and stretched-segments (a), and ECD spectra computed for Turn2 segment (b), Turn1 segment (c), Turn1+1 segment (d), Turn1+2 segment (e), Stretched1 segment (f), Stretched2 segment (g), and Stretched3 segment (h).

This aspect was further assessed by CD prediction of shorter sections cut out from the self-folded 13-monomeric-unit segment (Figure 2-10). It was found that a 4-monomeric-unit segment with central two units forming a turn caused negative CD signals in the lowest-energy region with much higher intensities compared with 2- and 3-unit segments.

In addition, the TEM image of poly(NMPF-E) exhibited string-like objects with

thicknesses of around 1.2 nm (Figure 2-2D). The thickness of single chain is around 1.2 nm from a molecular model (Figure 2-11), suggesting that the string-like objects may represent single, stretched chains. Also, the part marked by the circle may correspond to a self-folded segment. These images are in a sharp contrast to the fact that chiral polymers often form bundles of chains which result in enhanced CD intensity through chirality amplification.[6-10,11-16]

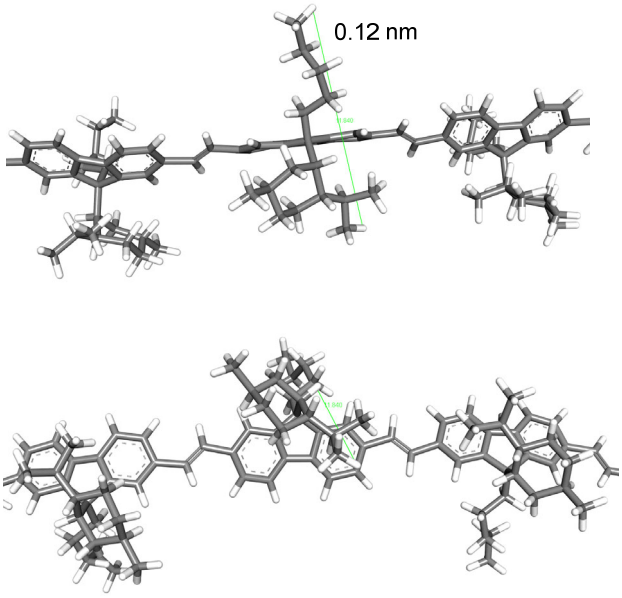

Figure 2-11. Chain models of poly(NMPF-E) with the thickness of single chain.

It should be noted that the higher-molar-mass poly(NMPF-E-co- DPF-E)]s (73%, 48%, and 23% chiral units) also showed remarkably amplified CD intensity in film and in THF-MeOH (67/33 (v/v)) where g_{CD} values after amplification were higher for a polymer with higher ratio of the chiral units (Figure 2-6). On the other hand, the lower-molar-mass poly(NMPF-E) and poly(NMPF-E-co-DPF-E)]s did not show any chirality amplification. These results suggest that intra-chain interactions between chiral and achiral monomeric units may also induce self-folding and that efficient self-folding needs a long enough chain.

Furthermore, chirality amplification through the formation of self-folded structure was found for poly(DPF-E) through chirality transfer from poly(NMPF-E) (Figure

2-12). Films prepared by casting THF solutions containing the two polymers at different ratios showed intense CD spectra with strong negative signals at around 450 nm which were similar to those of poly(NMPF-E) (100% chiral units) observed on chirality amplification (Figure 2-12A). The observed absolute CD intensity at 430 nm was much higher than expected from proportionality with the ratio between the two polymers and was close to that of pure poly(NMPF-E) film even at the ratios of poly(NMPF-E) 23% and 48%. Based on these results, achiral poly(DPF-E) is considered to undergo self-folding through chirality transfer effects from nearby self-folded poly(NMPF-E) chains.

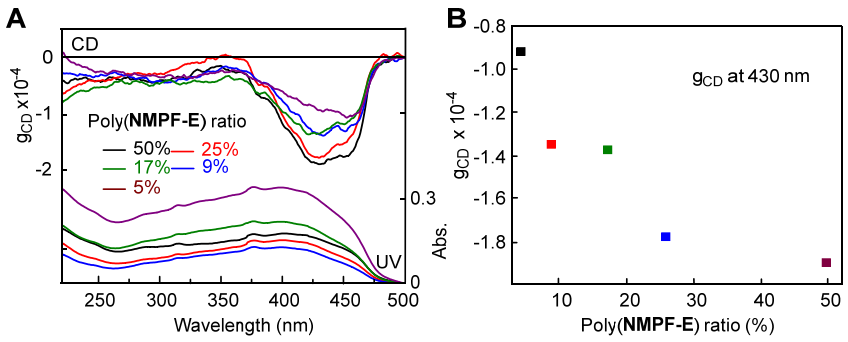

Figure 2-12. g_{CD}-UV spectra of films containing higher-molar-mass poly(**NMPF-E**) (100% chiral units) and poly(**DPF-E**) (0% chiral units) at different ratios (A) and a plot of g_{CD}-vs.-poly(**NMPF-E**) ratio.

Amplified chirality through self-folding of poly(NMPF-E) appeared to be maintained in excited states through circularly polarized light (CPL) emission properties (Figure 2-13). A film and a suspension in THF-MeOH (2/1 (v/v)) exhibited clear CPL emission in the range of 450-550 nm, and glum value was about -5 x 10^{-4} in film and -1.8 x 10^{-3} at 470 nm in suspension, which is in line with the fact that absolute g_{CD} was greater in suspension. On the other hand, THF solution of the polymer did not indicate any CPL emission within the limitation of sensitivity of the experimental setup. This indicates that the self-folded structure is indispensable in attaining efficient CPL emission. This observation was further confirmed through ab-initio molecular dynamics simulations in

the first singlet excited state (S1) within the TD-DFT framework at the wB97xD/6-31G level of theory, thereby calculating the CPL, PL and glum spectra from the ab-initio dynamics trajectories (Figure 2-14). The theoretical spectra clearly indicate an intense negative CPL signals between 440 and 480 nm, closely matching the signal experimental recorded.

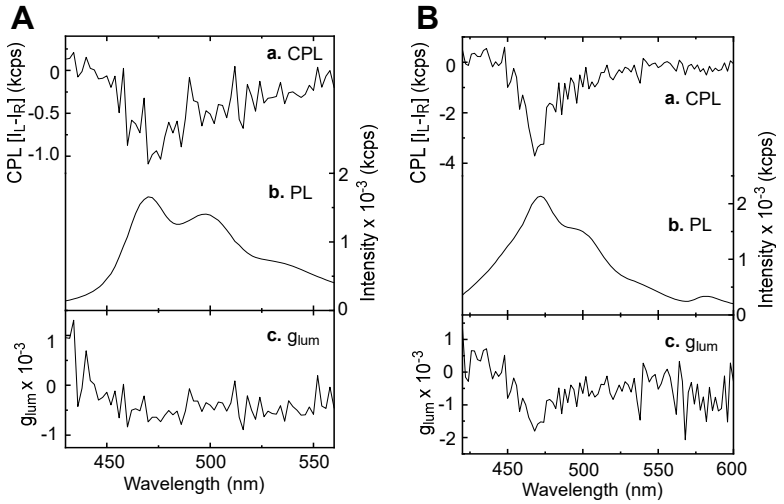

Figure 2-13. CPL spectra (a), total emission (PL) spectra (b), and g_{lum} spectra (c) of higher-molar-mass poly(**NMPF-E**) in film (A) and in suspension in THF-MeOH (2/1 (v/v)) (B). [1.0 x 10^{-4} M (B), 10-mm cell (B), λ_{ex} 260 nm].

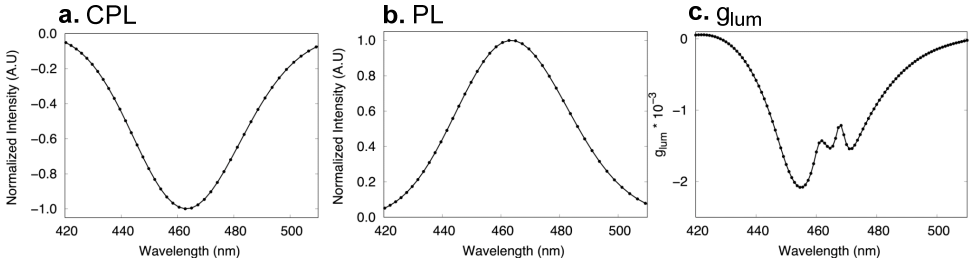

Figure 2-14. Predicted CPL (a), total emission (PL) (b) and g_{lum} spectra (c) at the wB97xD/6-31G level of theory on the self-folded 13-mer polymer section.

2.2.3 Theoretical study of self-folding

The folding process inducing turn formation was further investigated by calculating the rotational barrier around inter-ring bonds for the 55-mer polymer deposited on amorphous silica dioxide with an ensemble of chains. Figure 2-15 reports the

free-energy profiles as a function of dihedral angles around the first (terminal) and the third (internal) inter-ring bonds from a chain end, predicted using the parallel bias metadynamics approach. The free-energy profiles show two sets of minima at 76 and 175 degrees, corresponding to *cis* and *trans* configurations, with inter-ring rotational barrier values approaching 17 kcal/mol which may be too small for explaining the folding in terms only of the single chain energies. The free-energy predictions hence suggest a likelihood of inter-chain interactions in stabilizing the turn formation than rotational dynamics alone.

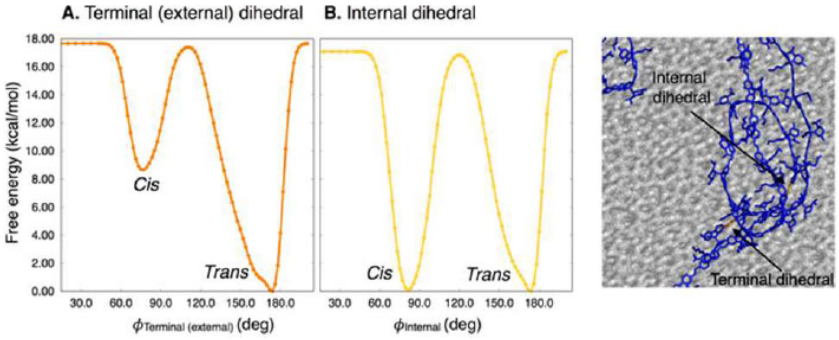

Figure 2-15. Free-energy profiles as a function of the external (A) and internal (B) dihedral angles of the 55-mer poly(NMPF-E) (100% chiral units) deposited in amorphous silicon dioxide slab in an ensemble of ten chains computed by using the parallel bias metadynamics approach. The bonds considered in calculation in A and B are indicated in orange and yellow, respectively, in the structure at the far right.

It is noteworthy that the *cis* and *trans* configurations were predicted degenerate for the internal torsion, presumably due to an increase in conjugation moving along the polymer chain while trans was more stable than cis by 9 kcal/mol for the terminal (external) torsion. These results may be connected with the more pronounced occurance of the "turn" moieties in internal moieties of the polymer and may explain the non-uniform self-folding of the polymer chain.

2.3 Conclusions

In conclusion, the optically active poly(fluorenevinylene) derivative bearing a neomenthyl group derived from *L*-menthol as the chirality source and a pentyl group at the 9-position of the fluorene unit was found to form a self-folded structure in which two neighboring monomeric units form a highly twisted, anisotropic conformation leading to remarkable chirality amplification in film and in suspension. Weaker amplification occurred also in $CHCl_3$-acetone solution. Copolymers composed of the chiral fluorene unit and achiral fluorene unit bearing two pentyl groups at the 9-position of fluorene unit also showed chirality amplification. Self-folding was disclosed to be induced and further stabilized by inter-chain interactions where the bent shape of the chain may be strengthened possibly through alkyl-π-interactions between the opportunely designed side-chain groups and the main chain. Moreover, through chirality transfer from the chiral homopolymer to the achiral homopolymer, self-folding of the latter was induced. Chain folding is known for peptides and peptide mimics for which hydrogen-bonding plays a role in folding.[17-19] Self-folding of completely synthetic chains has been reported for aromatic oligomers and polymers with restricted internal bond rotation represented by those called foldamers showing helical folding through hydrophobic and van der Waals force[20,21] and also for an oligomer composed of donor (D) and acceptor (A) moieties through D-A interactions.[22,23] While most of these examples are characterized by uniform self-folding, the poly(fluorenevinylene) derivatives studied in this work undergo non-uniform self-folding leading to a structure in which the turns connect the single strand, stretched segments and the turn moieties show amplified chiroptical properties. Such self-folding may be regarded as an unprecedented category of conformational transition of synthetic polymers.

2.4 Experimental

Materials.

Fluorene (TCI), (-)-Menthol (TCI), *p*-toluenesulfonyl chloride (tosyl chloride) (Wako), paraformaldehyde (TCI), n-BuLi (2.3 M cyclohexane solution) (TCI), 1-iodopentane (Aldrich), HBr (33 wt%, acetic acid solution) (Wako), t-BuOK (TCI), potassium hydroxide (Kanto), pyridine (Kanto), $CHCl_3$ (Kanto), methanol (Kanto), acetone (Kanto), Dimethylformamide (Wako) and Silica-gel 60 N (neutral) (Kanto) were used as purchased. Tetrahydrofuran (THF) (Wako) was dried with calcium hydride under nitrogen flow.

General instrumentation.

^{1}H NMR spectra in solution were recorded on a JEOL JNM-ECX400 spectrometer (400 MHz for ^{1}H measurement) and a JEOL JNM-ECA600 spectrometer (600 MHz for ^{1}H measurement). SEC measurements were carried out using a chromatographic system consisting of a Hitachi L-7100 chromatographic pump, a Hitachi L-7420 UV detector (254 nm), and a Hitachi L-7490 RI detector equipped with TOSOH TSK gel G3000HHR and G6000HHR columns (30 x 0.72(i.d.) cm) connected in series (eluent THF, flow rate 1.0 mL/min). Preparative SEC analyses were carried out using JAI LC-9201 recycling preparative HPLC with UV/VIS detector S-3740 and column JAIGEL-1H, 2H (eluent $CHCl_3$, flow rate 3.0 mL/min), JAI LC-9201 recycling preparative HPLC with UV/VIS detector UV-50, RI detector RI-50 and column JAIGEL-1H, 2H (eluent $CHCl_3$, flow rate 3.0 mL/min), A Laboace LC-5060 recycling preparative HPLC with UV/VIS detector 4ch800LA and RI detector 700LA equipped with JAIGEL-1RH, 2RH, and 3RH columns connected in series (eluent $CHCl_3$, flow rate 10.0 mL/min). UV-vis absorption spectra were measured at room temperature with a JASCO V-570 spectrophotometers. Steady-state emission spectra were taken on a JASCO FP-8500 fluorescence spectrophotometer. Circular dichroism (CD) spectra were taken with a JASCO-820 spectrometer. The spectra of films were obtained by averaging those recorded at four different film orientations (angles) at an interval of 90^o with the

film face positioned vertically to the incident light beam for measurement. The anisotropy factor (g_{CD}) was calculated according to g_{CD} = ΔAbs/Abs = (ellipticity/32980)/Abs. DLS measurements were performed using a Nicomp 380 ZLS particle sizer. CPL spectra were measured with a JASCO-300 spectrometer and with an assembled apparatus based on a photo elastic modulator and a photomultiplier designed according to the literature[24] with modifications. The emission anisotropy factor (g_{lum}) was calculated according to $g_{lum} = 2(I_L - I_R)/(I_L + I_R)$ where I_L and I_R are the emission intensities of *L*- and *R*-CPL, respectively. TEM images were obtained on a JEM-2100F microscope at 200 kV using a microgrid. XRD profiles were measured using a Rigaku MiniFlex600-C diffractometer.

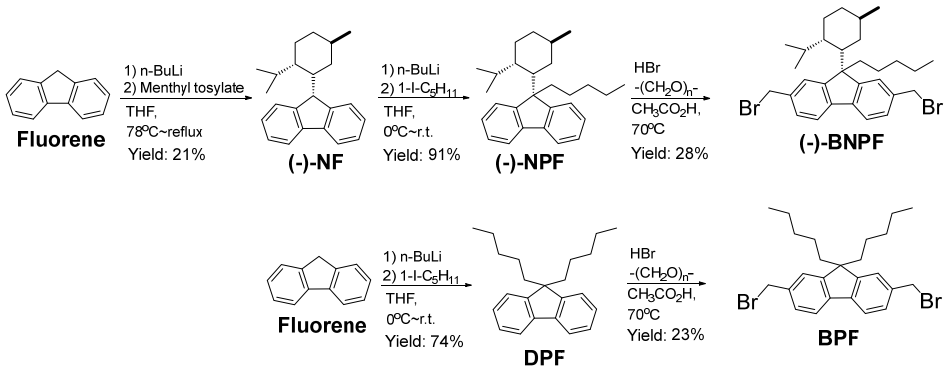

Scheme 2-2. Synthesis of the monomers and the precusors.

The monomers synthesis procedures are illustrated in Scheme 2-2 and the details are demonstrated following.

9,9-Dipentylfluorene (DPF).

Fluorene (11.47 g, 0.069 mol), 1-iodopentane (34.16 g, 0.173 mol), and KOH (46.75 g, 0.835 mol) were mixed with 200 mL of DMF. The system was stirred at r.t. for 36 h, and the mixture was then poured into a large excess of water and extracted with $CHCl_3$. After the organic layer was dried on $MgSO_4$ and the solvent was removed to give the crude material which was purified by silica-gel column chromatography using *n*-hexane as eluent, leading to a colorless oily product. Yield: 86.2 % (18.2 g). ^{1}H NMR (400

MHz, 298 K, $CDCl_3$) δ/ppm: 7.70 (2 H, d, J = 4 Hz), 7.28-7.35 (6 H, m), 1.91-1.99 (4 H, m), 0.97-1.12 (8 H, m), 0.67-0.73 (6 H, m), 0.56-0.66 (4 H, m).

2,7-Bis(bromomethyl)-9,9-dipentylfluorene (BPF).[25,26]

To a mixture of 9,9-dipentylfluorene (1.52 g, 0.005 mol) and paraformaldehyde (4.1 g, 0.005 mol) cooled at 0 ºC was added dropwise 21.5 mL of 33 wt% HBr (40 g, 0.5 mol) in an acetic acid solution. The reaction mixture was stirred at 60 ºC and for 36 h. The mixture was poured into a large excess of water and extracted with $CHCl_3$ to give the crude material which was purified by silica-gel column chromatography with a mixture of toluene and *n*-hexane (1/5, v/v) as eluent and further purified by preparative SEC, leading to a colorless solid product. Yield 46.1 % (1.4 g).). ^{1}H NMR (600 MHz, 298 K, $CDCl_3$) δ/ppm: 7.27-7.66 (6 H, m), 4.59 (4 H, s), 1.80-1.98 (4 H, m), 0.88-1.12 (8 H, m), 0.45-0.75 (10 H, m). ^{13}C NMR (150 MHz, 298 K, $CDCl_3$) δ/ppm: 151.8, 140.9, 137.0, 128.2, 123.8, 120.2, 55.3.

Menthyl tosylate.

This compound was synthesized according to the literature[25,27] with modifications. To a solution of *L*-(-)-menthol (20.00 g, 0.127 mol) in 41 mL of pyridine cooled at 0 ºC was slowly added tosyl chloride (26.60 g, 0.139 mol) dissolved in 60 mL of $CHCl_3$. The reaction mixture was warmed to room temperature and was stirred for 3 h. Removal of solvents gave a crude product which was recrystallized from a mixture of methanol and water afforded colorless crystals. Yield 35.6 g (90.7%).

9-Neomenthylfluorene ((-)-NF).

This compound was synthesized according to the literature[25,28] with modifications. The reactions were carried out under nitrogen atmosphere. To a solution of fluorene (26.07 g, 0.157 mol) in 120 mL of THF cooled at 0 ºC was slowly added 100 mL (0.157 mol) of *n*-BuLi (1.57 M in hexane solution). The reaction mixture was stirred for 25 min at 0 ºC. After the reaction system was cooled at -78 ºC, menthyl tosylate (24.00 g, 0.0774 mol) dissolved in 120 mL of dry tetrahydrofuran was added in three portions. The reaction mixture was stirred at room temperature for 30 min and then under reflux

for 15 h. The reaction mixture was poured into a large excess of water and was extracted with $CHCl_3$ to give the crude material which first purified by silica-gel column chromatography with a mixture of toluene and *n*-hexane (1/10, v/v) as eluent and was then recrystallized from methanol to afford colorless crystals. Yield 7.46 g (31.7 %).

9-Neomenthyl-9-pentylfluorene ((-)-NPF).

The reactions were conducted under nitrogen atmosphere. To a solution of 9-neomenthylfluorene (4.00 g, 0.0132 mol) in 70 mL of dry tetrahydrofuran cooled at 0 ^oC was slowly added 10.0 mL (0.0157 mol) of *n*-BuLi (1.57 M in hexane solution). The reaction system was stirred at 0 ^oC for 24 h. 1-Iodopentane (3.90 g, 0.0197 mol) dissolved in 10 mL of tetrahydrofuran was slowly added to the reaction mixture. The resulting mixture was stirred at ambient temperature for 24 h. The reaction mixture was poured into a large excess of water and extracted with $CHCl_3$ to give the crude material which was purified by silica-gel column chromatography with a mixture of toluene and *n*-hexane (1/5, v/v) as eluent to afford a colorless oily product. Yield 4.51 g (91.1 %). ^1H NMR (400 MHz, 298 K, $CDCl_3$) δ/ppm: 7.71-7.19 (m, 8H, ArH), 2.61-2.55 (m, 1H, -CH-), 2.19-0.07 (m, 29H).

2,7-Bi(bromomethyl)-9-neomenthyl-9-pentylfluorene ((-)-BNPF).

To a mixture of (-)-NPF (1.52 g, 0.005 mol) and paraformaldehyde (10.1 g, 0.125 mol) cooled at 0 ^oC was added dropwise 21.5 mL of 33 wt% HBr (10.1 g, 0.125 mol) in acetic acid solution. The reaction mixture was stirred at 65 ^oC for 36 h. The reaction mixture was poured into a large excess of water and extracted with $CHCl_3$ to give the crude material which was purified by silica-gel column chromatography with a mixture of toluene and *n*-hexane (1/5, v/v) as eluent and further purified by preparative SEC to afford a white solid product. Yield was 23 % (0.7 g). ^1H NMR (600 MHz, 298 K, $CDCl_3$) δ/ppm: 7.29-7.67 (6 H, m), 2.52-2.62 (1 H, m), 0.03-2.26 (29 H, m); ^{13}C NMR (150 MHz, 298 K, $CDCl_3$) δ/ppm: 152.0, 151.4, 141.2, 140.9, 136.7, 136.6, 127.9 (2C), 125.9, 125.0, 120.2, 120.1, 57.5.

Polymerization.

The detailed conditions and results of polymerization are summarized in Table 1-1. The detailed procedure is described for run 3 in Table 1-1. (-)-BNPF (46.90 mg, 0.084 mmol) and BPF (42.65 mg, 0.086 mmol) were dissolved in 0.95 mL of dry THF under N_2 atmosphere, and 0.47 mL of 1-M *t*-BuOK (0.47 mmol) in THF was injected to initiate the polymerization. The reaction mixture was allowed to stand at 23 ℃ for 12 h and was then terminated by the addition of 1 mL of water and stirring for 10 mins. The quenched reaction mixture was poured into a large excess of methanol. Precipitated polymer was collected with centrifuge. The MeOH-insoluble polymer was separated by preparative SEC to obtain the higher-molar-mass (11.9 mg, 13.3%) and lower-molar-mass products (48.7 mg, 54.4%).

Film preparation.

The procedure is described for the films of the higher-molar-mass polymer from run 5 in Table S1. The polymer (0.22 mg or 0.51 mg or 1.2 mg or 2.2 mg or 12 mg) was dissolved in THF (0.4 mL). An aliquot (ca. 0.05 mL) of the solution was dropped onto a 1-mm quartz plate (1cm x 2 cm x 1 mm) and dried under air at r.t.

Computational method.

The initial structure is represented by the 55-mer of atactic poly(**NMPF-E**) with a total size of 3742 atoms. Those coordinates have been energy-minimized through the steepest descent algorithm and equilibrated through molecular dynamic (MD) simulations at 300K in vacuo, in a simulation box of 60 x 15 x 15 nm^3, using the CHARMM-based general force field.[29]

Steered molecular dynamic (SMD) simulation[30] has been subsequently performed on the equilibrated conformation in order to sample different polymer conformations by using the gyration radius as collective variable (CV).

Within this procedure, ten polymer chains have been identified by a gyration radius of 3 nm, 6 nm, 8 nm, 10 nm, 12 nm, 13 nm, 15 nm, 17 nm, 18 nm and 20 nm.

Those sampled conformations have been stacked on top of amorphous silicon dioxide slab, and equilibrated through MD simulations at 300K in a simulation box of 80 x 80 x

16 nm^3, using CHARMM-based general force field.[29]

Electrostatic interactions were calculated using the Particle Mesh Ewald method,[31] a time-step of 2 fs has been set and the LINCS algorithm[32] has been applied to fix all bond lengths. Periodic boundary conditions have been applied only in the xy directions and the amorphous silica has been kept fixed during the simulations. The simulated MD trajectory has been clusterized by using the Daura and Van Gunsteren method[33] with a cutoff of 3.5 Å.

All simulations have been performed by using GROMACS 2020.3[34] equipped with PLUMED 2.7.0.[35]

Each chain clusterized from the MD trajectory has been divided in 4 sections and selected for the ECD spectra simulation. ECD spectra calculations have been performed at the ZINDO[36,37] level of theory as implemented in Gaussian16[38] suite of quantum-chemical program, by considering the first fifty singlet excited states. The calculations of the ECD spectrum at a given wavelength have been performed by assuming gaussian bands with 1000 cm^{-1} full width at half-height for all transition centered in a given excitation wavelength. A factor of 2.278 was applied during the conversion of rotatory strength and Δε values as reported in the literature.[39]

Born Oppenheimer Molecular Dynamic (BOMD) simulations at 300 K have been performed in the first electronic excited state (S_1) of the 13-monomeric-unit segment at wB97xD/6-31G level of theory, using Gaussian16,[38] to calculate the PL and CPL spectra with a total simulation time of 100 fs with a step size of 1 fs. 20 configurations have been extracted and from those excitation energies, oscillator strengths and rotatory strengths have been computed at wB97xD/6-31G level of theory.

PL and CPL intensities (I and ΔI, respectively) are derived by using the following expressions:[40]

$$I = \frac{4E^3\rho(E)D_{01}}{3\hbar^4c^3} = 1.27 \cdot 10^{-7}E^3\rho(E)D_{01} \qquad (1)$$

$$\Delta I = \frac{16E^3\rho(E)R_{01}}{3\hbar^4c^3} = 5.09 \cdot 10^{-13}E^3\rho(E)R_{01} \qquad (2)$$

Where D_{01} and R_{01} are the dipole and rotational strengths, respectively, associated to the transition 0←1, E is the emission energy of the given transition expressed in cm^{-1}, $\rho(E)$ is a Gaussian band shape and the calculated constants are coherently expressed in cgs units. The PL and CPL intensities have been then normalized to arbitrary relative units by assuming Gaussian bands with 800 cm^{-1} full width at half-height for all transitions in a given emission energy.

The emission dissymmetry factor (g_{lum}) has been computed by using equation 3:

$$g_{lum} = \frac{4R_{01}}{D_{01}} \qquad (3)$$

Parallel Bias Metadynamics (PBMetaD) simulations[41] were performed on the polymer chains stacked on top of amorphous silicon dioxide slab by using the first four dihedral torsions as collective variables. Moreover, in order to improve the sampling and the efficiency in the reconstruction of the free energy profiles, Multiple Walkers metadynamics (MW-MetaD) simulations were carried out. Within the MW-metaD approach, multiple interacting simulations have been used for accelerating the free-energy simulation convergence.[42] Specifically, two interacting simulations have been used identifying cis and trans conformation with 0 degrees and 180 degrees, respectively. Gaussians with an initial height equal to 1.2 kJ/mol and with a width of 0.1 rad were deposited with a bias factor of 5, and a temperature of 300 K. All the simulations were performed with GROMACS 2020.311 equipped with plumed 2.7.[35]

References

1. E. Yashima, K. Maeda, H. Iida, Y. Furusho, K. Nagai, Helical polymers: synthesis, structures, and functions, *Chem. Rev.* **2009**, *109*, 6102-6211.

2. E. Yashima, N. Ousaka, D. Taura, K. Shimomura, T. Ikai, K. Maeda, Supramolecular helical systems: helical assemblies of small molecules, foldamers, and polymers with chiral amplification and their functions, *Chem. Rev.* **2016**, *116*, 13752-13990.

3. T. Nakano, Y. Okamoto, Synthetic helical polymers: conformation and function, *Chem. Rev.* **2001**, *101*, 4013-4038.

4. Y. Okamoto, T. Nakano, Asymmetric polymerization, *Chem. Rev*. **1994**, *94*, 349-372.

5. M. M. Green, J. W. Park, T. Sato, A. Teramoto, S. Lifson, R. L. B. Selinger, J. V. Selinger, The macromolecular route to chiral amplification, *Angew. Chem. Int. Ed.* **1999**, *38*, 3138-3154.

6. J. H. K. K. Hirschberg, L. Brunsveld, A. Ramzi, J. A. J. M. Vekemans, R. P. Sijbesma, E. W. Meijer, Helical self-assembled polymers from cooperative stacking of hydrogen-bonded pairs, *Nature* **2000**, *407*, 167-170.

7. S. Cai, J. Chen, S. Wang, J. Zhang, X. Wan, Allostery-Mimicking Self-assembly of Helical Poly (phenylacetylene) Block Copolymers and the Chirality Transfer, *Angew. Chem. Int. Ed.* **2021**, *60*, 9686-9692.

8. H. Goto, H. Katagiri, Y. Furusho, E. Yashima, Oligoresorcinols fold into double helices in water, *J. Am. Chem. Soc.* **2006**, *128*, 7176.

9. S. Sakurai, K. Okoshi, J. Kumaki, E. Yashima, Two-dimensional hierarchical self-assembly of one-handed helical polymers on graphite, *Angew. Chem. Int. Ed.* **2006**, *45*, 1245-1248.

10. R. Ho, M. Li, S. Lin, H. Wang, Y. Lee, H. Hasegawa, E. L. Thomas, Transfer of chirality from molecule to phase in self-assembled chiral block copolymers, *J. Am. Chem. Soc.* **2012**, *134*, 10974-10986.

11. H. Gilch, W. Wheelwright, Polymerization of □-halogenated □-xylenes with base, *J. Polym. Sci. A1* **1966**, *4*, 1337-1349.

12. S. Jin, H. Park, J. Kim, K. Lee, S. Lee, D. K. Moon, H. Lee, Y. S. Gal, Poly (fluorenevinylene) derivative by gilch polymerization for light-emitting diode applications, *Macromolecules* **2002**, *35*, 7532-7534.

13. C. C. Lee, C. Grenier, E. W. Meijer, A. P. H. J. Schenning, Preparation and characterization of helical self-assembled nanofibers, *Chem. Soc. Rev.* **2009**, *38*, 671-683.

14. T. M. Clover, C. L. O'Neill, R. Appavu, G. Lokhande, A. K. Gaharwar, A. E. Posey, M. A. White, J. S. Rudra, Self-assembly of block heterochiral peptides into helical tapes, *J. Am. Chem. Soc.* **2020**, *142*, 19809-19813.

15. A. J. Varni, A. Fortney, M. A. Baker, J. C. Worch, Y. Qiu, D. Yaron, S. Bernhard, K. J. T. Noonan, T. Kowalewski, Photostable helical polyfurans, *J. Am. Chem. Soc.* **2019**, *141*, 8858-8867.

16. K. Suda, K. Akagi, Self-Assembled Helical Conjugated Poly(m-phenylene) Derivatives That Afford Whiskers with Hexagonal Columnar Packed Structure, *Macromolecules* **2011**, *44*, 9473-9488.

17. T. J. Deming, Synthesis of side-chain modified polypeptides, *Chem. Rev.* **2016**, *116*, 786-808.

18. J. Venkatraman, S. C. Shankaramma, P. Balaram, Design of folded peptides, *Chem. Rev.* **2001**, *101*, 3131-3152.

19. D. Priftis, L. Leon, Z. Song, S. L. Perry, K. O. Margossian, A. Tropnikova, J. Cheng, M. Tirrell, Self-assembly of α-helical polypeptides driven by complex coacervation, *Angew. Chem. Int. Ed.* **2015**, *54*, 11128-11132.

20. D. J. Hill, M. J. Mio, R. B. Prince, T. S. Hughes, J. S. Moore, A field guide to foldamers, *Chem. Rev.* **2001**, *101*, 3893-4012.

21. J. C. Nelson, J. G. Saven, J. S. Moore, P. G. Wolynes, Solvophobically driven folding of nonbiological oligomers, *Science* **1997**, *277*, 1793-1796.

22. R. S. Lokey, B. L. Iverson, Synthetic molecules that fold into a pleated secondary structure in solution, *Nature* **1995**, *375*, 303-305.

23. J. Q. Nguyen, B. L. Iverson, An amphiphilic folding molecule that undergoes an irreversible conformational change, *J. Am. Chem. Soc.* **1999**, *121*, 2639-2640.

24. S. Tanaka, K. Sato, K. Ichida, T. Abe, T. Tsubomura, T. Suzuki, K. Shinozaki, Circularly Polarized Luminescence of Chiral Pt (pppb) Cl (pppbH= 1-pyridyl-3-(4, 5-pinenopyridyl) benzene) Aggregate in the Excited State, *Chem. Asian J.* **2016**, *11*, 265–273.

25. J. Yu, T. Sakamoto, K. Watanabe, S. Furumi, N. Tamaoki, Y. Chen, T. Nakano, Synthesis and efficient circularly polarized light emission of an optically active hyperbranched poly (fluorenevinylene) derivative, *Chem. Commun.* **2011**, *47*, 3799–3801.

26. M. Zheng, L. Ding, Z. Lin, F. E. Karasz, Synthesis and characterization of fluorenediylvinylene and thiophenediylvinylene-containing terphenylene-based copolymers, *Macromolecules* **2002***, 35,* 9939–9946.

27. G. Erker, M. Aulbach, M. Knickmeier, D. Wingbermiihle, C. Kriiger, M. Nolte, S. Werne, The role of torsional isomers of planarly chiral nonbridged bis (indenyl) metal type complexes in stereoselective propene polymerization, *J. Am. Chem. Soc.* **1993**, *115*, 4590–4601.

28. A. Gutnov, H.-J. Drexler, A. Spannenberg, G. Oehme, B. Heller, Syntheses of chiral nonracemic half-sandwich cobalt complexes with menthyl-derived cyclopentadienyl, indenyl, and fluorenyl ligands, *Organometallics* **2004**, *23*, 1002–1009.

29. K. Vanommeslaeghe, E. Hatcher, C. Acharya, S. Kundu, S. Zhong, J. Shim, E. Darian, O. Guvench, P. Lopes, I. Vorobyov, A. D. MacKerell, Jr., CHARMM general force field: A force field for drug-like molecules compatible with the CHARMM all-atom additive biological force fields, *J. Comput. Chem.* **2010**, *31*, 671–690.

30. B. Isralewitz, M. Gao, K. Schulten, Reconstructing potential energy functions from simulated force-induced unbinding processes, *Curr. Opin. Struct. Biol.* **2001**, *11*, 224–230.

31. U. Essmann, L. Perera, M. L. Berkowitz, T. Darden, H. Lee, L. G. Pedersen, A smooth particle mesh Ewald method, *J. Chem. Phys.* **1995**, *103*, 8577–8593.

32. B. Hess, *J. Chem. Theory Comput.* **2008**, *4*, 116–1220.

33. X. Daura, K. Gademann, B. Jaun, D. Seebach, W. F. van Gunsteren, A. E. Mark, Peptide folding: when simulation meets experiment, *Angew. Chem. Int. Ed.* **1999**, *38*, 236-240.

34. B. Hess, C. Kutzner, D. van der Spoel, E. Lindahl, *J. Chem. Theory Comput.* **2008**, *4*, 435–447.

35. The PLUMED consortium, Promoting transparency and reproducibility in enhanced molecular simulations, *Nat. Methods* **2019**, *16*, 670–673.

36. J. Ridley, M. Zerner, *Theor. Chim. Acta* **1973**, *32*, 111–134.

37. J. Ridley, M. Zerner, *J. Mol. Spectrosc.* **1974**, *50*, 457–473.

38. Gaussian 16, Revision C01, M. J. Frisch, G. W. Trucks, H. B. Schlegel, G. E. Scuseria, M. A. Robb, J. R. Cheeseman, G. Scalmani, V. Barone, G. A. Petersson, H. Nakatsuji, X. Li, M. Caricato, A. V. Marenich, J. Bloino, B. G. Janesko, R. Gomperts, B. Mennucci, H. P. Hratchian, J. V. Ortiz, A. F. Izmaylov, J. L. Sonnenberg, D. Williams-Young, F. Ding, F. Lipparini, F. Egidi, J. Goings, B. Peng, A. Petrone, T. Henderson, D. Ranasinghe, V. G. Zakrzewski, J. Gao, N. Rega, G. Zheng, W. Liang, M. Hada, M. Ehara, K. Toyota, R. Fukuda, J. Hasegawa, M. Ishida, T. Nakajima, Y. Honda, O. Kitao, H. Nakai, T. Vreven, K. Throssell, J. A. Montgomery, Jr., J. E. Peralta, F. Ogliaro, M. J. Bearpark, J. J. Heyd, E. N. Brothers, K. N. Kudin, V. N. Staroverov, T. A. Keith, R. Kobayashi, J. Normand, K. Raghavachari, A. P. Rendell, J. C. Burant, S. S. Iyengar, J. Tomasi, M. Cossi, J. M. Millam, M. Klene, C. Adamo, R. Cammi, J. W. Ochterski, R. L. Martin, K. Morokuma, O. Farkas, J. B. Foresman, and D. J. Fox, Gaussian, Inc., Wallingford, CT, 2016.

39. A. Koslowski, N. Sreerama, R. Woody. Theoretical Approach to Electronic Optical Activity. In Circular Dichroism – Principles and Applications; N. Berova, K. Nakanishi, R. Woody, Eds.; Wiley-VCH: New York, **2000**, 55–95.

40. G. Longhi, E. Castiglioni, J. Koshoubo, G. Mazzeo, S. Abbate, Circularly polarized luminescence: a review of experimental and theoretical aspects, *Chirality* **2016**, *28*, 696–707.

41. J. Pfaendter, M. Bonomi, *J. Chem. Theory Comput*. **2015**, *11*, 5062.

42. P. Raiteri, A. Laio, F. L. Gervasio, C. Micheletti, M. Parrinello, Efficient

reconstruction of complex free energy landscapes by multiple walkers metadynamics, *J. Phys. Chem. B* **2006**, *110*, 3533.

Chapter 3. Chiral hyperbranched polyfluorenvinylenes and their interactions with external molecules

3.1 Introduction

Optically active molecules and polymers play important roles in life and in materials science. In this context, various optically active compounds have been prepared mainly by asymmetric synthesis in which asymmetry of a chirality-source compound, typically a ligand, is transferred through chemical modifications resulting in the chiral products.[1-3] Chirality transfer can be attained from a "chirality donor" to a "chirality acceptor" even without any changes in their chemical structure, which has been well presented for the systems involving host-guest complexes,[4-7] helical polymers with ordered conformation,[8-12] supramolecular crystals,[13-15] and aggregates and gel systems having chiral structure beyond the molecular level.[16,17] As for the preceding examples of chirality transfer involving polymers, linear polymers including those with well controlled, uniform, single-handed helical conformation[1-4] have been a focus.

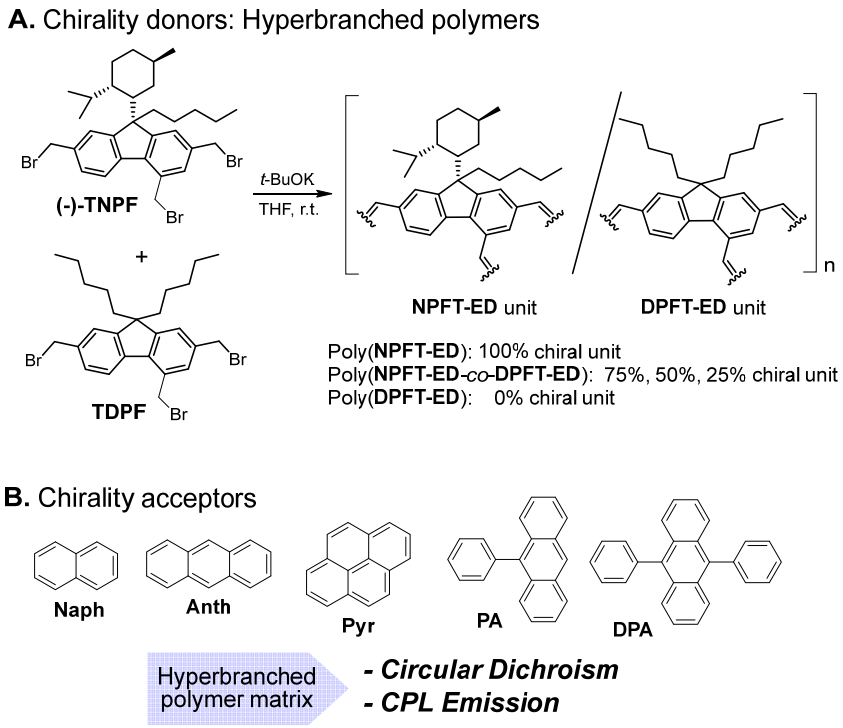

Scheme 3-1. Synthesis of hyperbranched, chiral poly(fluorene-2,4,7- triylethene-1,2-diyl) derivatives (A) and chirality transfer to aromatic, small molecules (B).

With such a background, we herein report the synthesis and properties of an amorphous, optically active, hyperbranched poly(fluorenevinylene) derivative as an efficient chirality donor that can include small molecules inside its interior space within the complex, hyperbranched structure. The chirality donor polymers are poly(9-neomenthyl-9-pentylfluorene-2,4,7- triylethene-1,2-diyl) (poly(**NPFT-ED**)) bearing chiral side-chain neomentyl group derived from *L*-menthol ((1*R*,2*S*,5*R*)-2-isopropyl-5- methylcyclohexanol) and also optically active, hyperbranched copolymers, poly(9-neomenthyl-9-pentylfluorene-2,4,7-triylethene-1,2-diyl-co-9,9-dipentylfluorene-2,4,7-triylethene-1,2-diyl) (poly(**NPFT-ED**-*co*-**DPFT-ED**)) (Scheme 3-1 A), and small molecular chirality acceptors are naphthalene (Naph), anthracene (Anth), pyrene (Pyr), 9-phenylanthracene (PA), and 9,10-diphenyanthracene (DPA) (Scheme 1 B). In addition, linear polymer analogues to the hyperbranched ones were also used for clear comparison, leading to a conclusion that chirality transfer efficiency was much higher with the hyperbranched polymers.

The hyperbranched polymers were prepared through homopolymerization and copolymerization of 2,4,7-tris(dibromomethyl)-9-neomenthyl-9-pentylflourene[18] ((-)-TNPF) and 2,4,7-tris(dibromomethyl)- 9,9-dipentylflourene (TDPF) by the Gilch reaction using t-BuOK in tetrahydrofuran (THF) at 23 ºC, resulting in the homopolymers and copolymers composed of chiral 9-neomenthyl-9-pentylfluorene-2,4,7-triylethene-1,2-diyl (NPFT-ED) units and/or achiral 9,9-dipenthylfluorene-2,4,7- triylethene-1,2-diyl (DPFT-ED) units at different ratios, i.e., poly(9-neomentyl-9- pentylfluorene-2,4,7-triylethene-1,2-diyl) [poly(TNPFT-ED)] (100% chiral units),[18] poly[(9-neomenthyl-9-pentyl-2,4,7-triylethene-1,2-diyl-co-9-dipentylfluorene-2,4,7-triylethene-1,2-diyl] [poly(NPFT-ED-co-DPFT-ED)] (25% or 50% or 75% chiral

monomeric units) and poly(9,9-dipentylfluorene-2,4,7-triylethene-1,2-diyl) [poly(DPFT-ED)] (0% chiral monomeric units) (Scheme 3-1A). The conditions and results of polymerization as well as synthetic details are reported in Table 3-1. The crude polymerization products had broad dispersities with two major components as found by SEC analysis and were separated into acetone-insoluble, higher-molar-mass (Mn 84500-140300) and acetone-soluble, lower-molar-mass (Mn 850-2100) parts (Figure 3-1). The 1H NMR spectra of these separated polymers are shown in Figure 3-2. From here on, the higher-molar-mass polymers are mainly discussed unless otherwise noted. While regularity of relative configuration of chirality centers at the 9-position of fluorene backbone (tacticity) in the polymers with 9-neomenthyl-9-pentylfluorene-2,4,7-triyl units is not known at this stage of work, the polymers may be assumed to have rather irregular relative configuration because steric repulsion between side-chain groups may not be significant enough to create ordered structure through the Gilch reaction. In addition, the polymers are considered to be composed of dendritic (branched) (D), linear (L), and terminal (T) units,[19,20] whose ratio was estimated according to the method of literature[21] by 1H NMR spectroscopy and was used to calculate the degree of branching (DB) defined as DB = ([D] + [T])/([D] + [L] + [T]).[19,20] DB was in the range of 0.78 to 0.86 (Table 3-2).

Table 3-1. Synthesis of poly(fluorene-2,4,7-triylethene-1,2-diyl) derivatives composed of chiral **NPFT-ED** unit and achiral DPF-E unit from optically active **TNPF** and achiral **TDPF** by the Gilch reaction in THF at 23°C for 12 h[a]

Run	**TNPF** (M)	**TDPF** (M)	*t*-BuOK (M)	Conv.[b] (%)	Acetone-insoluble part[c]			Acetone-soluble part[c]		
					Yield (%)	M_n[d]	M_w/M_n[d]	Yield (%)	M_n[d]	M_w/M_n[d]
1	0	0.08	0.33	99	20.1	140300	4.93	71.1	1800	1.25
2	0.02	0.06	0.33	99	17.2	114000	7.04	71.6	2100	1.53
3	0.04	0.04	0.33	99	19.2	135500	3.49	74	2100	2.13
4	0.06	0.02	0.33	99	19.9	84500	4.46	72.2	850	1.2
5	0.08	0	0.33	99	14.8	100200	3.86	65.2	2000	1.28

[a][*t*-BuOK] = 0.33 M; **TNPF** 25.5 mg (0.039 mmol) (run 2), 41.4 mg (0.063 mmol) (run 3), 73.1 mg (0.112 mmol) (run 4), 89.7 mg (0.137 mmol) (run 5); **TDPF** 136.6 mg (0.231 mmol) (run 1), 68.6 mg (0.117 mmol) (run 2), 37.1 mg (0.063 mmol) (run 3), 21.8 mg (0.037 mmol) (run 4). [b]Determined by ^{1}H NMR analysis of crude products. [c]Purified by reprecipitation in MeOH and further in acetone to result in acetone-insoluble and acetone-soluble parts. [d]Determined by SEC (eluent THF) using standard polystyrene samples.

Table 3-2. Ratios of dendritic (branched) (D), linear (L), and terminal (T) units of acetone-insoluble hyperbranched polymers[a]

	Run 1[b]	Run 2[b]	Run 3[b]	Run 4[b]	Run 5[b]
D	0.43	0.47	0.5	0.56	0.62
L	0.22	0.20	0.16	0.18	0.14
T	0.35	0.33	0.34	0.26	0.24
DB	0.78	0.80	0.84	0.82	0.86

[a]Determined using the NMR spectra in Figure 3-2 based on the relative intensities of the signals based on the aromatic and ethene protons (8.7-6.5 ppm), and -CH_2Br groups at the 2- and 7-positions (4.6 ppm) and the 4-position (4.8 ppm) of the fluorene backbone. [b]Runs in Table 3-1.

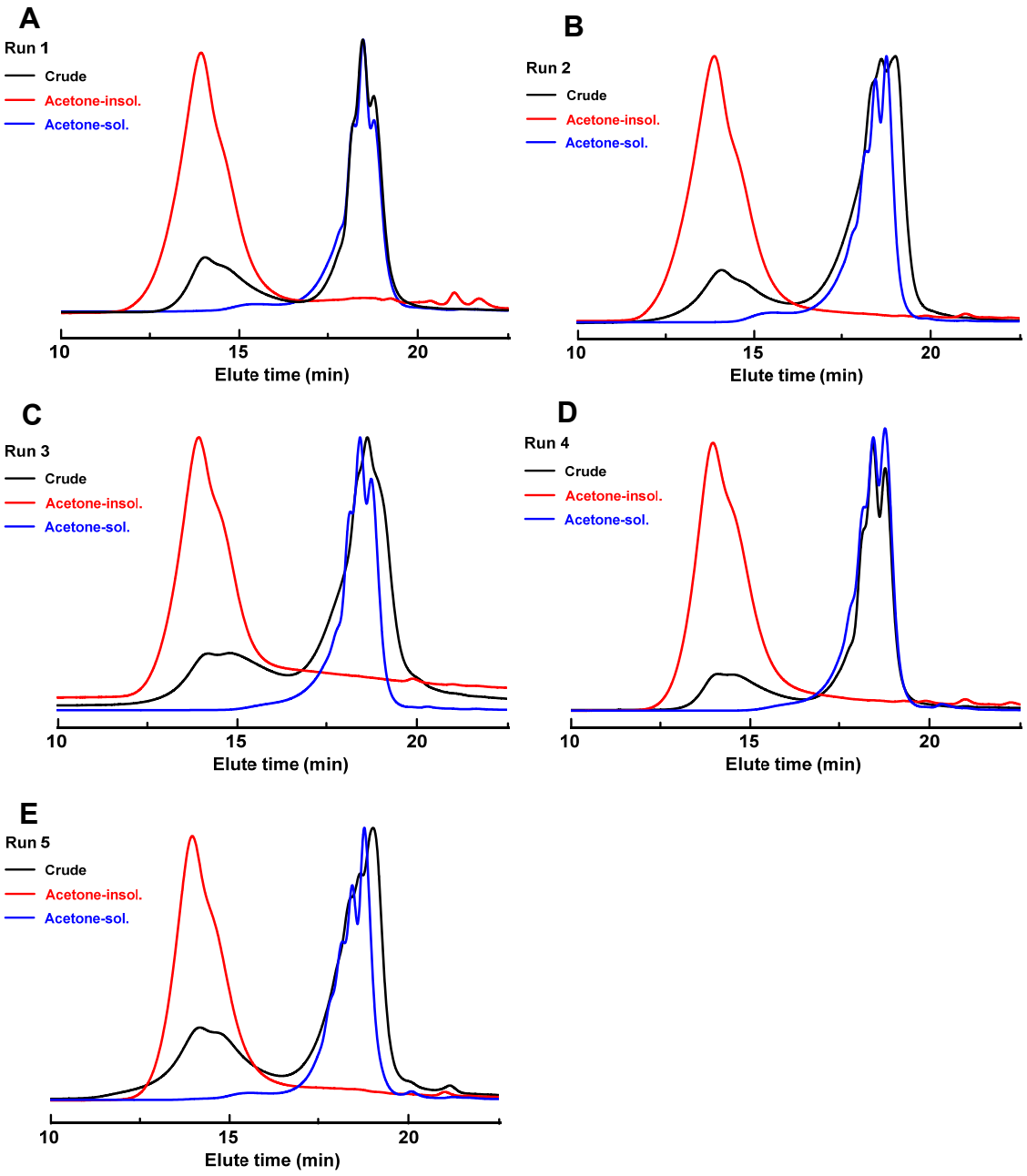

Figure 3-1. SEC profiles of crude mixtures, acetone-insoluble hyperbranched polymers, and acetone-soluble hyperbranched polymers from run 1 (A), run 2 (B), run 3 (C), run 4 (D), and run 5 (E) in Table 3-1.

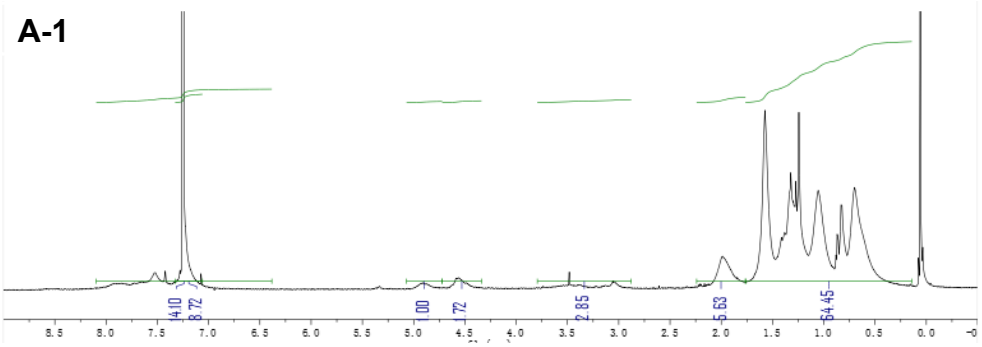
A-1

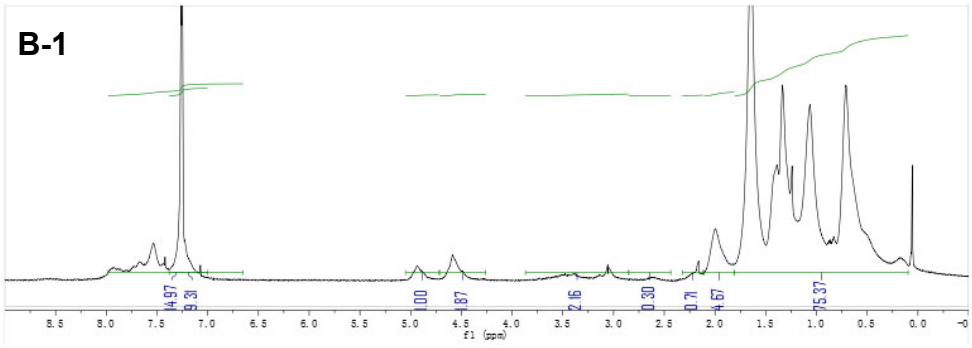
B-1

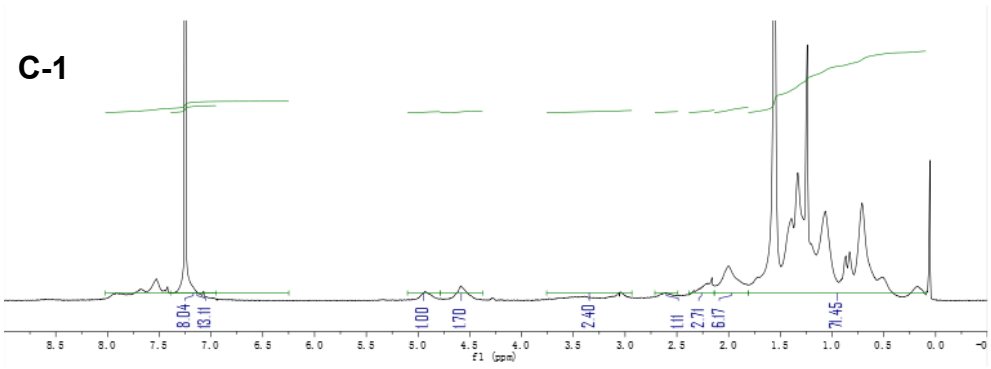
C-1

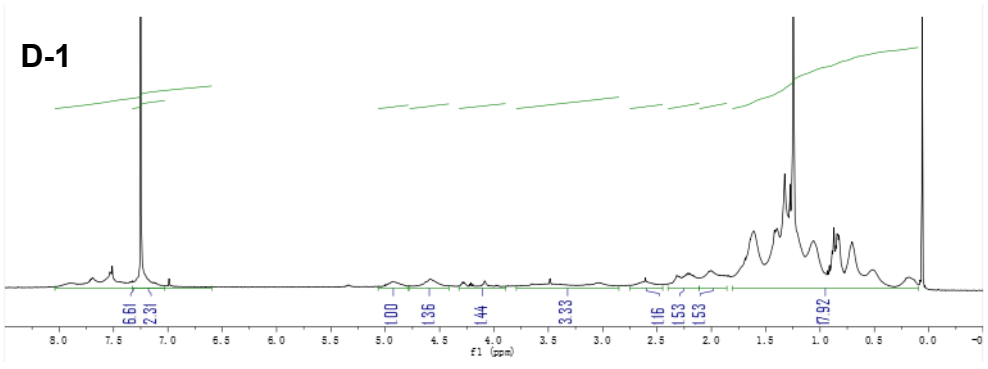
D-1

E-1

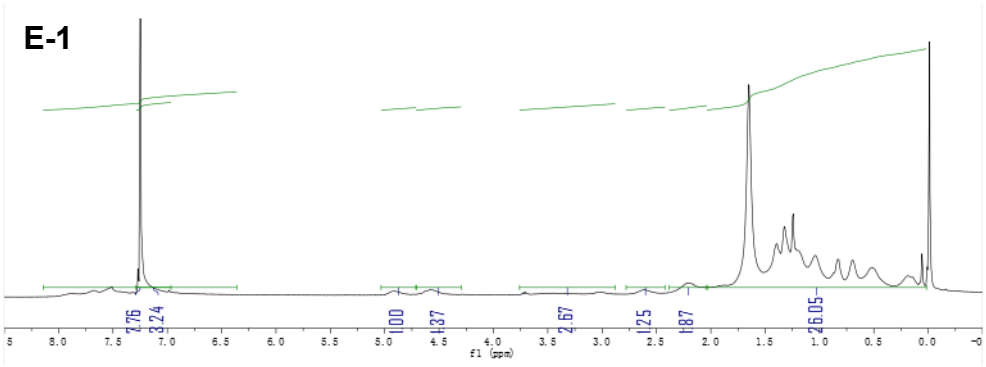

A-2

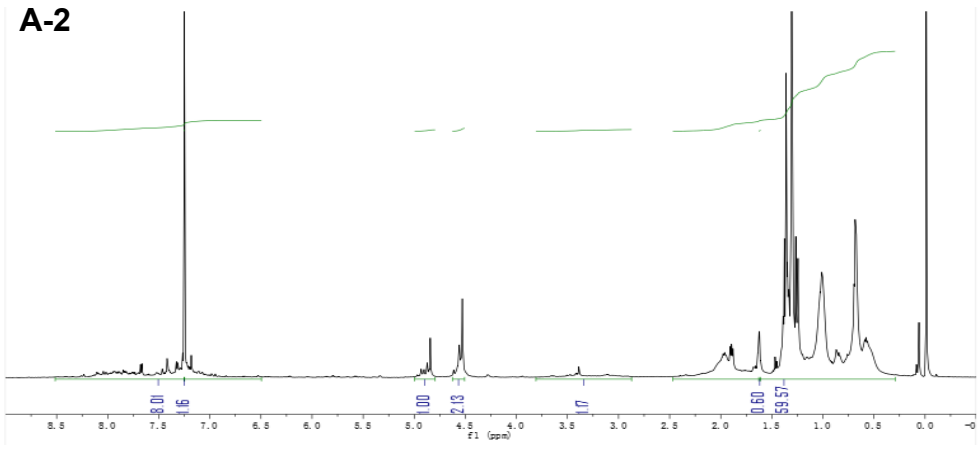

B-2

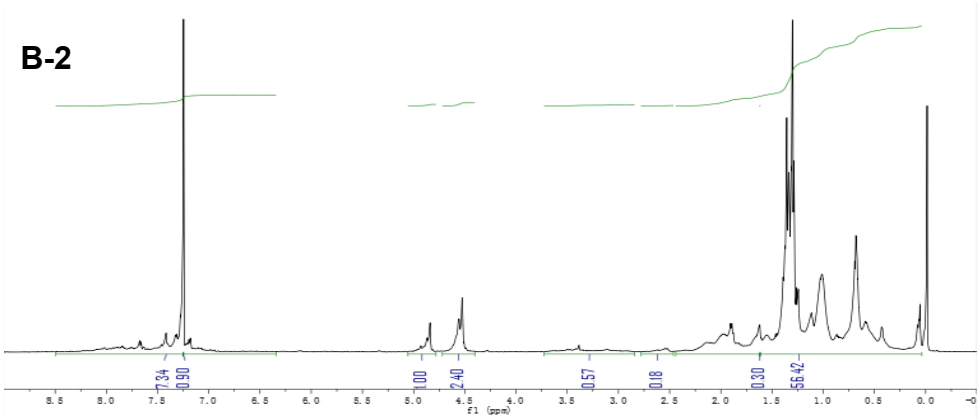

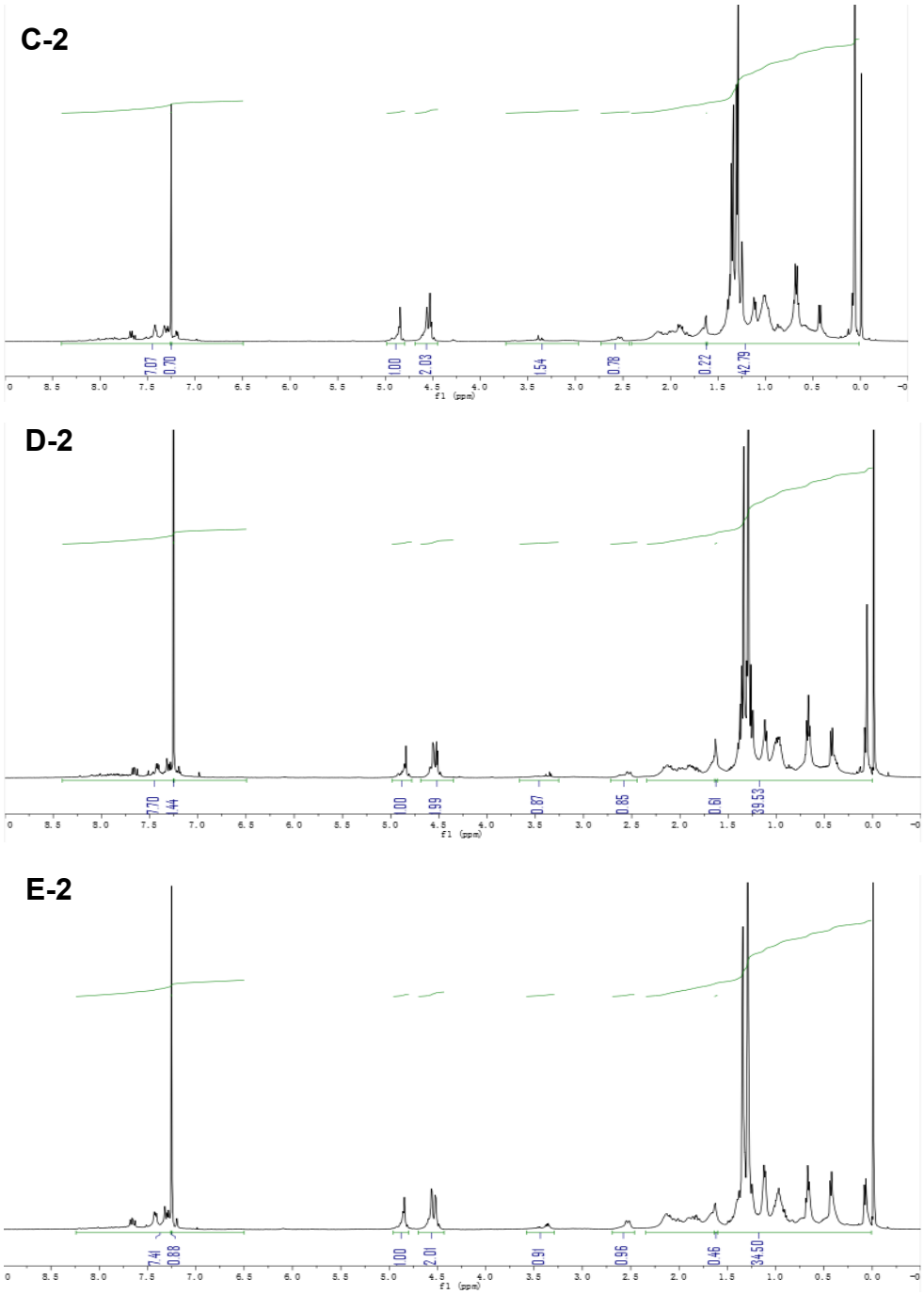

Figure 3-2. ^{1}H NMR spectra of acetone-insoluble hyperbranched polymers from run 1 (A-1), run 2 (B-1), run 3 (C-1), run 4 (D-1), run 5 (E-1) in Table 3-1. ^{1}H NMR spectra of acetone-soluble hyperbranched polymers from run 1 (A-2), run 2 (B-2), run 3 (C-2), run 4 (D-2), and run 5 (E-2) in Table 3-1 [400/600 MHz, $CDCl_3$, r.t.].

3.2 Results and Discussions

3.2.1 Chiroptical properties of polymers

The thermal properties of chiral acetone-insoluble and -soluble hyperbranched polymers (poly-(NPF-ED)) and the comparison with linear polymers (poly-(DPFT-ED)) are shown in Figure 3-3. As expected, the acetone-insol hyperbranched polymer and the higher molar mass linear polymer have higher decomposition temperature than these polymers with lower-molar-mass. All of these polymers are amorphous, as they do not show classical crystalline peaks in DSC files (Figure 3-3B).

The relations of molar ellipticity ([θ]) (solution) and g_{CD} value (film) with the ratio of chiral to achiral monomeric units are found in 3-6 (acetone-insoluble products). Both in solution and in film, all polymers showed similar UV spectral shapes with absorbance edges at around 460 nm and showed similar CD spectra patterns mainly contributed by negative signals in the wavelength ranges matching to those of the UV spectra, suggesting that the polymers have similar electronic conjugation systems with similar chirality through regardless of the ratio of chiral monomeric units as well as the state of the samples, solution or film. There seem to be no remarkable conformational aspects leading to chirality enhancement by the accumulation of chiral monomeric units. The acetone-soluble products (Figure 3-4) exhibit similar results that there is no remarkable chirality amplification.

Figure 3-5A shows the CD-UV spectra of the hyperbranched polymers in THF solution and in film. The optically active hyperbranched polymers were found to serve as efficient chirality donors toward the small molecules as chirality acceptors in mixed films (Figure 3-5B). The films fabricated on quartz glass by casting a solution of polymer and aromatic molecule exhibited intense CD spectra based mainly on the small molecules whose spectral shapes were remarkably different from those of the pure polymers. Hereafter, the results about Anth and DPA are mainly discussed.

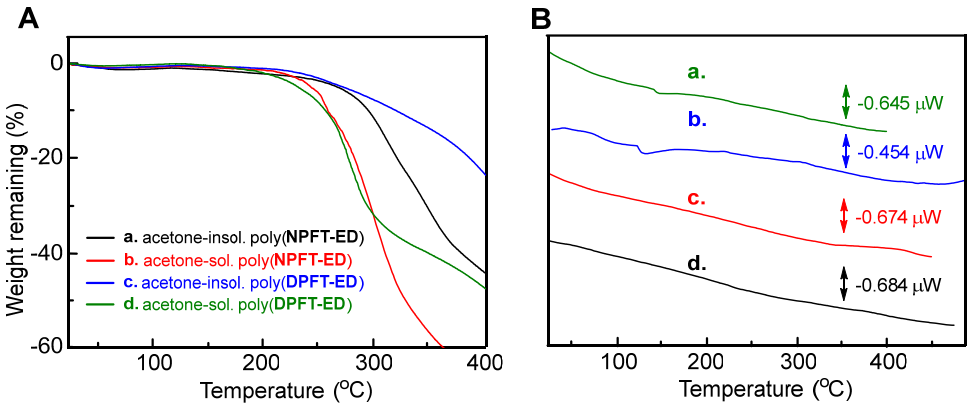

Figure 3-3. TG profiles (A) and DSC profiles on the second heating scan (B) of acetone-insoluble poly(**NPFT-ED**) (run 5 in Table 3-1) (a), acetone-soluble poly(**NPFT-ED**) (run 5 in Table 3-1) (b), acetone-insoluble poly(**DPFT-ED**) (run 1 in Table 3-1) (c), and acetone-soluble poly(**DPFT-ED**) (run 1 in Table 3-1) (d). [Heating rate 10°C/min]

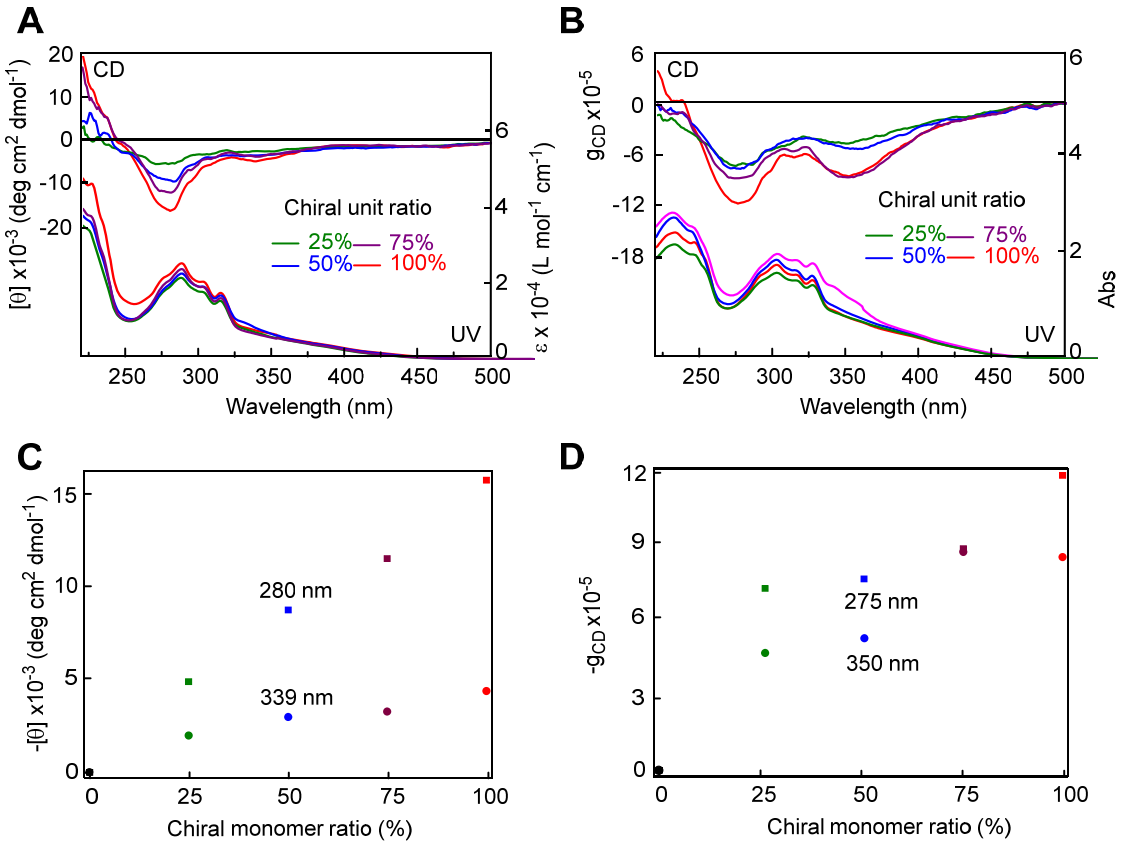

Figure 3-4. CD and UV spectra (top) and CD intensity-vs-chrial monomer unit ratio plots of acetone-soluble hyperbranched polymers in THF (A, C) and in film (B, D). [r. t., conc. 4.3~6.7 x 10^{-4} M, 1-mm cell (A)].

A. Hyperbranched polymer only

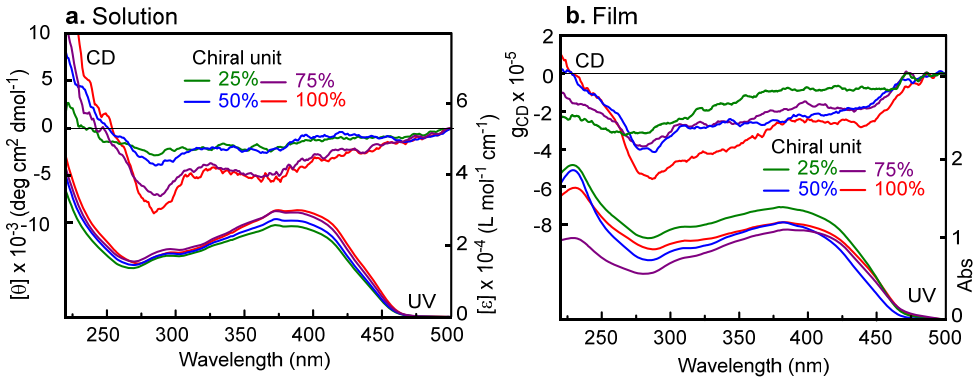

B. Hyperbranched polymer-aromatic moleules

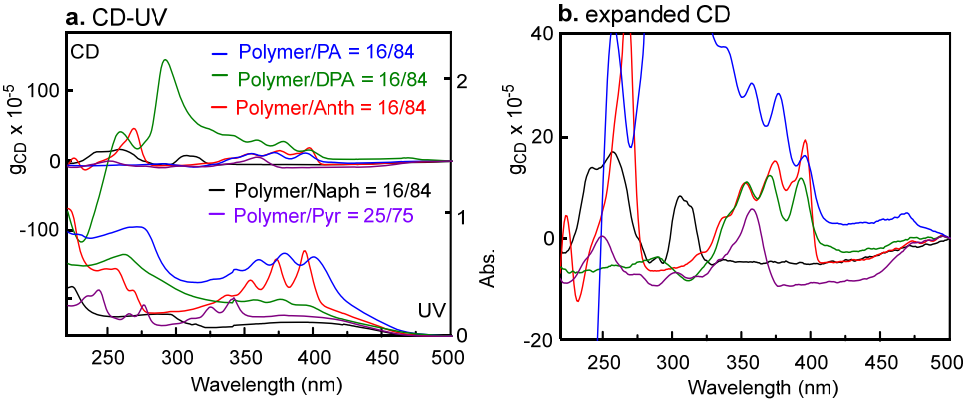

C. Effects of chiral monomer unit ratio on g_{CD} of mixed film

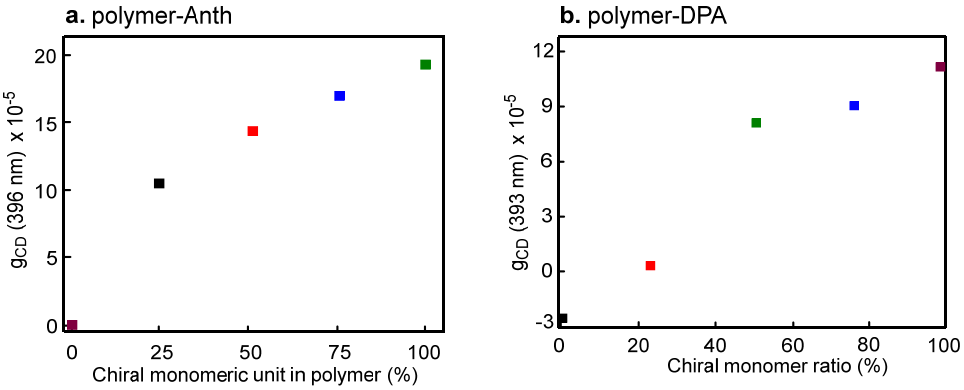

D. Effects of [polymer]/[Anth or DPA] ratio on g_{CD} of mixed film

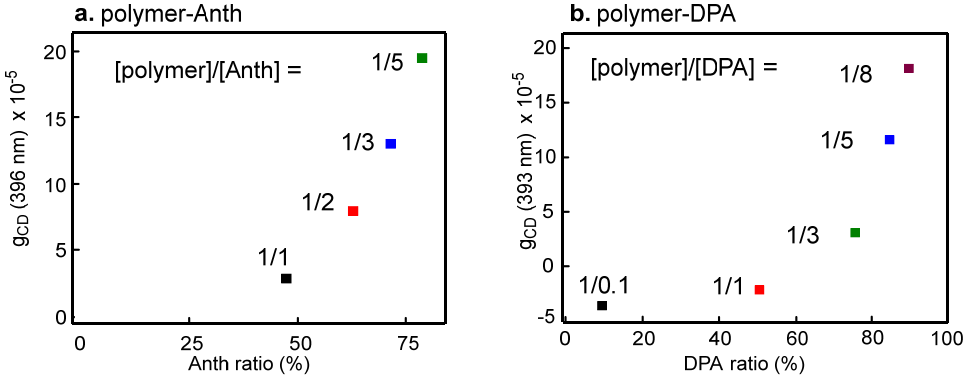

Figure 3-5. CD-UV spectra of hyperbranched polymers at different chiral monomer unit ratios in THF solution and in film (A), g_{CD} spectra of film samples of mixtures of acetone-insoluble, higher-molar-mass poly(**TNPFT-ED**) (M_n 100200) and aromatic small molecules (B), g_{CD} (396 nm)-vs.-chiral monomeric unit ratio plot for the mixed film samples of acetone-insoluble, higher-molar-mass hyperbranched polymers (M_n 84500-140300) with Anth (a) and DPA (b) at [polymer]/[Anth or DPA] = 1/5 (C), and g_{CD} (396 or 393nm)-vs.-Anth or DPA ratio plot for the mixed film samples of acetone-insoluble, higher-molar-mass poly(**TNPFT-ED**) (M_n 100200) with Anth (a) and DPA (b) (D). [(A-a) conc. (per residue) 5.3~6.0 x 10^{-4} M, cell path 1-mm]

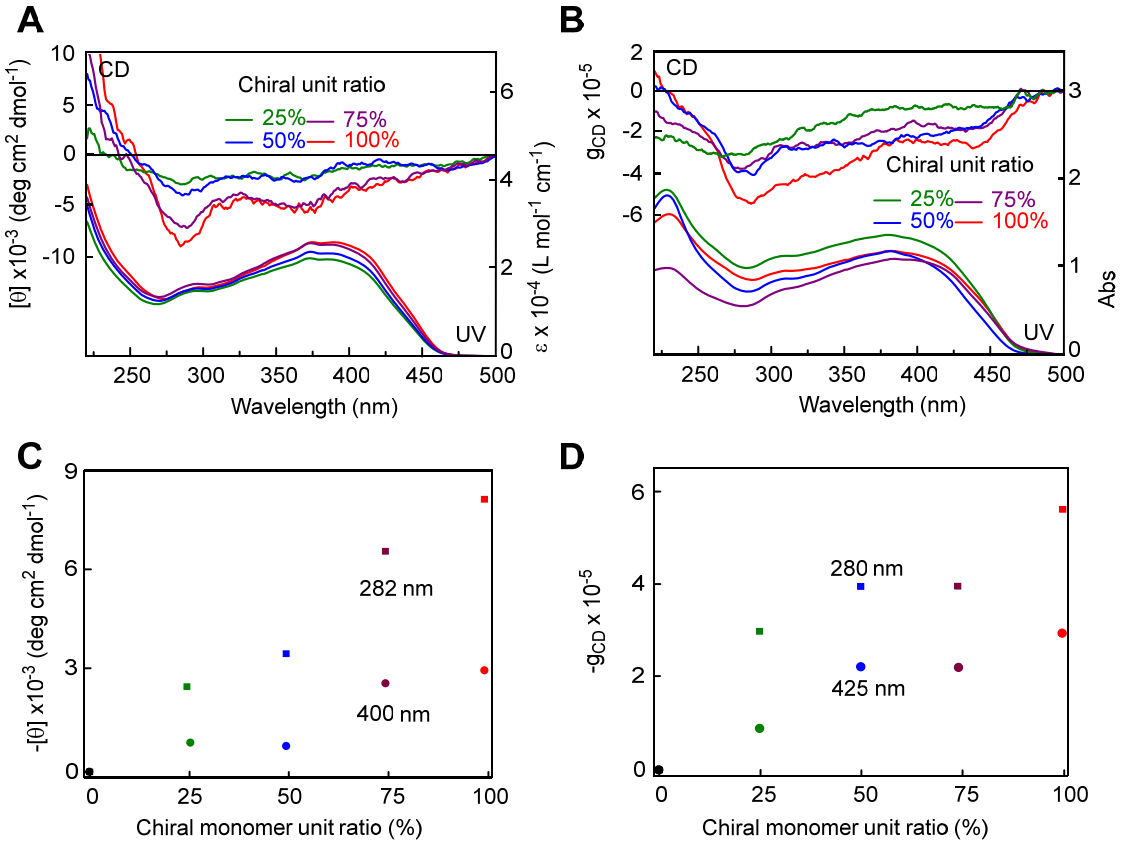

Figure 3-6. CD and UV spectra (top) and CD intensity-vs-chrial monomer unit ratio plots of acetone-insoluble hyperbranched polymers in THF (A, C) and in film (B, D). [r. t., conc. 3.3~4.0 x 10^{-4} M, 1-mm cell (A)]

3.2.2 Chiroptical properties of chirality transfer systems

The CD spectral intensity of the aromatic molecules remarkably varied depending on the chiral monomeric unit ratio of the polymer as presented for the polymer-Anth systems (Figure 3-5C) where the g_{CD} (396 nm)-vs.-chiral monomeric unit ratio relation appeared rather nonlinear, and g_{CD} rose sharply from chiral monomeric unit ratio = 0% to 25% and increased more moderately from the ratio of 25% to 100%, which may suggest saturation of chirality.

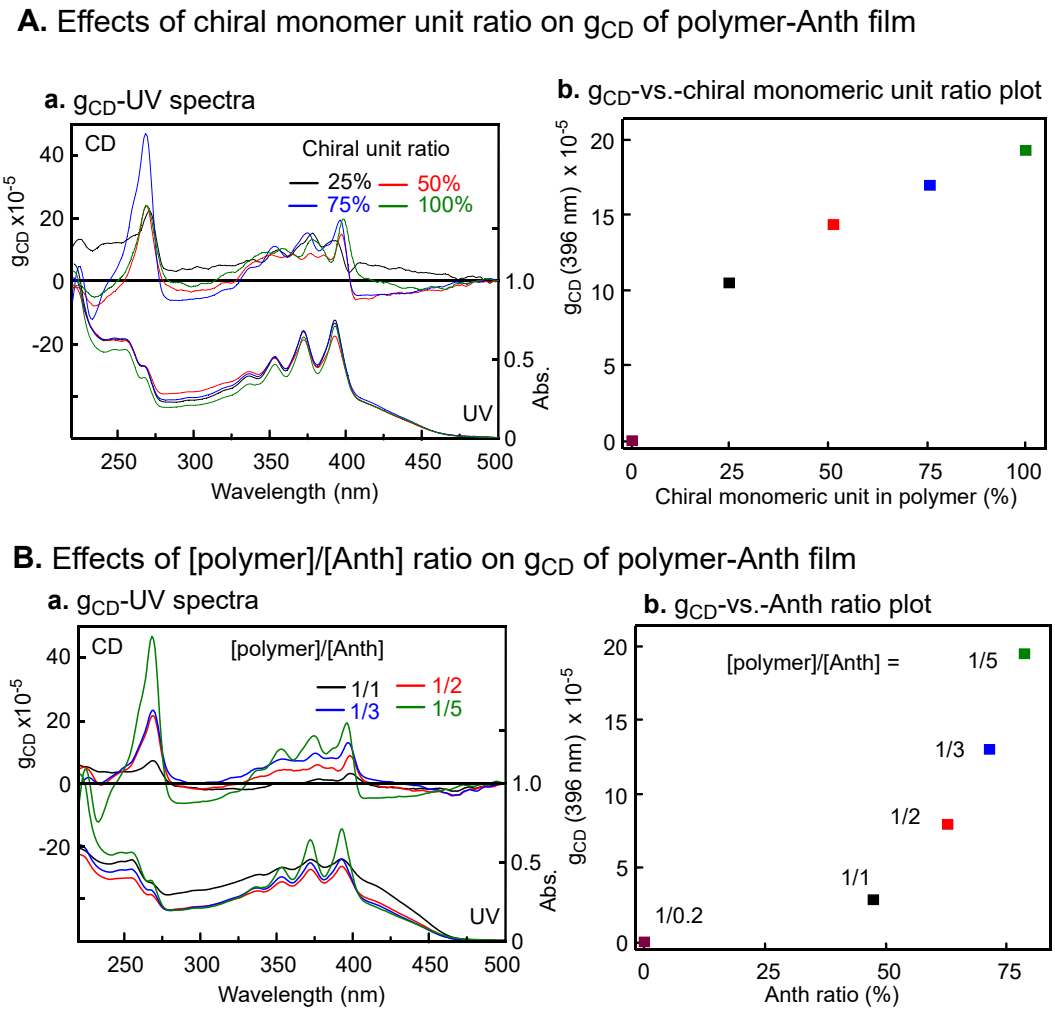

Figure 3-7. g_{CD}-UV spectra and g_{CD} (396 nm)-vs.-chiral monomer unit ratio plot of film samples of acetone-insoluble, higher-molar-mass hyperbranched polymers (M_n 84500-140300) and Anth at [polymer]/[Anth] = 1/5 (A), and g_{CD}-UV spectra and g_{CD} (396 nm)-vs.-Anth ratio plot of film samples of acetone-insoluble, higher-molar-mass poly(**TNPFT-ED**) (M_n 100200) and Anth (B).

In addition, g_{CD} of Anth rose rather exponentially as the [Anth]/[polymer (residue)] ratio increased (Figure 3-5D). This observation is surprising because an increase in this ratio means a decrease in relative concentration of the chiral polymer in film and strongly suggests that chirality is largely amplified between Anth molecules. The amplification may imply that chiral intermolecular ordering was induced to Anth molecules. Full spectral data for the Anth and DPA systems are found in Figure 3-7.

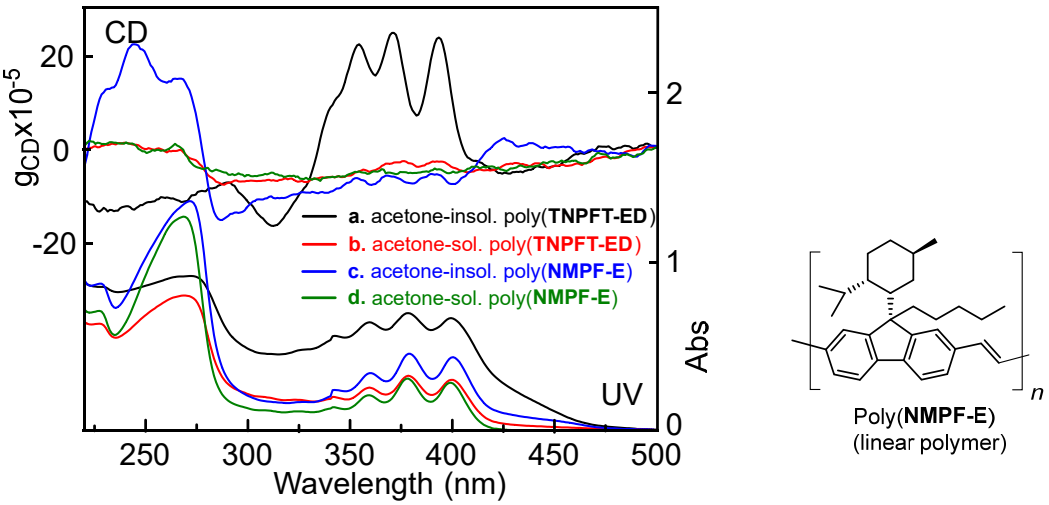

Figure 3-8. g_{CD}-UV spectra of acetone-insoluble poly(**TNPFT-ED**) (Mn 100200)-DPA film (a), acetone-soluble poly(**TNPFT-ED**) (Mn 2000)-DPA film (b), linear poly(**NMPF-E**) (Mn 21900)-DPA film (c), and linear poly(**NMPF-E**) (Mn 1400)-DPA film (d) at [polymer (residue)]/[DPA] = 16/84.

It is interesting that chirality transfer was far more efficient for the acetone-insoluble, higher-molar-mass poly(TNPFT-ED) (Mn 100200) compared with the acetone-soluble, lower-molar-mass poly(TNPFT-ED) (Mn 2000) and also with poly(9-neomenthyl-9-pentylfluorene- 2,7-diylethene1,2-diyl) [poly(NMPF-E)] (Mn 21900 and 1400) which is a linear analougue of poly(TNPFT-ED) as confirmed using DPA (Figure 3-8). The extended hyperbranched strcture appears to play a role in chirality transfer.

3.2.3 Molecular ordering of chirality transfer systems

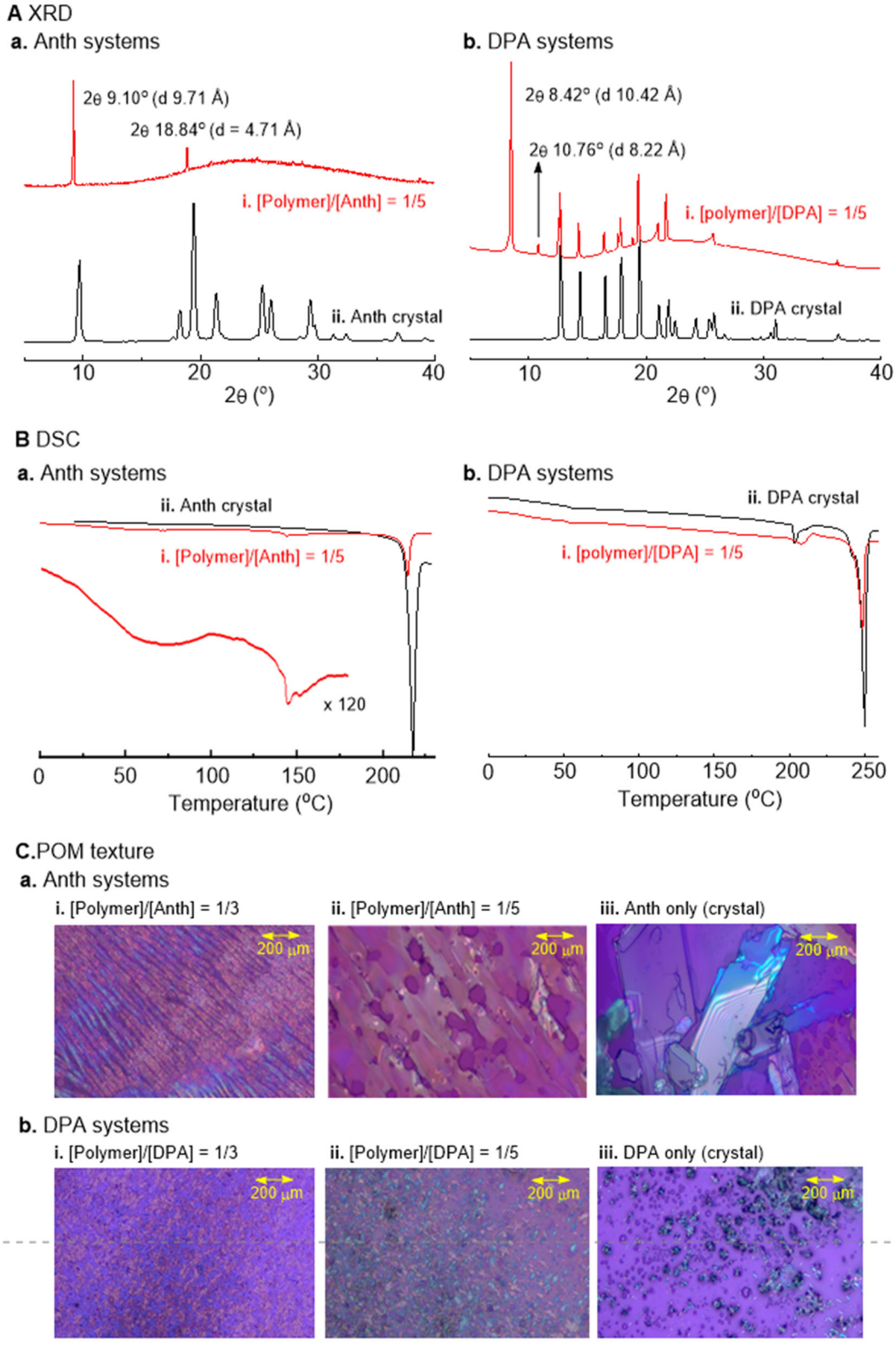

Figure 3-9. XRD (A) and DSC (B) profiles of polymer-Anth mixture at [polymer (residue)]/[Anth] = 1/5 (a) and of pure Anth crystal (b), proposed ordering of Anth molecules (C), and textures of Anth-polymer mixture observed by polarized optical microscopy (POM) (D) at [polymer (residue)]/[Anth] = 1/3 (a) and 1/5 (b). [Sample quantities: Anth 2.49 mg (B-a-i), polymer 1.34 mg + Anth 2.47 mg (B-a-ii), DPA 2.00 mg (B-b-i), polymer 0.41 mg + DPA 1.95 mg (B-b-ii)]

In order to obtain information on molecular ordering in the polymer-Anth and -DPA films, wide-angle x-ray diffraction (XRD) profiles were measured for pure Anth and DPA crystals and polymer-Anth and -DPA mixtures at [polymer]/[Anth or DPA] = 1/5 (Figure 3-9A). While the pure Anth sample showed reflection signals consistent with its crystal structure (Figure 3-9A-b), the mixture sample exhibited a broad halo at around $2\theta = 25$ deg as the main signal due to amorphous structure as well as two sharp signals at $2\theta = 9.1$ deg (d = 9.7 Å) with higher intensity and at 18.8 deg (d = 4.7 Å) with lower intensity which do not coincide the crystal-based signals (Figure 3-9A-a). The polymer-DPA mixture also showed signals which do not coincide with those based on crystal at $2\theta = 10.4$ deg (d = 9.4 Å) with higher intensity and at 10.7 deg (d = 8.2 Å) in addition to a broad halo and crystal-based signals (Figure 3-9A-b). In addition, in differential scanning calorimetry (DSC), the polymer-Anth mixture showed a broad endothermic response at around 70 ^{o}C and a group of endothermic signals at around 140 ^{o}C in addition to a melting transition of Anth crystal at around 210 ^{o}C whose intensity was much smaller than the same signal of the pure Anth sample (Figure 3-9B-a). On the basis of the normalized melting peak intensities in Figure 3-9B-a, the majority (80 %) of Anth molecules are in a non-crystalline, amorphous state where partial, intermolecular order characterized by the spacings indicated by XRD may be present. On the other hand, the DSC profiles of the DPA systems indicate that about 50% of DPA may be in an ordered amorphous state characterized by the by the aforementioned spacings (Figure 3-9B-b). Further, polarized optical microscopy (POM) observations of the polymer-Anth mixtures indicated optical textures which are clearly different from that of pure Anth crystal (Figure 3-9C-a-iii) and may be recognized as banded focal conic

fan texture (Figure 3-9C-a-i) and mosaic texture (Figure 3-9C-a-ii). The polymer-DPA mixture at [polymer]/[DPA] = 1/3 also showed mosaic texture (Figure 3-9C-b-i) while that at [polymer]/[DPA] = 1/5 performs similar as the original crystals. The textures observed for the mixtures are similar to those reported for smectic liquid crystals.[22] The proposed order of Anth and DPA molecules may have some similarity to those of liquid crystals.

Considering the chemical structures of the polymers and the small molecules, specific and directional interactions such as hydrogen-bonding or strong interactions such as ionic at would not be plausible between the polymer and the molecules, and only non-specific and weak interactions based on van deer Waals force would be available. Nevertheless, the chirality transfer and chirality amplification effects are remarkable. The chirality transfer and the proposed ordering may be interpreted in terms of inclusion of the small molecules within the interior space of the polymers. Unlike linear polymers, the hyperbranched polymers may have a complex stereostructure having interior space large enough to include many small molecules due to a complex structure based on the extended hyperbranched architecture.

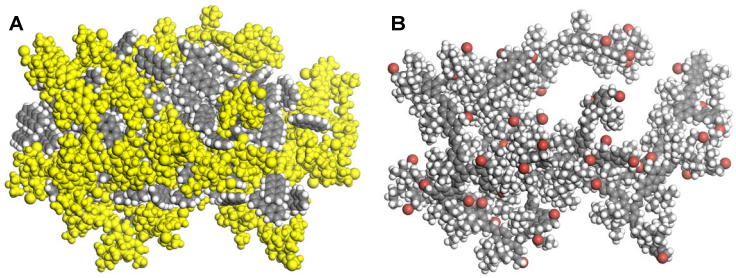

Figure 3-10. Structure of poly(**TNPFT-ED**) 50-mer model hosting 100 Anth molecules where the polymer is highlighted in yellow (A) and poly(**TNPFT-ED**) 50-mer extracted from A obtained by molecular dynamics simulations. [NVT, 300 K, COMPASS force field]

Inclusion of small molecules in the hyperbranched structure was supported by molecular dynamics simulations using a 50-mer polymer model and 100 Anth molecules as visualized in Figure 3-10. Anth molecules whose number is greater than

that of the monomeric units can be included in the polymer as if the polymer embraces the small molecules. The fact that the ratio of the amorphous part was greater for Anth than DPA may indicate that the capacity of inclusion, *i.e.*, the maximum number of small molecules that can be included is greater for a smaller molecule.

3.2.4 Chirality transfer in solution

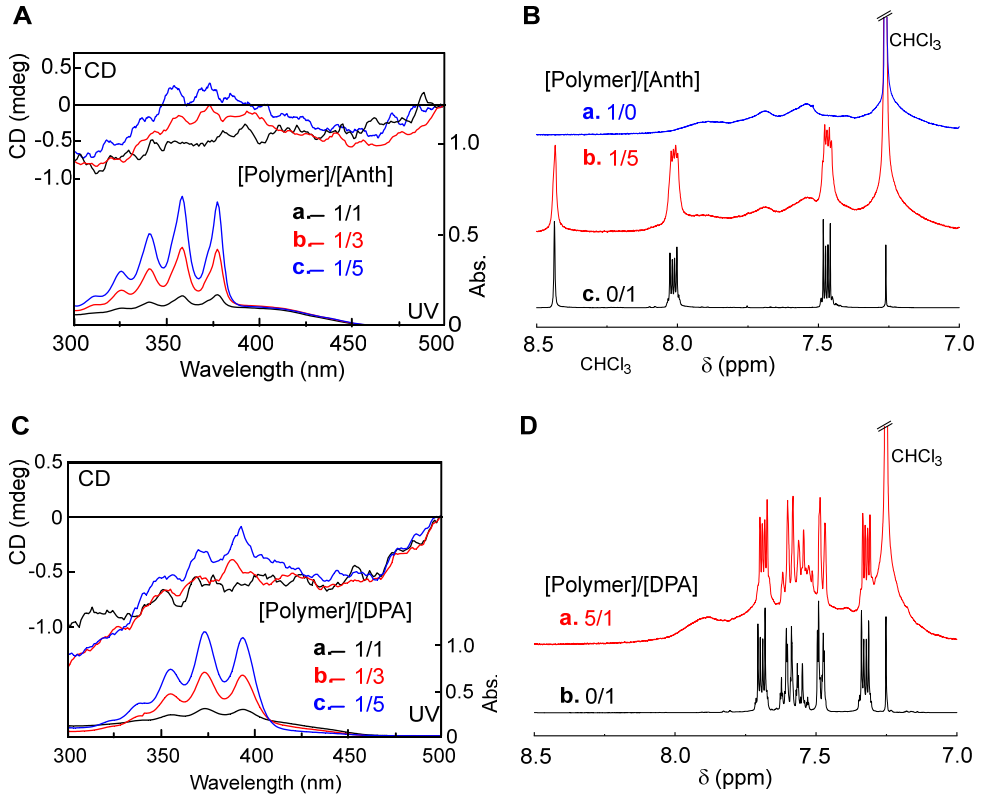

Figure 3-11. CD-UV spectra in THF solution (A) and ^{1}H NMR spectra in $CDCl_3$ solution (B) of poly(**TNMPFT-ED**)-Anth mixtures at different [polymer (residue)]/[Anth] ratios. [[polymer] = 2.0 x 10^{-4} M (A,C-a,b,c), 1.5 x 10^{-2} M (B-a), 1.0 x 10^{-2} M (B-b, D-a); [Anth] = 2.0 x 10^{-4} M (A-a), 6.0 x 10^{-4} M (A-b), 1.0 x 10^{-3} M (A-c), 2.0 x 10^{-3} M (B-b), 1.5 x 10^{-2} M (B-c); [DPA] = 2.0 x 10^{-3} M (D-a), 1.8 x 10^{-2} M (D-b)]

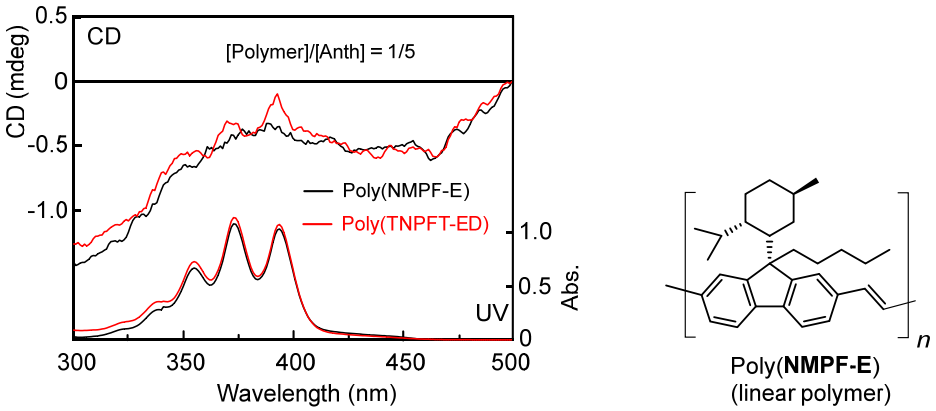

Figure 3-12. g_{CD}-UV spectra of a THF solution containing linear poly(**NMPF-E**) (Mn 21900) and DPA and that containing hyperbranched poly(**TNPFT-ED**) (Mn 100200) and DPA at [polymer]/[DPA] 1/5 (B). [[polymer (residue) = 2 x 10^{-4} M]

Further, it is notable that chirality transfer was observed for Anth and DPA in the presence of poly(**TNMPFT-ED**) even in THF solution at a low concentration ([polymer (residue)] = 2.0 x 10^{-4} M) while g_{CD} values were smaller than those in the corresponding film samples (Figure 3-11A, C). With an increase in [polymer]/[Anth or DPA] ratio, CD spectrum became clearer. The hyperbranched polymer can thus include the small molecules in a dilute solution in THF without any specific or strong interactions. The complex hyperbranched structure is responsible for such effects poly(**NMPF-E**) (M_n), a linear analougue of poly(**TNPFT-ED**), did not induce CD to Anth in THF solution (Figure 3-11).

Interactions between the polymer with Anth and DPA in solution were further studied by ^{1}H NMR spectroscopy (Figure 3-11B,D). At [polymer]/[Anth or DPA] = 1/5 at the same polymer concentration, the Anth signals were clearly broadened, suggesting that the mobility of Anth molecules was reduced by being included in the polymer (Figure 3-11B). In contrast, no clear changes were observed on the DPA signals, indicating DPA molecules are not effectively included under the NMR conditions (Figure 3-11C). In addition, for both the Anth and DPA systems, no clear shifts due to magnetic anisotropy were confirmed, which would rule out the possibility of π-stacking interactions of the polymer with Anth and DPA.[23,24] The different effects on NMR

spectra between Anth and DPA suggest that the polymer may recognize the size and also possibly the same of small molecules to be included.

3.2.5 CPL emission properties of chirality transfer systems

The films of mixture of poly(**TNMPFT-ED**) with Naph, Pyr, Anth, and PA exhibited clear CPL emission based on the small molecules (Figure 3-14). Pure poly(**TNMPFT-ED**) film showed broad CPL emission in the range of 450-700 nm with a moderate g_{lum} of around 1 x 10^{-3} (500 nm) (Figure 3-13). On the other hand, the emission spectra of the polymer-aromatic molecule mixtures appear to compose of broad emission bands in the longer wavelength ranges may arise mainly from the polymer and those in the shorter wavelength ranges (blow around 450 nm) which may be based mainly on the small molecules. The separate emission bands from the polymer and small molecules would mean that the two species are not homogeneously mixed and that the potential energy transfer from the higher-energy small molecules to the lower-energy polymer was not efficient, which may mean that part of the small molecules are not in direct contact with the polymer.

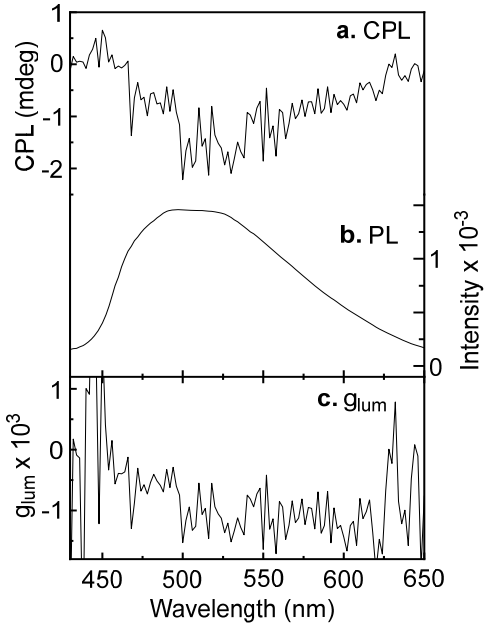

Figure 3-13. CPL spectrum (a), total emission (PL) spectrum (b), and g_{lum} spectrum (c) of acetone-insoluble, higher-molar-mass poly(**TNMPFT-ED**) in film [λ_{ex} 375 nm].

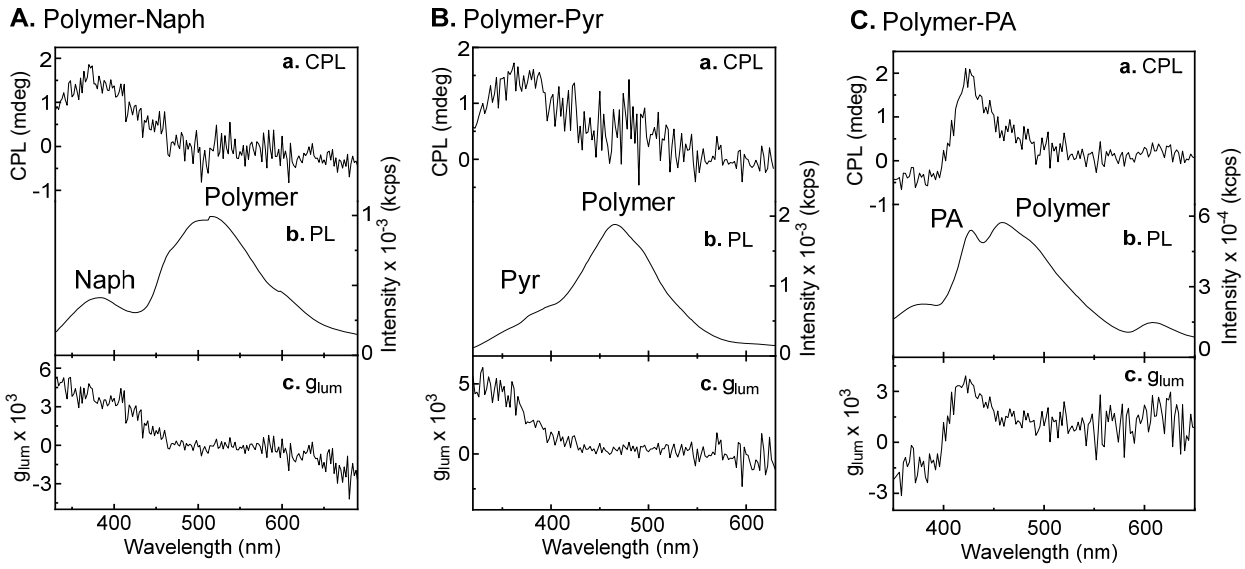

Figure 3-14. CPL spectra (a), total emission (PL) spectra (b), and g_{lum} spectra (c) of poly(**TNMPFT-ED**)-Naph (1/5) film (A), poly(**TNMPFT-ED**)-Pyr (1/3) film, and poly(**TNMPFT-ED**)-PA (1/5) film (C). [λ_{ex} 260 nm]

In addition, the CPL emission bands arising from the small molecules showed much greater anisotropy than the polymer-based bands (Figure 3-14). The g_{lum} values of Naph, Pyr and PA films with poly(**TNMPFT-ED**) were as high as around 5 x 10^{-3} which are a few times higher than that of the pure polymer. In addition, because the g_{CD} values of poly(**TNMPFT-ED**)-Naph, -Pyr, and -Anth films were of the orders of 10^{-4} or 10^{-5} at 260 nm (excitation wavelength), it can be concluded that chirality of the small molecules was amplified to a remarkable extent in excited states in the proposed intermolecular order induced by the polymer.

As for the origin of the observed chiroptical properties, the possibility of preferential crystallization leading to the formation of enantiomer-enriched crystals is ruled out in all cases because the space groups of pure crystals of Naph,[25] Anth,[25] Pyr,[25,26] DPA,[27]

and PA[28] are $P2_1/a$, $P2_1/a$, $P2_1/a$, C2/c, and P-1, respectively, indicating that the crystals have achiral structures. Relative spatial arrangement of the molecules in the proposed intermolecular order may hence have a single-handed twist character leading to chiroptical properties.

Another possibility may be intramolecular twist formation in the case of DPA and PA. However, DFT calculations based on the twisted conformation in the PA crystal predicted a CD spectrum with two bands of the same sign which are not in good agreement with the observed CD spectrum (Figure 3-17, Figure 3-5B). The observed chiroptical properties of PA may also be mainly contributed by chiral intermolecular order.

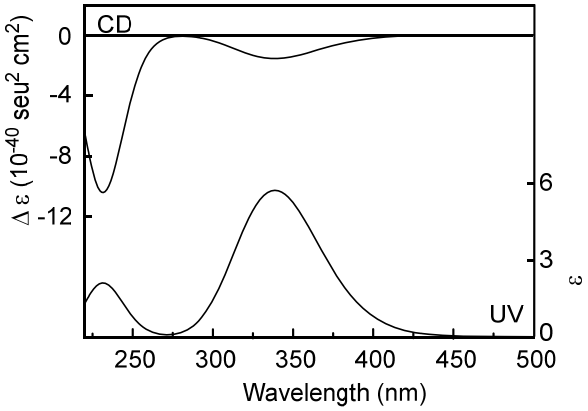

Figure 3-17. DTF-predicted CD and UV spectra of PA molecule having the conformation in its single crystal. [wB97XD/6-31G(d)]

3.3 Conclusions

In conclusion, the optically active, hyperbranched poly(fluorenevinylene) derivatives bearing a neomenthyl group derived from L-menthol as the chirality source and a pentyl group at the 9-position of the fluorene unit was found to serve as an efficient polymer matrix for aromatic small moleules having different sizes and shapes and transfer chirality to the gest molecules. The small molecules are mostly not crystals in the hyperbranched polymer matrix but are amorphous or in chiral intermolecular order

induced in the interior space of the hyperbranched polymer which may be similar to liquid crystals. In the cases with Anth and DPA, chirality in the ground state was amplified among the molecules embraced in chiral intermolecular order. In addition, Naph, Pyr and PA mixed with the hyperbranched polymer exhibited efficient CPL emission where the chirality induced in the ground state was remarkably amplified in excited states. Because these chirality transfer and amplification effects were not clearly observed with lower-molar mass hyperbranched polymers and also with linear analogue of the hyperbranched polymers, the extended hyperbranched structure is concluded to play a role in effectively including the small molecules. While there have been excellent systems of chirality transfer, it is very rare to the best of our knowledge that amorphous, hyperbranched polymers effectively host external molecules not on the basis of any specific or strong intermolecular forces or shape recognition effects known for templated polymer gels.[29-31] Further studies are in progress to clarily the details of the intremolecule structure of the small molecules and to expand the scope chirality receptors to be included by the polymer from small molecuels to macromolecules as well as to design novel hyperbranched polymers with wider functions including reaction control in the interior space.

3.4 Experimental

Materials.

Fluorene (TCI), (-)-menthol (TCI), *p*-toluenesulfonyl chloride (tosyl chloride) (Wako), paraformaldehyde (TCI), *n*-BuLi (2.3 M cyclohexane solution) (TCI), 1-iodopentane (Aldrich), HBr (33 wt%, acetic acid solution) (Wako), t-BuOK (TCI), potassium hydroxide (Kanto), pyridine (Kanto), 9-bromoanthracene (TCI), phenylboronic acid (TCI), tetrakis(triphenylphosphine)palladium(0) (TCI), $CHCl_3$ (Kanto), methanol (Kanto), acetone (Kanto), dimethylformamide (Wako) and silica-gel 60 N (neutral) (Kanto) were used as purchased. Tetrahydrofuran (THF) (Wako) was dried over calcium hydride and distilled under nitrogen flow. 9,9-Dipentylfluorene (DPF), menthyl tosylate,

9-neomenthylfluorene (NF), and 9-neomenthyl-9-pentylfluorene (NPF) (Scheme S1) were available from our recent work.[32]

General instrumentation.

^{1}H NMR spectra in solution were recorded on a JEOL JNM-ECX400 spectrometer (400 MHz for ^{1}H measurement) and a JEOL JNM-ECA600 spectrometer (600 MHz for ^{1}H measurement). SEC measurements were carried out using a chromatographic system consisting of a Hitachi L-7100 chromatographic pump, a Hitachi L-7420 UV detector (254 nm), and a Hitachi L-7490 RI detector equipped with TOSOH TSK gel G3000HHR and G6000HHR columns (30 x 0.72(i.d.) cm) connected in series (eluent THF, flow rate 1.0 mL/min). Preparative SEC analyses were carried out using JAI LC-9201 recycling preparative HPLC with UV/VIS detector S-3740 and column JAIGEL-1H, 2H (eluent $CHCl_3$, flow rate 3.0 mL/min), JAI LC-9201 recycling preparative HPLC with UV/VIS detector UV-50, RI detector RI-50 and column JAIGEL-1H, 2H (eluent $CHCl_3$, flow rate 3.0 mL/min), A Laboace LC-5060 recycling preparative HPLC with UV/VIS detector 4ch800LA and RI detector 700LA equipped with JAIGEL-1RH, 2RH, and 3RH columns connected in series (eluent $CHCl_3$, flow rate 10.0 mL/min). UV-vis absorption spectra were measured at room temperature with a JASCO V-570 spectrophotometers. Steady-state emission spectra were taken on a JASCO FP-8500 fluorescence spectrophotometer. Circular dichroism (CD) spectra were taken with a JASCO-820 spectrometer. The spectra of films were obtained by averaging those recorded at four different film orientations (angles) at an interval of 90^o with the film face positioned vertically to the incident light beam for measurement. The anisotropy factor (g_{CD}) was calculated according to g_{CD} = ΔAbs/Abs = (ellipticity/32980)/ Abs. DLS measurements were performed using a Nicomp 380 ZLS particle sizer. CPL spectra were measured with an assembled apparatus based on a photo elastic modulator and a photomultiplier designed according to the literature[33] with modifications. The emission anisotropy factor (g_{lum}) was calculated according to $g_{lum} = 2(I_L - I_R)/(I_L + I_R)$ where I_L and I_R are the emission intensities of *L*- and *R*-CPL,

respectively. TEM images were obtained on a JEM-2100F microscope at 200 kV using a microgrid. XRD profiles were measured using a Rigaku MiniFlex600-C diffractometer.

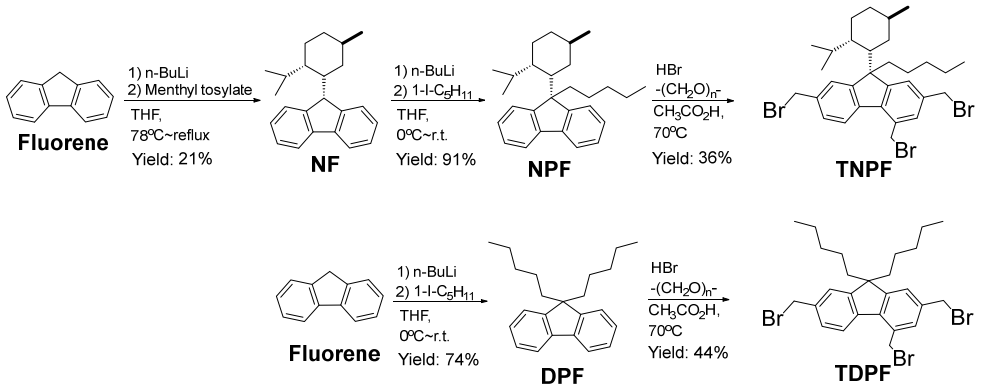

Scheme 3-2. Synthesis of the monomers and the precusors.

The monomers synthesis procedures are illustrated in Scheme 3-2 and the details are demonstrated following.

9-Phenylanthrathene.

9-Bromoanthrathene (514.2 mg, 2 mmol), benzeneboronic acid (146.3 mg, 1.2 mmol), KOAc (117.8 mg, 1.2 mmol) and bis(triphenylphosphine)palladium(II) dichloride (43.8 mg, 0.625 mmol) were mixed with toluene (5 mL), and the reaction mixture was stirred at 120 ºC for 24 h. After the mixture was cooled at r.t., raw products were collected by filtration and were recrystallized from hexane to lead to a slight yellow powder the pure target compound. Yield 365.1 mg (71 %). ^{1}H NMR (400 MHz, 298 K, $CDCl_3$) δ/ppm: 8.50 (s), 8.05 (d, 2H), 7.66 (d, 2H), 7.60-7.30 (m, 9H).

2,4,7-Tri(bromomethyl)-9,9-dipentylfluorene (TPF) (Scheme S1).

To a mixture of 9,9-dipentylfluorene (3.04 g, 0.01 mol) and paraformaldehyde (16.56 g, 0.20 mol) cooled at 0 ºC was added dropwise 43.0 mL of 33 wt% HBr (20 g, 0.25 mol) in an acetic acid solution. The reaction mixture was stirred at 70 ºC and for 36 h. The mixture was poured into a large excess of water and extracted with $CHCl_3$ to give the crude material which was purified by silica-gel column chromatography with a

mixture of toluene and *n*-hexane (1/5, v/v) as eluent, leading to a colorless solid product. Yield 44.0 % (1.87 g). ^{1}H NMR (600 MHz, 298 K, $CDCl_3$) δ/ppm: 7.27-7.66 (5 H, m), 4.91-4.76 (m, 2H, CH_2Br at 5-position of fluorene), 4.62-4.55 (m, 4H, CH_2Br at 2- and 7-position of fluorene), 1.80-1.98 (4 H, m), 0.88-1.12 (8 H, m), 0.45-0.75 (10 H, m).

2,4,7-Tri(bromomethyl)-9-neomenthyl-9-pentylfluorene (TNPF).[34]

To a mixture of NPF (3.78 g, 0.01 mol) and paraformaldehyde (20.2 g, 0.25 mol) cooled at 0 ºC was added dropwise 43.0 mL of 33 wt% HBr (20.2 g, 0.25 mol) in acetic acid solution. The reaction mixture was stirred at 70 ºC for 36 h. The reaction mixture was poured into a large excess of water and extracted with $CHCl_3$ to give the crude material which was purified by silica-gel column chromatography with a mixture of toluene and *n*-hexane (1/5, v/v) as eluent to afford a white solid product. Yield was 36 % (2.37 g). ^{1}H NMR (600 MHz, 298 K, $CDCl_3$) δ/ppm: 7.29-7.67 (5 H, m), 4.91-4.76 (m, 2H, CH_2Br at 5-position of fluorene), 4.62-4.55 (m, 4H, CH_2Br at 2- and 7-position of fluorene), 2.52-2.62 (1 H, m), 0.03-2.26 (29 H, m).

Polymerization.[34]

The detailed conditions and results of polymerization are summarized in Table 3-1. The procedure is described for run 3 in Table 3-1. TNPF (41.39 mg, 0.0634 mmol) and TPF (37.08 mg, 0.0634 mmol) were dissolved in 1.062 mL of dry THF under N_2 atmosphere, and 0.523 mL of 1-M *t*-BuOK (0.523 mmol) in THF was injected to initiate the polymerization. The reaction mixture was allowed to stand at 23 ºC for 12 h and was then terminated by the addition of 1 mL of water and stirring for 10 mins. The quenched reaction mixture was poured into a large excess of methanol. Precipitated polymer was collected with centrifuge. The MeOH-insoluble polymer was further separated by re-precipitated in acetone to obtain the acetone-insoluble product (15.06 mg, 19.2%) and acetone-soluble products (58.06 mg, 74%).

Film preparation.

The procedure is described for the films of the higher-molar-mass polymer from run 5 in Table 3-1. The polymer (0.41 mg, 1 mmol) was dissolved in THF (0.33 mL). An

aliquot (ca. 0.05 mL) of the solution was dropped onto a 1-mm quartz plate (1cm x 2 cm x 1 mm) and dried under air at r.t.

For film of the mixture of polymer and small molecule, here take polymer/DPA as example. The chiral pure polymer from Run 5 in Table 3-1 (0.41 mg, 1 mmol) was mixed with DPA (0.03, 0.33, 0.99, 1.65 or 2.64 mg, 0.1, 1, 3, 5, or 8 mmol) in 0.33 mL of $CHCl_3$. An aliquot (ca. 0.05 mL) of the solution was dropped onto a 1-mm quartz plate (1cm x 2 cm x 1 mm) and dried under air at r.t.

Computational method.

Molecular mechanics and dynamics simulations were conducted using the COMPASS[35] force field implemented in the Material Studio 4.2 software package. Molecular mechanics optimization was performed with the Fletcher-Reeves[36] conjugate gradient algorithm until the RMS residue went below 0.01 kcal/mol/Å. Molecular dynamic simulation was performed in vacuum under a constant NVT ensemble in which the numbers of atoms, volume, and thermodynamic temperature were held constant. Berendsen's thermocouple[37] was used for coupling to a thermal bath. UV and CD spectral calculations by DFT were run using Gaussian16W[38] package where ten singlet excited states were estimated in the time dependent framework using the WB97XD functional and the 6-31G(d) basis set.

References

1. S. K. Barry, Searching for new reactivity (Nobel lecture), *Angew. Chem. Int. Ed.* **2002**, *41*, 2024-2032.

2. N. Ryoji, Asymmetric catalysis: Science and opportunities (Nobel lecture), *Angew. Chem. Int. Ed.* **2002**, *41*, 2008-2022.

3. W. S. Knowles, Asymmetric hydrogenations (Nobel lecture), *Angew. Chem. Int. Ed.* **2002**, *41*, 1998-2007.

4. K. Kano, H. Matsumoto, Y. Yoshimura, S. Hashimoto, Binding sites of pyrene and related compounds and chiral excimer formation in the cavities of cyclodextrins and branched cyclodextrins, *J. Am. Chem. Soc.* **1988**, *110*, 204-209.

5. D. A. Lightner, J. K. Gawronski, K. Gawronska, Conformational enantiomerism in bilirubin. Selection by cyclodextrins, *J. Am. Chem. Soc.* **1985**, *107*, 2456-2461.

6. H. Shimizu, A. Kaito, M. Hatano, nduced circular dichroism of β-cyclodextrin complexes with azanaphthalenes-polarization directions of the $\pi \rightarrow \pi$ transitions in azanaphthalenes, *J. Am. Chem. Soc.* **1982**, *104*, 7059-7065.

7. M. Miyauchi, Y. Takashima, H. Yamaguchi, A. Harada, Chiral supramolecular polymers formed by host−guest interactions, *J. Am. Chem. Soc.* **2005**, *127*, 2984-2989.

8. E. Yashima, K. Maeda, H. Iida, Y. Furusho, K. Nagai, Helical polymers: synthesis, structures, and functions, *Chem. Rev.* **2009**, *109*, 6102-6211.

9. E. Yashima, N. Ousaka, D. Taura, K. Shimomura, T. Ikai, K. Maeda, Supramolecular helical systems: helical assemblies of small molecules, foldamers, and polymers with chiral amplification and their functions, *Chem. Rev.* **2016**, *116*, 13752-13990.

10. T. Nakano, Y. Okamoto, Synthetic helical polymers: conformation and function, *Chem. Rev.* **2001**, *101*, 4013-4038.

11. Y. Wang, N. Zavradashvili, Y. Wang, A. Pietropaolo, Z. Song, M. Bando, R. Katsarava, T. Nakano, Optically Active Polymers with Cationic Units Connected through Neutral Spacers: Helical Conformation and Chirality Transfer to External Molecules, *Macromolecules* **2020**, *53*, 9916-9928.

12. X. Yang, X. Jin, L. Zhou, P. Duan, Y. Fan, Y. Wang, Modulating the Excited State Chirality of Dynamic Chemical Reactions in Chiral Micelles, *Angew. Chem. Int. Ed.* **2022**, **61**, e202115600.

13. M. Miyata, M. Shibakami, S. Chirachanchai, K. Takemoto, N. Kasai, K. Miki, Guest-responsive structural changes in cholic acid intercalation crystals, *Nature* **1990**, *343*, 446-447.

14. H. Wang, A. Pietropaolo, W. Wang, C.-Y. Chou, I. Hisaki, N. Tohnai, M. Miyata, T. Nakano, Right-handed 2/1 helical arrangement of benzene molecules in cholic acid crystal

established by experimental and theoretical circular dichroism spectroscopy, *RSC Advances* **2015**, *5*, 101110-101114.

15. M. Miyata, K. Sada, in Comprehensive Supramolecular Chemistry, ed. D. D. MacNicol and F. Toda and T. R Bishop, Pergamon, Oxford, **1996**, vol. 6, pp. 147-176.

16. D. Yang, P. Duan, L. Zhang, M. Liu, Chirality and energy transfer amplified circularly polarized luminescence in composite nanohelix, *Nat. Commun.* **2017**, *8*, 1-9.

17. T. Zhao, J. Han, P. Duan, M. Liu, New Perspectives to Trigger and Modulate Circularly Polarized Luminescence of Complex and Aggregated Systems: Energy Transfer, Photon Upconversion, Charge Transfer, and Organic Radica, *Acc. Chem. Res.* **2020**, *53*, 1279-1292.

18. J.-M. Yu, T. Sakamoto, K. Watanabe, S. Furumi, N. Tamaoki, Y. Chen, T. Nakano, Synthesis and efficient circularly polarized light emission of an optically active hyperbranched poly (fluorenevinylene) derivative, *Chem. Commun.* **2011**, *47*, 3799-3801.

19. C. J. Hawker, J. M. J. Frechet, Preparation of polymers with controlled molecular architecture. A new convergent approach to dendritic macromolecules, *J. Am. Chem. Soc.* **1990**, *112*, 7638-7647.

20. M. P. Stevens, Polymer Chemistry, Oxford University Press, New York, **1999**, 353–354.

21. L.-R. Tsai, Y. Chen, Hyperbranched poly (fluorenevinylene) s obtained from self-polymerization of 2, 4, 7-tris (bromomethyl)-9, 9-dihexylfluorene, *Macromolecules* **2008**, *41*, 5098.

22. G. W. Gray, J. W. Goodby, HEYDEN & SON, 247 SOUTH 41 ST ST., PHILADELPHIA, PA 19104, USA, **1984**, 256, 1984.

23. T. Nakano, T. Yade, Synthesis, structure, and photophysical and electrochemical properties of a π-stacked polymer, *J. Am. Chem. Soc.* **2003**, *125*, 15474-15484.

24. T. Nakano, K. Takewaki, T. Yade, Y. Okamoto, Dibenzofulvene, a 1, 1-diphenylethylene analogue, gives a π-stacked polymer by anionic, free-radical, and cationic catalysts, *J. Am. Chem. Soc.* **2001**, *123*, 9182-9183.

25. F. P. Fabbiani, D. R. Allan, S. Parsons, C. R. Pulham, High-pressure elastic properties of polycyclic aromatic hydrocarbons obtained by first-principles calculations, *Acta Crystallogr B* **2006**, *62* (Pt 5), 826-842.

26. A. Camerman, J. Trotter, The crystal and molecular structure of pyrene, *Acta Crystallogr.* **1965**, *18*, 636-643.

27. J.M. Adams, S. Ramdas, The crystal structure of solution-grown 9, 10-diphenylanthracene. A combined computational and X-ray study, *Acta Cryst. B* **1979**, *35*, 679-683.

28. H. Iwahara, T. Kushida, S. Yamaguchi, A planarized 9-phenylanthracene: a simple electron-donating building block for fluorescent materials, *Chem. Commun.* **2016**, *52*, 1124-1127.

29. R. Arshady, K. Mosbach, Synthesis of substrate-selective polymers by host-guest polymerization, *Die. Makromol. Chem.* **1981**, *182*, 687-692.

30. K. J. Shea, T. K. Dougherty, Molecular recognition on synthetic amorphous surfaces. The influence of functional group positioning on the effectiveness of molecular recognition, *J. Am. Chem. Soc.* **1986**, *108*, 1091; b) K. J. Shea, D. Y. Sasaki, On the control of microenvironment shape of functionalized network polymers prepared by template polymerization, *J. Am. Chem. Soc.* **1989**, *111*, 3442.

31. G. Wulff, H.-G. Poll, M. Minárik, Enzyme-analogue built polymers. XIX. Racemic resolution on polymers containing chiral cavities, *J. Liq. Chromatogr. Relat. Technol.* **1986**, *9*, 385-405.

32. P. Wu, A. Pietropaolo, M. Fortino, S. Shimoda, K. Maeda, T. Nishimura, M. Bando, N. Naga, T. Nakano, Non-uniform Self-folding of Helical Poly (fluorenevinylene) Derivatives in the Solid State Leading to Amplified Circular Dichroism and Circularly Polarized Light Emission, *Angew. Chem. Int. Ed.* **2022**, DOI: 10.1002/anie.202210556.

33. S. Tanaka, K. Sato, K. Ichida, T. Abe, T. Tsubomura, T. Suzuki, K. Shinozaki, Circularly Polarized Luminescence of Chiral Pt (pppb) Cl (pppbH= 1-pyridyl-3-(4, 5-pinenopyridyl) benzene) Aggregate in the Excited State, *Chem. Asian J.* **2016**, *11*, 265–273.

34. R. Arshady, K. Mosbach, Synthesis of substrate-selective polymers by host-guest polymerization, Synthesis and efficient circularly polarized light emission of an optically active hyperbranched poly (fluorenevinylene) derivative, *Die. Makromol. Chem.* **1981**, *182*, 687-692.

35. H. Sun, COMPASS: an ab initio force-field optimized for condensed-phase applications overview with details on alkane and benzene compounds, *J. Phys. Chem. B* **1998**, *102*, 7338-7364.

36. R. Fletcher, C.M. Reeves, Function minimization by conjugate gradients, *Comput. J.* **1964**, *7*, 149-154.

37. H. J. Berendsen, J. V. Postma, W. F. van Gunsteren, A. R. H. J. DiNola, J. R. Haak, Molecular dynamics with coupling to an external bath, *J. Chem. Phys.* **1984**, *81*, 3684-3690.

38. Gaussian 16, Revision C01, M. J. Frisch, G. W. Trucks, H. B. Schlegel, G. E. Scuseria, M. A. Robb, J. R. Cheeseman, G. Scalmani, V. Barone, G. A. Petersson, H. Nakatsuji, X. Li, M. Caricato, A. V. Marenich, J. Bloino, B. G. Janesko, R. Gomperts, B. Mennucci, H. P. Hratchian, J. V. Ortiz, A. F. Izmaylov, J. L. Sonnenberg, D. Williams-Young, F. Ding, F. Lipparini, F. Egidi, J. Goings, B. Peng, A. Petrone, T. Henderson, D. Ranasinghe, V. G. Zakrzewski, J. Gao, N. Rega, G. Zheng, W. Liang, M. Hada, M. Ehara, K. Toyota, R. Fukuda, J. Hasegawa, M. Ishida,

T. Nakajima, Y. Honda, O. Kitao, H. Nakai, T. Vreven, K. Throssell, J. A. Montgomery, Jr., J. E. Peralta, F. Ogliaro, M. J. Bearpark, J. J. Heyd, E. N. Brothers, K. N. Kudin, V. N. Staroverov, T. A. Keith, R. Kobayashi, J. Normand, K. Raghavachari, A. P. Rendell, J. C. Burant, S. S. Iyengar, J. Tomasi, M. Cossi, J. M. Millam, M. Klene, C. Adamo, R. Cammi, J. W. Ochterski, R. L. Martin, K. Morokuma, O. Farkas, J. B. Foresman, and D. J. Fox, Gaussian, Inc., Wallingford, CT, 2016.

Chapter 4. General Conclusions

The optically active poly(fluorenevinylene) derivatives having linear and hyperbranched architectures were synthesized, and their chiropitcal properteis were studied in this theis work. The polymers bear a neomenthyl group derived from *L*-menthol as the chirality source and a pentyl group at the 9-position of fluorene core.

The linear poly(fluorenevinylene) derivatives were found to form a self-folded structure in which two to four neighboring monomeric units form a highly twisted, anisotropic conformation (“turn”) leading to remarkable chirality amplification in film, in suspension, and even in solution in a rather poor solvent. Self-folding was disclosed to be induced and further stabilized by inter-chain interactions where turns of the main chain may be strengthened possibly through alkyl-π-interactions between the opportunely designed side-chain groups and the main chain. Moreover, through chirality transfer from the chiral homopolymer to the achiral homopolymer, self-folding of the latter was induced. Chain folding is known for peptides and peptide mimics for which hydrogen-bonding plays a role in folding. Self-folding of completely synthetic chains has been reported for aromatic oligomers and polymers with restricted internal bond rotation represented by those called foldamers showing helical folding through hydrophobic and van der Waals force and also for an oligomer composed of donor (D) and acceptor (A) moieties through D-A interactions. While most of these examples are characterized by uniform self-folding, the poly(fluorenevinylene) derivatives studied in this work undergo non-uniform self-folding leading to a structure in which the turns connect the single-strand, stretched segments and the turn moieties show amplified chiroptical properties.

In addition, in the discipline of chiral polymers, helix has been extensively studied as a conformation leading to intense chiroptical properties, other structures have been paid little atttention. Uon-uniform self-folding may hence be regarded as an unprecedented category of conformational transition of synthetic polymers.

On the other hand, the optically active, hyperbranched poly(fluorenevinylene) derivatives did not indicate any remarkable enhancement of chirality in the solid state or in suspension that may suggest conformational transitions. However, they were found to serve as an efficient polymer matrix for aromatic small molecules having different sizes and shapes and transfer chirality to the gest molecules. The small molecules included in the hyperbranched polymer matrix are mostly amorphous where chiral intermolecular order may be induced in the interior space of the hyperbranched polymer. The proposed order may be similar to liquid crystals to an extent. In the cases with anthracene and 9,10-diphenylanthracene, chirality in the ground state was amplified among the small molecules included in chiral intermolecular order. In addition, naphthalene, pyrene, anthracene, and 9-phenylanthracene mixed with the hyperbranched polymer exhibited efficient CPL emission where the chirality induced in the ground state was remarkably amplified in excited states. CPL properties are especially significant with anthracene where the total emission spectra were very similar in shape to pure anthracene and the emission anisotropy (glum) was remarkably high. Without any derivatization such as that by the introduction chiral group attached to anthracene by significant synthetic efforts, CPL emission which appear to arise almost from pure anthracene was realized.

Because these chirality transfer and amplification effects were not clearly observed with lower-molar mass hyperbranched polymers and also with linear analogues of the hyperbranched polymers, the extended hyperbranched structure is concluded to play a role in effectively including the small molecules. While there have been excellent systems of chirality transfer, it is very rare to the best of our knowledge that amorphous, hyperbranched polymers effectively host external molecules without the aid from any specific interactions or strong intermolecular forces or shape recognition effects known for templated polymer gels. That no specific and intense interactions are necessary in the chirality transfer studied here would mean that the scope of chirality acceptor molecules is wide, indicating that the hyperbranched polymers studied here is versatile.

Through this thesis work, the polymers composed of fluorene core and ethen-1,2-diyl

group connected to form long conjugation systems were studied from a view of chirality. While fluorenevinylene as well as phenylenevinylene polymers have been long studied as light-emitting polymers, this work has brought about a new insight into this class of polymers as chiral polymer materials.

Acknowledgment

I am indebted to my supervisor, Prof. Dr. Tamaki Nakano, whose stimulating motivation, valuable ideas, and warm encouragement were indispensable in completing this thesis work.

I gratefully acknowledge Prof. Dr. Keiji Tanino, Prof. Dr. Yashichika Hasegawa, and Prof. Dr. Jun-ya Hasegawa for their reviewing my thesis and helpful advises.

Also, I would love to thank Prof. Dr. Adriana Pietropaolo (Catanzaro University), Prof. Dr. Katsuhiro Maeda (Kanazawa University), Dr. Hiroyasu Sato (Rigaku corporation), and Mr. Shuhei Shimoda (ICAT) for their experimental supports.

I feel grateful to all members of Nakano Laboratory and ICAT for their friendship and encouragement. Also, great gratitude goes to all of my friends who helped me complete this work.

Finally, I want to show deep love to my parents and all family members for their comprehension and supporting.

Finally, I acknowledge with a deep sense of reverence my parents and all family members who always understood and respected my decision to become a scientist and provided me with financial support.

Scholarships: My stay in Hokkaido University for 3.5 years was supported in part by the MEXT scholarhip from the government of Japan.

Thank you all.

2023/3/24
Pengfei WU